Universidade do Porto
FEUP Faculdade de Engenharia

U.PORTO
INSTITUTO DE CIÊNCIAS BIOMÉDICAS ABEL SALAZAR
UNIVERSIDADE DO PORTO

# Amoxicillin-loaded lipid nanoparticles against *Helicobacter pylori* infections

Ana Rita Oliveira Macedo Pinto

Master Thesis for the degree in Master of Science in Bioengineering – Specialization in Molecular Biotechnology

**Supervisor:**
Prof. PhD Salette Reis
UCIBIO/REQUIMTE, Departamento de Ciências Químicas, Faculdade de Farmácia, Universidade do Porto

**Co-supervisors:**
PhD Cláudia Nunes
UCIBIO/REQUIMTE, Departamento de Ciências Químicas, Faculdade de Farmácia, Universidade do Porto

MSc Daniela Lopes
UCIBIO/REQUIMTE, Departamento de Ciências Químicas, Faculdade de Farmácia, Universidade do Porto

June 2016

# Abstract

Nowadays, the increasing antibiotic resistance verified at a worldwide level lead to the failure of many treatments available for infectious diseases, such as *Helicobacter pylori*. This bacterium affects around 50% of the world population and is classified as human carcinogenic by the World Health Organization. Unfortunately, the efficacy of the standard triple therapy against this infection has been declined, mainly due to the increasing number of emergent antibiotic resistant bacterial strains. However, other factors are associated with the lack of efficacy, namely the degradation of antibiotics under acidic conditions, their low diffusion across the mucus layer, their insufficient residence time in the stomach, among others. Therefore, lipid nanoparticles emerged as a promising biocompatible drug delivery strategy. They can improve drugs pharmacokinetic properties, leading to an improvement of the efficacy and a decrease in the incidence of side effects. Further, the risk of development of bacterial resistance against antibiotics-loaded nanoparticles is reduced.

In this work, amoxicillin-loaded solid lipid nanoparticles (SLNs) were developed to protect amoxicillin against acidic degradation and to enhance its absorption, with the aim to increase the bioavailability. Preliminary studies were performed in order to select the most adequate lipid and preparation method of the lipid nanoparticles. From these screenings, cetyl palmitate was selected as the solid lipid and double emulsion technique was chosen as the most suitable preparation technique. Further, SLNs composed of cetyl palmitate, linolenic acid, dioleoylphosphatidylethanolamine (DOPE), Tween®80 and amoxicillin were optimized by Box-Behnken design. The optimal formulation had a low polydispersity index around 0.137 with a mean size diameter around 200 nm and a zeta potential superior to |30| mV. Additionally, the loading capacity was satisfactory high, being around 7%. The optimal formulation was stable in a suspension form at 4ºC during at least 2 months, while in the lyophilized SLNs amoxicillin degradation was visible after 1 month. *In vitro* release studies revealed an initial burst release (less than 30%) followed by an increased release at the simulated mucosa medium (pH 5). Then, a sustained and controlled phase was observed at physiologic pH 7.4. Methylthiazolydiphenyl-tetratozium bromide (MTT) assay revealed that the optimal SLNs suspension does not have cytotoxic effects in both L929 and MKN28 cell lines. Additionally, other three formulations with decreasing complexity compared with the abovementioned nanoparticles composition were prepared for future evaluation of the most important parameters involved in the nanoparticles-bacteria interactions. These formulations were also characterized and evaluated in *in vitro* release and cell viability studies, with similar results comparative to the optimal formulation.

***Keywords:*** antimicrobial resistance, *Helicobacter pylori* infections, amoxicillin, lipid nanoparticles, oral administration, lipid nanoparticles preparation techniques, nanoparticles characterization, Box-Behnken design, MTT assay.

*-This page was intentionally left blank-*

# Acknowledgments

I'm deeply grateful to Prof. Dr. Salette Reis for the great opportunity to work in such a fantastic research group and for all the guidance, concern and enthusiasm.

To Dr. Cláudia Nunes, thank you for your positive energy and enthusiastic way to see every result. Thank you also for your support, guidance and for the good moments.

To Daniela Lopes, thank you for everything you did during this project and for always being by my side. Thank you for your patience, I know that sometimes I was annoying and had some crazy ideas of doing many things at the same time. You never said no to anything, even when it seemed impossible. I think we were bought super women these last months.

I'm am grateful to Dr. Sofia Lima for all the guidance, knowledge and patience during the cellular assays.

I also want to thank all the people from the lab for making my days more fun. Thank you all for the good moments that I will take with me. A special thanks to my "roomie" Andreia for always being available when I needed something and to care about me.

To my friends "Nenas" for the friendship, care and for making my life better. You made my last 5 years wonderful. I will miss our adventures and maybe the days we passed like crazy studying in "Biblioteca da Maia".

To Helena, thank you for your "eternal" friendship, since I was 6 years old you walked by my side.

To Thomas, thank you for your support and for listening to me. I know sometimes I was annoying but you were always patient. Thank you also for making me see that work is not everything that matters.

Last but not least, to my parents, brother and grandmother. Thank you for understanding my late arrivals for dinner and the enthusiasm you showed when I talked about my project and my days in the lab. Thank you for all your support.

*-This page was intentionally left blank-*

# Table of Contents

*-This page was intentionally left blank-*

# List of Figures

# List of Tables

*-This page was intentionally left blank-*

# List of Appendices

*-This page was intentionally left blank-*

# List of Abbreviations

| | |
|---|---|
| AMR | Antimicrobial Resistance |
| AMX | Amoxicillin |
| ANOVA | Analysis of variance |
| BBD | Box-Behnken design |
| CSK | CSKSSDYQC peptide |
| DLS | Dynamic Light Scattering |
| DMEM | Dulbecco's Modified Eagle's Medium |
| DMSO | Dimethyl Sulfoxide |
| DNA | Deoxyribonucleic acid |
| DOPE | Dioleoylphosphatidylethanolamine |
| DSC | Differential Scanning Calorimetry |
| EDTA | Ethylenediaminetetraacetic acid |
| EE | Encapsulation Efficiency |
| ELS | Electrophoretic Light Scattering |
| FBS | Fetal Bovine Serum |
| FDA | Food and Drug Administration |
| GRAS | Generally Recognized As Safe |
| *H. pylori* | *Helicobacter pylori* |
| HPH | High-Pressure Homogenization |
| IARC | International Agency for Research on Cancer |
| IRQ | IRQRRRR peptide |
| IUPAC | International Union of Pure and Applied Chemistry |
| LC | Loading Capacity |
| LNPs | Lipid Nanoparticles |
| MTT | Methylthiazolydiphenyl-tetratozium Bromide |
| NLCs | Nanostructured Lipid Carriers |
| NPs | Nanoparticles |
| OVAT | One-Variable-At-a-Time |
| PBS | Phosphate Buffered Saline |
| PDI | Polydispersity Index |
| PE | Phosphatidylethanolamine |
| PLX | Polymixin B Sulphate |
| PVA | Polyvinyl Alcohol |
| Pen Strep | Penicillin- Streptomycin |

| | |
|---|---|
| RI | Recrystallization Index |
| RPMI | Roswell Park Memorial Institute |
| RT | Room Temperature |
| SA | Sodium Alginate |
| sCT | Salmon calcitonin |
| SD | Standard Deviation |
| SLNs | Solid Lipid Nanoparticles |
| SPC | Soybean Phosphatidylcholine |
| TEM | Transmission Electron Microscopy |
| TMC | *N*-trimethyl chitosan |
| WHO | World Health Organization |

# Chapter 1 – Introduction

## 1.1 Introducing Infectious Diseases

At the beginning of the 20th century, infectious diseases were the leading cause of death at a worldwide level [1]. However, since the introduction of penicillin in the 1940s the field of antibiotics emerged [2]. Consequently, various natural products capable of killing bacteria were discovered, which led to a significant decrease in morbidity and mortality resultant from infectious diseases [2]. Nevertheless, we are currently living in a new era, driven by the development of antimicrobial resistance (AMR) [3]. In the United States, AMR is estimated to be responsible for the addition of $20 billion to the total health care costs and $35 billion in costs to society [4]. AMR is also a concern in the European Union, since it is estimated that the phenomenon causes 25 000 deaths and costs more than US$1.5 billion per year [5]. These costs include both healthcare expenses and losses in productivity [5].

AMR is a natural evolutionary process in bacteria, since antimicrobial resistance genes existed long before the therapeutic application of antibiotics [4]. The occurrence of mutations is highly probable in an infection cycle due to the large number of bacteria and the high intrinsic rate of mutation [6]. If one of the mutations confers resistance to an administered antibiotic, a natural selection occurs, where all the sensitive bacteria are killed, while the bacteria with the mutation grow [6]. Due to the wide use of antimicrobial agents at a global level, there is a preferential selection for bacteria that are able to express resistance genes against antibiotics [4]. Thus, AMR has been rapidly evolving and spreading, leading to no assurance that new antimicrobial drugs can timeously respond to the increasing rates of bacterial resistance [2]. Thus, AMR is becoming a worldwide threat to the efficient treatment of infectious diseases [7].

Besides AMR, other drawbacks of the current antimicrobial therapies lead to unsuccessful eradication of pathogens. Intrinsic factors of antimicrobial agents can also compromise their therapeutic effects [8]. These factors include poor cellular penetration, limited intracellular retention, inefficient subcellular distribution and decreased intracellular activity [8]. Antibiotics are usually administered by oral or intravenous routes [2]. Oral administration is the most convenient and safest route for drug administration [9]. This route is cost-effective, presents less complications and it is less intrusive than intravenous administration, increasing therapeutic compliance [9, 10]. In addition, prolonged intravenous drug administration can cause local and vascular infection and patient discomfort [9, 10]. However, both routes present a major drawback characterized by systemic side effects, due to nonspecific drug distribution [2]. Oral administration is also associated with a poor bioavailability, due to poor solubility and/or poor permeability of drugs [9]. The acidic pH of the stomach, the contact with enzymes and biliary salts can also reduce drugs' bioavailability through their degradation [9, 11].

Further, the hepatic first-pass metabolism contributes to reduce the concentration of drugs in the systemic circulation, since during this phenomenon drug metabolism occurs [9, 12]. Consequently, infection conditions usually require high-doses of antibiotics in order to achieve an adequate concentration in serum, which commonly lead to adverse side effects [13]. However, even applying an aggressive antibiotic treatment, the complete eradication of the infection can be difficult to achieve [13].

The increasing of antibiotic resistance, the loss of antibiotic efficacy and the lack of new antibiotics in the market have become a worldwide challenge to provide adequate treatment for infectious diseases [7, 14]. Thus, novel effective therapies are necessary to overcome these limitations.

## 1.2 NANOPARTICLES AS DRUG DELIVERY SYSTEMS

### 1.2.1 INTRODUCING NANOTECHNOLOGY

Nanotechnology is a multidisciplinary branch of science that integrates the fields of medicine, chemistry, biology and engineering [15]. According to International Union of Pure and Applied Chemistry (IUPAC) definition, nanoparticles (NPs) are structures of any shape with an equivalent diameter of approximately 1 to 100 nm [16]. However, the definition of nanomaterial is controversial with some definitions supporting that particles of dimensions greater than 100 nm might also have physicochemical properties that are characteristic to the nanoscale [17]. Hence, it is important that the accepted definition of NPs is not restricted to the size per se, but also to the physicochemical properties such as charge, shape and surface characteristics [17]. Herein, in this thesis, the term nanoparticle will be applied for particles in the range of 1-999 nm. Due to their nanoscale, these materials have novel physicochemical and biological features with potential for biosciences applications [18]. The high surface area-to-volume ratio of nanostructures is responsible for their different behaviour from the bulk material [19]. Consequently, nanomaterials have mechanical, electrical, chemical, optical and magnetic properties that can be advantageous in the design of drug delivery systems [19].

In the past few decades, NPs emerged as a promising drug delivery strategy to overcome AMR [4]. To design an ideal nanocarrier some characteristics must be considered. Nanocarriers must be biocompatible, biodegradable, nontoxic and be able to target the infection sites [14]. In addition, they must have a high drug payload and prevent drug release before reaching the target [14]. Thus, therapeutic concentrations at these sites can be achieved, reducing side effects related to non-targeted drug release [14].

NPs have been explored in the treatment of infectious diseases since they improve the antibacterial activity of antibiotics on several bacteria [20]. This activity is dependent on the size, shape, morphology, surface modifications and stability of NPs [20]. Nonetheless, some NPs have intrinsic antibacterial activity, such as silver NPs [21]. NPs are able to protect drugs from the acidic conditions of the stomach, improve their half-life and maintain a sustained drug

release at the target site [22]. These factors lead to higher concentrations of antibacterial agents near the bacterium, even with lower doses [22]. Hence, these drug delivery systems can minimise side effects and improve the therapeutic efficacy, decreasing the potential development of bacterial resistance [22]. Moreover, many types of lipophilic and water-soluble antibiotics can be carried at the core or at the surface of NPs by chemical conjugation, physical encapsulation or surface adsorption [23, 24]. However, covalent linking is the only technique that allows a precise control of the amount of drug loaded into the nanoparticle [18]. Through these methods, NPs are capable of loading multiple antimicrobial agents within their structure [4]. As a consequence, antimicrobial resistance mechanisms are unlikely to be developed against these systems, since it requires multiple simultaneous gene mutations in the microbial DNA [4].

Antimicrobial NPs improve drugs pharmacokinetics and their therapeutic index, including serum solubility and stability [2, 24]. Further, they prolong drugs half-life in systemic circulation, promoting a sustained and controlled release of the drug and a uniform distribution at the infection site [2, 24]. The target can be achieved using a passive or active strategies [4]. The passive targeting results from enhanced vascular permeability at the target infection site, if associated to inflammation, which allows a selective extravasation and retention of NPs [4]. On the other hand, in active targeting, the NPs are functionalized with specific ligands (e.g. antibodies, peptides, folic acids, among others) that recognise and bind to receptors at the target cells [4, 18]. For instance, drug delivery systems can be conjugated with antibodies against a specific antigen selectively found at the surface of the target microorganism [18]. The targeting can also be achieved through an activation upon an external stimuli, producing physicochemical changes that lead to drugs release at the target site [25]. These stimuli include magnetic and electric fields, ultrasounds, temperature, enzymatic activity, pH, ionic strength and redox potential [25]. Among these stimuli, pH stimuli has been widely researched [25]. One of its applications consist in the improvement of oral drug delivery systems [25]. For instance, Lin *et al*. (2009) formulated heparin-chitosan NPs, self-assembled by mixing heparin and chitosan at pH 1.2-2.5 to apply in the treatment of *Helicobacter pylori (H. pylori)* infections [26]. The system was stable at the gastric lumen (pH 1.2-2.5) due to electrostatic interactions within the structures [26]. After, the NPs infiltrated into the mucus layer (pH 4.5-7.0) and contacted with *H. pylori* along the gastric epithelium (pH~7.4) [26]. At the site of infection, the deprotonation of chitosan occurred, which weakened electrostatic interactions and led to system instability and disintegration [26]. As a consequence, the drug was released, acting locally on the bacteria at a bactericidal concentration [25, 26].

After drug-loaded NPs efficiently reach the infected tissue, they can deliver their payloads into target cells through three different pathways: adsorption, contact release or endocytosis [8]. In the last pathway, nanocarriers penetrate the target cells and release the antibiotics in the internal medium, avoiding resistant mechanisms related with activation of efflux systems and decreasing of membrane permeability [22, 24]. Due to these target delivery strategies, it is expected to reach a higher dose of antibiotic at the infection site with a lower administration

frequency and dose [4]. Consequently, systemic adverse effects of therapy are minimized, which improves patient compliance to the treatment [2, 4].

Currently, a number of nanoparticle-based drug delivery systems have been approved for clinical use in a variety of diseases, while many other nanoparticle formulations are under clinical trials [24]. In January 2012, 67 nanodevices were identified in the market, from which 33 were associated to nanotherapeutics [27]. According to the BCC Research report, the market value of the worldwide nanomedicine industry was $214.2 billion in 2013 and $248.3 billion in 2014. By the year of 2019, it is projected that the global market of nanomedicine reach $528 billion [28]. The progress of nanomedicine market over the past few years is a consequence of the increasing investment of companies on nanotechnology [2]. Therefore, this phenomenon is changing the paradigm of current treatments against many diseases, including infectious diseases [2]. However, the clinical nanoparticle-based drug delivery systems safety profiles must be considered upon a long-term exposure, being this parameter the most concerning in the use of nanotechnology for medical applications [2].

### 1.2.2 Lipid Nanoparticles (LNPs)

In the last decades, many colloidal drug carriers have been studied to improve drugs solubility by oral administration [29]. These carriers include micelles, nanoemulsions, nanosuspensions, polymeric NPs and liposomes [29]. For the majority of these carriers, a low cost large-scale production method is currently not available [29]. Nevertheless, LNPs adopted the best features of other colloidal systems and emerged as a strategy to overcome their limitations [29]. These NPs are usually composed of a matrix of physiological or physiologically related lipids characterized by their versatility, biocompatibility and biodegradability [29-31]. Lipids are natural materials that can be degraded by natural processes, such as enzymatic activity [31]. Due to these processes, complex lipids are easily and completely degraded in the human body [31]. Therefore, the excipients that compose the matrix of LNPs are generally recognized as safe (GRAS) for oral and topical administration [32].

LNPs exhibit other outstanding advantages when compared with other colloidal drug delivery systems, including improved kinetic stability, drug solubility and controlled drug release [30, 31]. Besides, LNPs production is cost-effective, being easy to scale up according to the production process, which increases the researchers' interest on these nanocarriers [30, 32].

Formulations for oral administration are possible as aqueous dispersion or alternatively transformed into tablets, pellets, capsules or powders in cachets [30, 32]. These formulations can protect encapsulated drugs from the environment of gastrointestinal tract and their nanoparticulate state promotes the uptake by M cells of Peyer's patches [30]. Consequently, LNPs enables the system to bypass the effect of first-pass metabolism, through lymphatic absorption [30, 33].

Different types of LNPs have been engineered, such as solid lipid nanoparticles (SLNs) and nanostructured lipid carriers (NLCs) [34]. These NPs demonstrated high drug loading for

hydrophilic and lipophilic drugs and long-term shelf stability [29]. Despite the increasing interest in the field of LNPs, a low number of formulations are currently in the market [32]. Consequently, more investment on LNPs investigation is required [32].

#### 1.2.2.1 SOLID LIPID NANOPARTICLES

SLNs were introduced in 1991 as an alternative to colloidal drug carriers [35]. SLNs are nanospheres with a matrix composed of lipids in a solid state at both room and body temperatures and with a mean particle size from 50 to 1000 nm (**Figure 1.1**) [32]. Fatty acids, waxes, monoglycerides, diglycerides and triglycerides are widely used to construct the rigid core of SLNs [34]. To stabilize the solid matrix, various non-toxic surfactants can be added during SLNs preparation, such as poloxamers, polysorbates or polyvinyl alcohol (PVA) [14, 34, 36]. From these, PVA is the most commonly used due to its physical and chemical properties, biocompatibility and low acute oral toxicity [36, 37]. Besides, PVA is approved by Food and Drug Administration (FDA) for use in medical and food applications [36, 37].

SLNs combine advantages of other drug delivery systems, while overcome some of their limitations [38]. These drug delivery systems are characterized by a good physical stability, biodegradability and they are able to incorporate both lipophilic and hydrophilic drugs, depending on the preparation method [14, 18]. Due to their solid core identical to polymeric NPs, SLNs provide simultaneously a protection of the encapsulated drug and its controlled delivery [32, 38]. Furthermore, these LNPs are easily produced at an industrial scale being possible to avoid the use of organic solvents [29]. Many drug delivery systems based on SLNs have been prepared for various administration routes, showing improved bioavailability and targeted delivery of antimicrobial drugs [2, 38].

Besides the advantages, several drawbacks are still associated with the use of SLNs as drug delivery systems. The loading capacity (LC) of SLNs is determined by the crystalline structure of the solid core [29]. In fact, the drug is incorporated in the spaces between the fatty acid chains, the lipid layers or in the amorphous clusters in crystal imperfections [29]. SLNs composed of a highly purified lipid can form a perfect crystalline lattice, which reduces the available spaces to accommodate the drug [29]. Consequently, these carriers have a limited drug loading capacity [29, 34]. Other disadvantages of SLNs are associated with a relatively high water content (70-99.9%) and with storage conditions. More specifically, during the storage, the degree of order of the solid matrix is increased, which contributes to the formation of a perfect crystalline lattice [29, 31]. Therefore, the number of imperfections in the crystal lattice is reduced, leading to an early drug release [29, 31]. Moreover, gelation phenomenon and the increase of the particle size may occur with storage time [29, 39].

SLNs constitute an attractive drug delivery system due to their advantages when compared with other drug carrier systems [40]. However, due to the drawbacks associated with these systems, a second generation of LNPs emerged: nanostructured lipid carriers [32].

### 1.2.2.2 NANOSTRUCTURED LIPID CARRIERS

NLCs were developed to overcome the potential limitations of SLNs. The second generation of LNPs are composed of a lipid matrix with both solid and liquid lipids [34]. This matrix has a melting point depression when compared with the pure solid lipid matrix of SLNs, being however solid at body temperature [30]. Besides, NLCs matrices are less-ordered and have imperfections between the liquid lipid and the solid lipid, providing more spaces to incorporate drugs (**Figure 1.1**) [32, 34]. In NLCs the drug can be accommodated between the fatty acid chains, lipid layers and imperfections [31]. Consequently, using NLCs, drug loading capacity is enhanced, while drug release during storage is minimized [29, 34]. Besides, these nanocarriers are less susceptible to gelation during both preparation and storage processes, having a lower water content when compared to SLNs [31, 34].

According to the preparation method and the lipid composition, there are three types of NLCs: imperfect type, multiple type and amorphous type [30, 40]. The imperfect type NLCs is obtained when small amounts of liquid lipids are added to the solid matrix, which leads to imperfections in the structure [30, 40]. Therefore, these imperfections create free spaces for drug accommodation in amorphous clusters (**Figure 1.1, I**) [40]. Multiple type NLCs are prepared by mixing higher amounts of oil with the solid lipid [38]. In this phenomenon, the solubility of oil molecules in the solid lipid is exceeded, which leads to a phase separation [38, 40]. Consequently, oily nanocompartments are formed in the solid matrix [38, 40]. This type of NLCs can be advantageous, since the solubility of many lipophilic drugs in oils is higher than in a solid lipid [38, 40]. Hence, the existence of oily nanocompartments improves drug solubility, while the solid lipid matrix prevents degradation and drug release during storage (**Figure 1.1, II**) [38, 40]. Finally, the amorphous type of NLCs is composed of a structureless solid amorphous matrix [40]. This amorphous matrix is obtained by mixing solid lipids with specific lipids (e.g. Miglyol®812 or isopropylmyristate) [40]. Due to the amorphous state of the matrix in this type of NLCs, crystallization process upon cooling is avoided [38, 40]. Thus, drug release during storage time is minimized (**Figure 1.1, III**) [40].

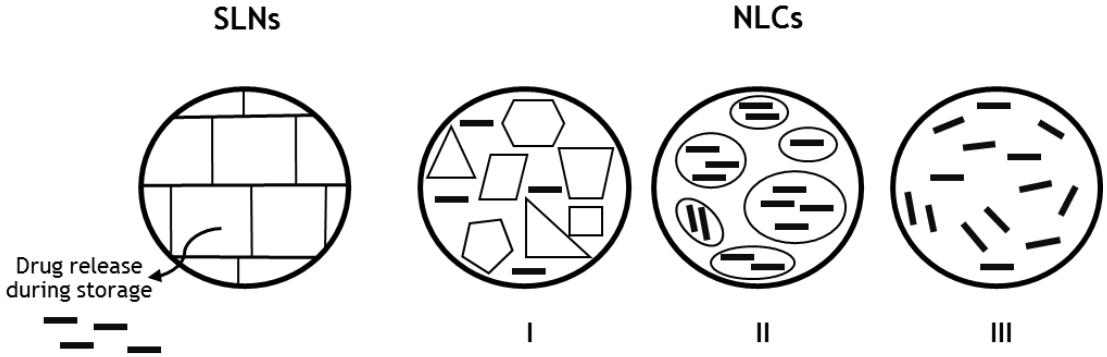


**Figure 1.1:** SLNs crystalline matrix and different types of NLCs matrices. I – Imperfect type NLCs, II – Multiple type NLCs, III – Amorphous type NLCs. Adapted from [41].

### 1.2.2.3 LNPs Synthesis Techniques

Various synthesis techniques can be used for the production of LNPs. Some important parameters must be considered in the selection of the most suitable technique for LNPs preparation, such as the physicochemical properties and the stability of the drug to be incorporated [42]. Besides, the desirable particle characteristics and stability should also be considered [42].

**High-Pressure Homogenization (**HPH) is a suitable technique for preparation of LNPs [38]. This technique can be performed at high temperatures (hot HPH) or at temperatures below room temperature (RT) (cold HPH) [38]. In hot HPH, both the lipid and the drug are melted at approximately 5-10ºC above the lipid melting point [38]. After, the homogeneous dispersion is mixed with an aqueous surfactant solution prepared at the same temperature [38]. Consequently, a hot pre-emulsion is formed by high speed stirring [29]. The hot pre-emulsion is processed in a high-pressure homogenizer at the same temperature until a nanoemulsion is obtained [29]. The lipid droplets of the nanoemulsion recrystallize into LNPs upon cooling down at RT [29]. The cold HPH is similar to hot HPH, since both the lipid and drug are melted [29, 38]. However, in cold HPH the cooling down process occurs rapidly using liquid nitrogen or dry ice, which leads to the formation of solid lipid microparticles [29, 38]. These microparticles are then suspended in a cold aqueous surfactant and homogenized at/or below RT [29]. Through this process, LNPs are produced [29]. Cold HPH is suitable for hydrophilic or thermo-labile drugs, since avoids drug degradation at high temperatures and drug distribution into aqueous phase during homogenization [29]. HPH technique has been widely used for LNPs production since it is easy to scale up, avoids organic solvents and has a short production time [30, 31]. However, the use of high operating temperatures and cavitation forces can cause thermodynamic and mechanic stress [30]. In order to overcome these disadvantages and to encapsulate drugs with a wide variety of physicochemical features, new production methods for LNPs preparation have been extensively investigated [30].

**Microemulsion** technique was developed and optimized by Gasco and his co-workers and has been adapted and/or modified by other researchers [38]. In this method, the solid lipid is melted and the drug dispersed in the melted lipid [29]. After, an aqueous solution, containing both the surfactant and co-surfactants, is prepared at the same temperature and added to the melted lipid [29]. The mixture is subjected to stirring, which leads to the formation of a microemulsion [38]. Subsequently, it is dispersed in cold water (2-10ºC) using stirring [29]. Consequently, the microemulsion breaks into ultrafine nanoemulsion droplets that crystallize to form LNPs [29]. This technique can be used at an industrial scale [29]. However, the removal of the surplus water, usually using ultrafiltration or lyophilisation, is the main concern of this technique [29]. The high concentration of surfactant and co-surfactants required in this method is also a disadvantage, since it is less desirable for regulatory purposes and applications [29, 38].

In the **emulsification-sonification** method, both lipid and drug are melted at approximately 5-10ºC above the lipid melting point [29]. After, an aqueous surfactant solution at the same

temperature is added to the homogenously dispersed mixture by a high shear mixing device [29]. The resultant emulsion is then ultrasonicated until a nanoemulsion is obtained and, afterward, cooled down at RT, forming LNPs [29]. However, the possible contamination of the emulsion by probe sonicator during sonication process is a concern in the use of the method [29].

In **solvent emulsification-evaporation**, the lipid is dissolved in a water-immiscible organic solvent (e.g. chloroform, cyclohexane) [29]. After, the mixture is emulsified in an aqueous phase containing surfactants under continuous stirring [29]. The solvent is evaporated during emulsification at a reduced pressure, which leads to lipid precipitation into NPs [29]. This method can be performed at RT, avoiding heat during the preparation [29, 38]. Consequently, solvent emulsification-evaporation technique is suitable for thermo-labile drugs [29]. However, the main concerns are associated with possible solvent residues in the final dispersion and the production of a very diluted dispersion due to the limited solubility of the lipid in the organic solvent [29, 38]. Consequently, the dispersion needs to be concentrated by ultrafiltration or evaporation [29].

In **solvent diffusion** technique, partially water-miscible organic solvents (e.g. benzyl alcohol, ethyl formate) are used [29]. In this method, the organic solvents are mutually saturated with water to ensure initial thermodynamic equilibrium of both lipids [29]. The oil-in-water emulsion is passed into water under continuous stirring, which leads to solidification of the dispersed phase, forming LNPs due to diffusion of the organic solvent [29]. However, similarly to the microemulsion technique, the dispersion is very diluted [29]. Consequently, it needs to be concentrated by ultrafiltration or lyophilisation [29]. Besides, the use of organic solvents that can remain in the final preparation is also a concern of this technique [29].

The **solvent injection** technique is similar to the solvent diffusion method [29]. Lipids are dissolved in a water-miscible solvent (e.g. acetone, isopropanol and methanol) or water-miscible solvent mixture [29]. Then, using an injection needle, the mixture is quickly injected into an aqueous solution of surfactants [29]. This preparation method is fast and easy to handle [29]. Besides, it does not require technically sophisticated equipment [29]. However, the main concern is associated with the use of organic solvents [29].

The **double emulsion** technique was first described by Cortesi *et al*. (2002) [43]. This method is based on the solvent emulsification-evaporation technique and is suitable for loading hydrophilic drugs into LNPs [29]. During LNPs preparation, both the drug and the stabilizer are encapsulated in the inner aqueous phase of the water-in-oil-in-water double emulsion [29]. The stabilizer is required to prevent drug partition to the external water phase during solvent evaporation [29, 38]. In the double emulsion procedure, an aqueous solution of drug is emulsified in molten lipid to obtain a primary water-oil emulsion, stabilized by the addition of emulsifiers to the aqueous phase [42]. Then, the primary emulsion is dispersed in a second aqueous solution containing stabilizers, under constant stirring [42]. Thus, a water-oil-water double emulsion is generated [42]. The formulations obtained through this method are usually named as “lipospheres” due to their larger particle size when compared with SLNs [29].

In the **high speed stirring and/or ultrasonication** technique, LNPs are produced by spray congealing [38]. After, these particles are subjected to high speed stirring or sonication, which leads to the formation of lipid nanopellets [38]. LNPs preparation by this method is easy and does not require technical and sophisticated equipment [38]. The main concern is associated to a broader particle size distribution, which fluctuates into the micrometer range due to the high speed stirring process [38]. Consequently, this phenomenon can lead to physical instabilities during storage [38]. Besides, the possible metal contamination due to ultrasonication is also a disadvantage of the technique [38].

## 1.3 EXPERIMENTAL DESIGN AND OPTIMIZATION OF FORMULATIONS

In the development of drug delivery systems, experimental design and optimization are crucial tools to facilitate the definition of the formulation composition and the manufacturing process [44, 45].

The traditional optimization of an experimental response involves monitoring the influence of one-variable-at-a-time (OVAT), while the remaining variables are kept at a constant level [44, 46]. However, this approach does not guarantee the optimum composition, since the interactive effect of one or more variables on others is not considered [44, 46]. Consequently, the final formulation obtained applying OVAT methodology is satisfactory, but mostly sub-optimal [44]. Besides, it is costly and time-consuming once an increased number of experiments are required, leading to a higher consumption of reagents and materials [46, 47].

Currently, to overcome the inconveniences of the traditional approach, multivariate statistic techniques have been widely applied to optimize the design of formulations [46-48]. These strategies involve designs for which the levels of all variables are changed simultaneously, allowing the assessment of interaction effects among the variables in study [48]. Consequently, a multivariate approach requires fewer experiments when compared to univariate approaches, leading to a lower reagent consumption and considerably less laboratorial work [48]. One of the most relevant multivariate techniques is the response surface methodology [46]. This approach consists in mathematical and statistical methods, based on linear or square polynomial equations [46]. Hence, the behaviour of an experimental data set is mathematically described in order to perform statistical previsions [46]. In an experimental procedure, several variables or factors may influence the final formulation [45]. Therefore, an initial screening is performed to select the independent variables and interactions that have a significant influence on the system, leading to a delimitation of the experimental region [46]. Consequently, a suitable design can be performed accordingly to the stablished by the previous screening [46]. The resultant data is then processed through mathematic-statistical treatment using a polynomial function [46]. Therefore, the optimum value for each variable is determined [46].

### 1.3.1 BOX-BEHNKEN DESIGN (BBD)

In a BBD the levels of independent variables must be adjusted at three levels (-1, 0, +1) with equally spaced intervals between the levels [46]. In this model, computer optimization processes and a mathematical function of response surface methodology evaluate the effect of the levels of independent variables on the responses [49].

The BBD is a very useful approach when several variables are simultaneously studied in an optimization process [49]. This approach exhibits outstanding advantages when compared with full three-level factorial designs, since it requires fewer runs, is more efficient and has lower costs for a large number of variables [46, 47]. Moreover, in BBD the combinations for which all factors are simultaneously at their lowest or highest are rejected [48]. Therefore, experiments performed under extreme conditions are avoided [48]. The BBD is being widely used to evaluate the effect of different variables on SLNs and NLCs formulations [47, 50]. One interesting application of optimized formulations obtained by this methodology is to improve bioavailability of oral drug delivery systems using NPs [49].

Usually, BBD applied to LNPs production requires approximately 15 to 17 runs for three or four dependent variables [49, 51, 52]. In this methodology, independent variables are selected to investigate their influence in the behaviour of dependent variables previously fixed [49, 51]. The most common dependent variables reported in studies for synthesis of SLNs and NLCs are the particle size, encapsulation efficiency (EE) and LC [49, 51]. However, other dependent variables such as zeta potential [53], turbidity [52] and polydispersity index (PDI) [50] have also been reported. On the other hand, drug to lipid ratio [51], surfactant concentration and homogenization speed [51] are the independent variables usually selected for LNPs preparation. Nonetheless, lipid concentration [52], homogenization time [53] and surfactant/lipid molar ratio [54] are also investigated for optimization of LNPs.

BBD is commonly represented by a multidimensional cube with a variable number of points. For instance, in a BBD involving 15 experimental runs, three replicated central points are used to determinate the experimental error and the precision of the design [55]. The remaining runs are associated to points located at the edges of the cube (**Figure 1.2**) [50].

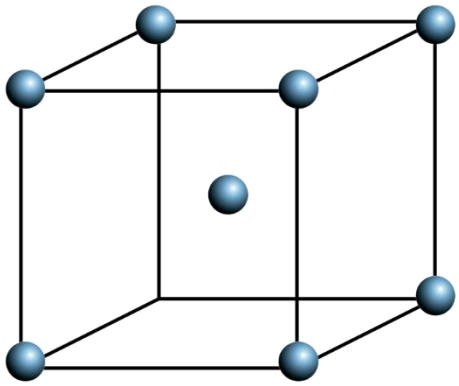

**Figure 1.2:** Cubic representation of the BBD for the optimization of three variables.

## 1.4 LIPID NANOPARTICLES FOR ORAL ADMINISTRATION

As abovementioned, the oral delivery is the most cost-effective route and simultaneously the most comfortable to the patient [9, 10]. However, due to the extreme and severe conditions of the gastrointestinal tract, SLNs and NLCs have been widely studied to improve drugs pharmacokinetics and to treat a wide range of diseases (**Appendix 1**). For that purpose, oral absorption is a crucial step. Thus, Zhang *et al.* (2012) studied the absorption of SLNs both in stomach and intestine [56]. In this work, oral candesartan cilexetil-loaded SLNs were formulated by a film-homogenization technique [56]. They verified that absorption of the resultant SLNs occurred mainly in the intestine via internalization into the enterocytes [56]. Besides, the developed SLNs were absorbed more rapidly than the free drug [56]. In order to investigate cellular uptake, internalization pathways and transcytosis routes of both SLNs and NLCs, Neves and her colleagues (2016) used Caco-2 cell monolayers as an intestinal model [57]. From this study, the authors concluded that LNPs internalization occurs manly through a clathrin-mediated endocytosis [57]. In addition, both SLNs and NLCs crossed the intestinal barrier predominantly by a transcellular route [57]. The internalization across the intestinal barrier can also be promoted by specific ligands, such as was performed by Fan *et al.* (2014) [58]. They used salmon calcitonin (sCT)-loaded SLNs modified with CSKSSDYQC (CSK) peptide or IRQRRRR (IRQ) peptide [58]. Both peptides showed to improve SLNs cellular uptake using Caco-2/HT29-MTX co-cultured cells [58]. Moreover, it was observed that SLNs modified with CSK and IRQ were internalized by clathrin- and caveolae-dependent endocytosis [58]. These results are in accordance with the mechanisms of SLNs internalization at intestinal level described by Neves and her colleagues [57, 58].

An interesting advantage of LNPs is their ability to be modified in order to improve their physicochemical stability for oral administration. For instance, Ramalingam *et al.* (2016) developed a nontoxic surface modified formulation of resveratrol-loaded SLNs using *N*-trimethyl chitosan (TMC) graft palmitic acid [59]. The modified NPs showed a sustained release and enhanced bioavailability of resveratrol due to the mucoadhesive and high absorption properties of TMC [59]. The relative bioavailability of the drug was found to be 3.8-fold higher from SLNs than free drug [59]. Pandita *et al.* (2014) were also focused on the development of a SLN-based delivery system to encapsulate resveratrol [60]. In this study, the system was composed of a lipid matrix of stearic acid coated with poloxamer 188 and lecithin [60]. The resultant SLNs showed a sustained drug release and a significant 8.035-fold improvement in oral bioavailability as compared to resveratrol suspension [60]. Another example of a compound used to functionalize LNPs in order to enhance drugs bioavailability is biotin. Zhou *et al.* (2015) studied the effect of biotin in oridonin-loaded NLCs [61]. Biotin-modified NLCs showed a relative bioavailability of 171.01%, while non-modified NLCs had a relative bioavailability of 143.48% [61]. Additionally, no significant differences in release were observed between non-modified NLCs and biotin-modified NLCs [61].

In order to improve the optimization of LNPs for oral delivery, the abovementioned experimental design, BBD, has been applied. More specifically, Varshosaz *et al*. (2010) used the BBD in the optimization of buspirone HCL-loaded SLNs prepared by emulsification-evaporation and sonification method [49]. A preliminary screening was performed to identify the independent variables, namely lipid type, surfactant percentage, speed of homogenizer and acetone:dichloromethane ratio, which significantly affected particles size [49]. These variables were considered in the 17 experimental runs of the BBD to obtain a formulation with a maximum level of LC and minimum levels of both particle size and zeta potential [49]. The optimized formulation revealed an enhanced oral bioavailability of the drug in 2.53-fold compared to that of the drug solution [49]. In a study performed by Neupane and co-workers (2014), decitabine-loaded NLCs were also optimized using BBD [62]. In this process, 17 experimental runs were obtained to investigate the effect of independent variables in particle size, PDI and EE [62]. The selected independent variables were lipid and surfactant concentrations and the number of homogenization cycles [62]. According to the study, the desired formulation should have a particle size in a range of 100-200 nm, the minimum PDI and the maximum EE [62]. The optimal formulation showed more affinity towards tumour cells and increased cytotoxicity activity against cancer cells than the plain drug [62].

Regarding the application of LNPs for oral administration, it can be very extensive. For example, LNPs have been applied to load nutraceutics. Luan and co-workers prepared and optimized baicalin-loaded NLCs [63]. The NPs showed a biphasic drug release pattern with an initial burst release and a sustained release afterwards [63]. Thus, a significant enhancement of bioavailability was observed [63]. Zhuang *et al*. (2010) optimized vinpocetine-loaded NLCs to obtain the most favourable physicochemical characteristics [64]. The optimized formulation showed a sustained release profile without an observable burst-release effect [64]. Furthermore, *in vivo* studies revealed that the relative bioavailability of the resultant formulation was 322% in comparison with the free drug [64]. Anticancer delivery systems based on NLCs have also been studied by many research teams around the globe. For instance, How and co-workers (2013) developed a stable anticancer tamoxifen-loaded NLCs formulation [65]. In *in vitro* studies it was verified that encapsulation in NLCs preserved the cytotoxicity of the drug against tumour cancer cell lines [65]. LNPs for oral administration have also been studied for administration of hypolipidemic drugs, such as lovastatin and simvastatin. Chen *et al*. (2010) investigated the effect of the surfactants myverol and soybean phosphatidylcholine (SPC) in lovastatin-loaded NLCs [66]. They concluded that NLCs with myverol were more stable in the gastric environment and showed significantly higher bioavailability than NLCs containing SPC [66]. However, SPC system exhibited slower release [66]. In a study performed by Tiwari and Pathak (2011), optimized simvastatin-loaded NLCs showed a significantly higher EE and improved gastrointestinal absorption when compared with simvastatin-loaded SLNs [67]. As a consequence, in *in vivo* pharmacokinetic studies, NLCs revealed 2.29 folds increase in bioavailability as compared to SLNs [67].

LNPs loading antimicrobial agents have been extensively studied. A more detailed description of the oral administration of LNPs to combat infectious diseases was reviewed in a book chapter (Rita M. Pinto, Daniela Lopes, Cláudia Nunes, Bruno Sarmento, Salette Reis. Oral administration of lipid-based delivery systems to combat infectious diseases. Accepted at *Nanoparticles in the Life Sciences and Biomedicine*, Pan Stanford Publishing). In particular, antibiotics-loaded LNPs were proved as a successful delivery system with increased antibacterial efficiency. For instance, Xie *et al*. (2011) formulated ofloxacin-loaded SLNs using palmitic acid as the lipid matrix and PVA as emulsifier by hot homogenization and ultrasonication method [36]. The formulation exhibited an initial fast release of the drug followed by a slow and sustained phase, which contributed to maintain the effective therapeutic drug concentrations and increased bioavailability [36]. Consequently, the NPs developed in this study demonstrated i*n vitro* and *in vivo* antibacterial efficacy against *Staphylococcus aureus* [36]. A similar study was performed by Dong *et al*. (2011) where norfloxacin was loaded into SLNs for oral administration [68]. The resultant SLNs demonstrated an effective antibacterial activity while no cytotoxic effects were detected [68]. More recently, the polymixin B sulphate (PLX) was also studied [69]. However, the salt form of PLX is a hydrophilic antibiotic with a cationic charge, which is an obstacle for an efficient loading into SLNs [69]. Thus, Severino *et al*. (2015) developed a novel lipid-polymer hybrid SLNs-based system to encapsulate the drug [69]. For that purpose, the hydrophilicity of the drug was decreased via previous cross-linking with the anionic polymer sodium alginate (SA), in a SA/PLX ratio (1:1) [69]. The resultant SLNs revealed an improved LC [69].

In the previously described studies, both SLNs and NLCs formulations showed an enhanced bioavailability and pharmacological activity of the loaded drug, requiring less frequency of dosage. Although SLNs and NLCs only recently emerged as drug delivery systems, many researchers have developed formulations for oral delivery that showed potential for further clinical applications.

## 1.5 *HELICOBACTER PILORY* INFECTIONS: A STEP TOWARDS INNOVATION IS NEEDED

*H. pylori* is a gram-negative bacterium, usually characterized by a spiral-shaped form that can be converted in coccoid cells under a hostile environment [70]. This bacterium is a human pathogen able to resist to the acidic pH (1 or 2) of the stomach lumen and to penetrate within the mucosa (**Figure 1.3**) [22, 70]. Thus, the bacteria colonize the region between the mucus layer and epithelial cells, where the pH is near to neutral (pH 4-6) [22, 70]. The colonization process occurs due to several virulence factors, including bacteria flagella that allow bacteria mobility and adhesins responsible for the adherence to the mucosa and to epithelial cells [22, 70]. Other factors, such as urease production, phospholipase secretion and cytotoxic production, are crucial for the bacteria pathogenesis [70].

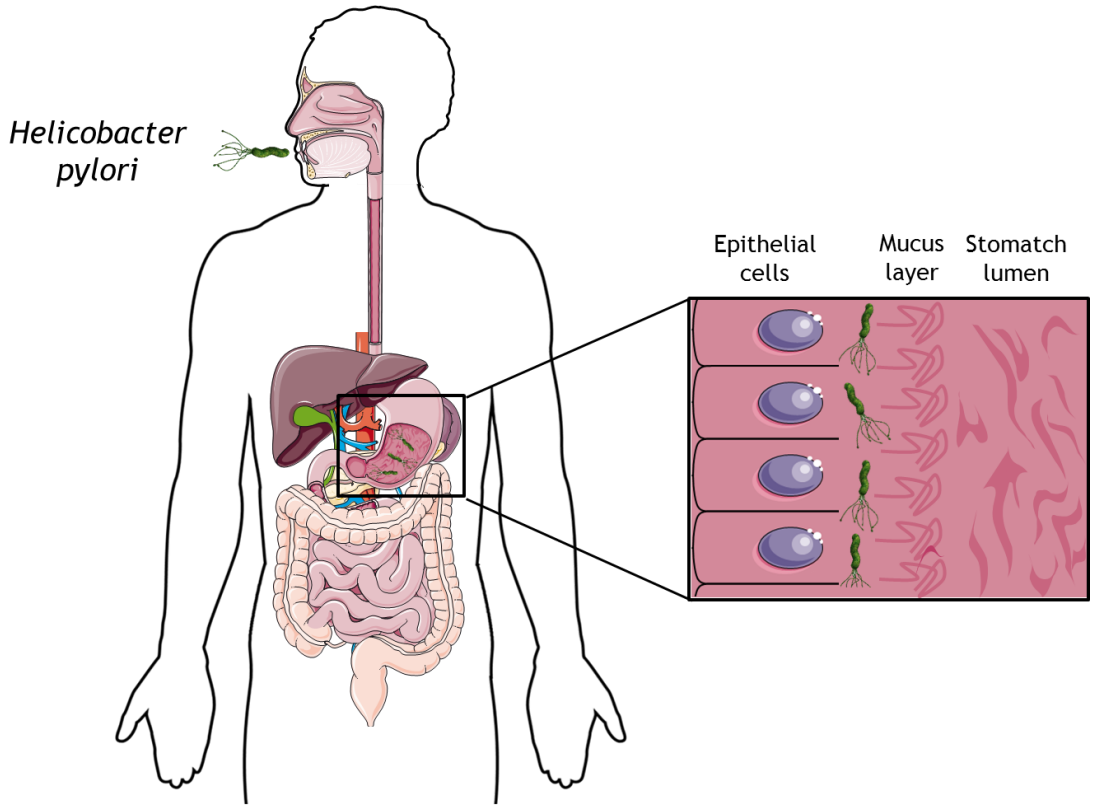


**Figure 1.3:** Schematic representation of the *H. pylori* infection. The bacterium is acquired by oral ingestion and colonizes the region between the mucus layer (pH 5) and epithelial cells (pH 7). Adapted from [22].

Nowadays, *H. pylori* bacteria have a huge impact worldwide, affecting around 50% of the global population [70]. However, the infection incidence is variable among countries and groups of people, reaching over 80% of the middle-aged adults in developing countries [71]. Several conditions are responsible for these variations among prevalence rates, including race/ethnic, aging and socioeconomic conditions [70]. The bacteria are acquired by oral ingestion and usually an asymptomatic colonization occurs [70, 71]. In fact, only approximately 20% of the infected patients develop chronic gastritis and peptic ulcer [22]. A more severe condition caused by the persistent colonization of *H. pylori* can be developed, namely gastric cancer [22, 70]. Due to this clinical outcome, the bacteria are classified as a human carcinogen (Group 1) according to the International Agency for Research on Cancer (IARC) and the World Health Organization (WHO) [22]. Although without a clear explanation, *H. pylori* have also been associated to other diseases, such as idiopathic thrombocytopenic purpura, iron deficiency anaemia, ischemic heart disease, stroke, Parkinson's diseases and Alzheimer's disease [22].

Currently, a standard triple therapy combining a proton pump inhibitor and two to three antibiotics is used against *H. pylori* infections, according to International Guidelines [70, 72]. The therapy is usually applied twice a day, for about 7 to 14 days [70]. The most common antibiotics used in this treatment are amoxicillin (AMX), clarithromycin and metronidazole or tinidazole [70]. Nonetheless, the efficacy of this therapy has been declining over the last years, especially when applied just for 7 days [73]. The decrease in the number of successfully treated

infections is mainly a consequence of the increasing number of emergent antibiotic resistant *H. pylori* bacteria strains [73]. Thus, the standard 7-day triple-therapy is recommended only for the cases where clarithromycin resistance is lower than 15-20%, while a higher antibiotic resistance rate requires a 14-day regime [73]. Nonetheless, the successful cases of *H. pylori* eradication using the prolonged therapy are far from the desirable, with a rate of eradication of 70% in non-ulcer dyspepsia patients and 81.7% in peptic ulcer patients [73].

Besides the intrinsic *H. pylori* antimicrobial resistance, other factors compromise the success of the triple therapy. The acidic pH of the stomach presents a huge drawback for the oral administration of both AMX and clarithromycin, since these antibiotics are easily degraded in the stomach conditions [22]. Thus, lower amount of effective drug is maintained *in vivo* [22]. Furthermore and as a consequence of the gastric transit, antibiotics remain in the stomach for an insufficient time, hindering their diffusion across the mucus layer [22, 70]. This lead to a lower concentration of drug that reaches the bacteria, located between the mucus layer and the epithelial cells [22, 70]. To overcome this limitation, higher and multiple doses are required, which may lead to discomfortable side effects, such as nausea, vomiting, abdominal pain, among others [22, 70]. The frequency of side effects combined with the duration of the therapy are the main reasons for a lack of patient compliance [22]. Thus, the discontinuation of the therapy commonly leads to an incomplete eradication of the bacteria and to potential development of antibiotic resistance [70, 74]. In the last years, the resistance prevalence of *H. pylori* to metronidazole has increased in around 40% and 90% in developed and developing countries, respectively [75].

In an attempt to overcome the drug resistance verified for the triple therapy, several regimens have been tested [75]. For instance, the efficacy of new antibiotics or new antibiotic combinations was evaluated for the eradication of *H. pylori* [73]. Nevertheless, the therapies failed mainly due to the high costs associated and the adverse effects that lead to a poor patient compliance, among other factors [75]. Moreover, the development of vaccines to prevent *H. pylori* infections is still in an experimental phase [73].

Besides some approaches are emerging, the lack of a suitable therapy is still a concern. Thus, a step towards innovation in anti-*H. pylori* therapies is urgently needed, which lead to the aim of the current project.

## 1.6 AIM AND STRATEGY

As previously mentioned, AMX is one of the most commonly antibiotics used in the standard triple therapy against *H. pylori* infections [70]. Usually this antibiotic is orally administered to eradicate the bacteria [76]. Nevertheless, some limitations are associated to this administration route for AMX. For instance, Lozniewski *et al.* (1999) reported that AMX is unstable at the normal gastric pH (1 to 2), which may be a consequence of hydrolytic degradation of AMX [76]. Therefore, a delivery system able to protect the drug from the acidic environment and to release it near the bacterium (almost neutral pH) would be advantageous

to avoid the drug's degradation [4]. Furthermore, and taking into account the advantages already mentioned regarding the oral administration of LNPs, they have a huge potential as AMX delivery systems, since they are able to protect it from the acidic gastric environment [22]. Moreover, AMX is considered a low permeability drug according to the Biopharmaceutics Classification System, with low affinity to lipid phases [77, 78]. This limitation leads to a poor absorption through the gastric mucus layer and, consequently, an enhanced intestinal absorption and first-pass metabolism. Due to the lipid composition of LNPs, they already proved their usefulness in improving drugs bioavailability, by enhancing their absorption. Hence, they can be a promising strategy to deliver low permeability drugs.

In this context, the present project consists in the development of an innovative AMX delivery system based on LNPs. The main purpose of this system is to improve the efficiency of the treatment for *H. pylori* infections, improving the residence time of AMX in stomach, protecting it from degradation, enhancing their absorption and, ultimately, increasing antibiotic concentration at the target site [22]. To achieve this purpose, AMX-loaded LNPs were developed. The ideal NPs are composed of the solid lipid, chosen by a lipid screening, Tween®80, linolenic acid and dioleoylphosphatidylethanolamine (DOPE) (**Figure 1.4**). According to literature, linolenic acid is a fatty acid that has been recently highlighted due to its antibacterial activity against all strains of *H. pylori* bacteria, including the ones resistant to metronidazole [75]. Thus, in the current work, linolenic acid was encapsulated with AMX, as an adjuvant to the therapy. On the other hand, DOPE was selected for functionalization and also as a surfactant, since it is an unsaturated phosphatidylethanolamine (PE) [22]. Lingwood and his colleagues (1992) observed that PE, which is a predominant lipid in the antrum of the human stomach, is a receptor for *H. pylori* adhesion [79, 80]. Considering the interaction between PE and the bacterium, it is possible to develop anti-adhesion drug delivery systems based on PE, acting simultaneously as an active targeting [22, 80]. In the present project, DOPE was used at the surface of the NPs to target and block the bacteria adhesion to the gastric mucosa.

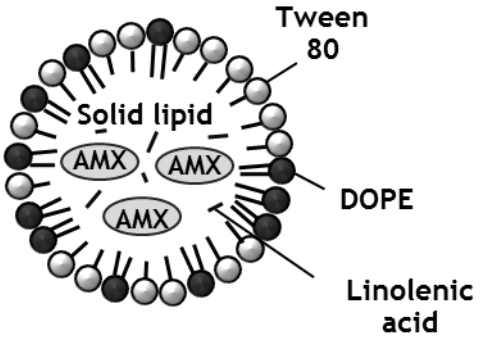


**Figure 1.4:** Schematic representation of the composition of the ideal formulation.

Besides, other three formulations (F1, F2, F3) (**Figure 1.5**) with decreasing degrees of complexity were characterized. The main goal of studying these formulations is to have a full physicochemical and morphologic evaluation of the NPs to be applied in future studies of NPs-

bacteria interactions. Thus, these formulations vary in the presence or absence of the adjuvant (linolenic acid) and the targeting (DOPE).

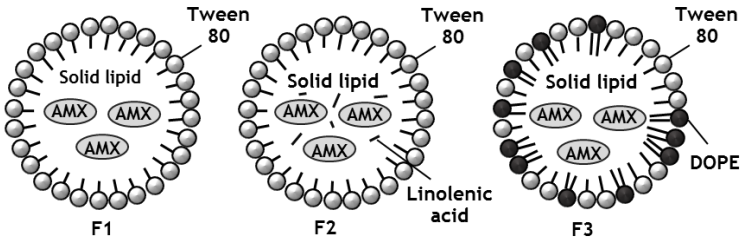


**Figure 1.5:** Schematic representation of the three formulations (F1, F2 and F3) that will be studied in this work.

The specific goals of this thesis can be enumerated as follows:

- Perform a lipid screening to evaluate the affinity of AMX to each one of the selected solid lipids;
- Perform a method screening to select the most suitable LNPs preparation method;
- Use a rational designed, namely a Box-Behnken statistical design, to optimized the AMX-loaded SLNs;
- Full-characterization of the designed formulations regarding storage stability through particle size, PDI, zeta potential and LC measurements;
- Comparison of the storage stability of lyophilized LNPs, in the form of powder or after resuspension with the stability of LNPs in suspension;
- Morphological characterization of lyophilized LNPs and LNPs suspensions using transmission electron microscopy (TEM);
- Assessment of the degree of lipid crystallinity and the lipid polymorphism of lyophilized LNPs;
- Evaluation of the *in vitro* AMX release of both lyophilized LNPs and LNPs suspensions, through simulation of the gastric absorption of AMX-loaded LNPs at body temperature.
- *In vitro* evaluation of the effect of LNPs in the L929 and MKN28 cell lines viability using the methylthiazolydiphenyl-tetratozium (MTT) assay.

*-This page was intentionally left blank-*

# Chapter 2 - Materials and Methods

## 2.1 MATERIALS

The lipids Gelucire 43/01, Gelucire 44/14, Cetyl palmitate, Compritol 888 ATO and Precirol ATO 5 were a kind gift from Gattefossé (Gattefossé, France). Softisan 100, Dynasan 116, Imwitor 900 K and Imwitor 491 were gently offered by Sasol (Johannesburg, South Africa). Miglyol 812 and Aerosil 200 were purchased from Acofarma® (Terrassa, Spain). Thiazolyl Blue Tetrazolium Bromide 98% (MTT), Amoxicillin Trihydrate, Linolenic acid ≥99%, Tween®80, Dimethyl sulfoxide ≥99.9% (DMSO), Sodium chloride, Sodium acetate, HEPES hemisodium salt ≥99% and Sodium hydroxide were obtained from Sigma-Aldrich® (St. Louis, MO, USA). 1,2-di-(9Z-octadecenoyl)-*sn*-glycero-3-phosphoethanolamine (DOPE) was purchased from Avanti® Polar Lipids (Alabaster, AL, USA). Acetonitrile 99%, Chloroform and Acetic glacial acid were obtained from VWR International LLC (Radnor, PA, USA). SIF® Powder was obtained from Biorelevant.com (Whitechapel, London, United Kingdom). Hydrochloric acid (HCl) was purchased from Fisher Scientific International Inc (Pittsburgh, PA, USA). Dulbecco's Modified Eagle's Medium (DMEM), Roswell Park Memorial Institute (RPMI) medium, trypsin-EDTA (1x), Penicillin- Streptomycin (Pen Strep), Dulbecco's Phosphate Buffered Saline 10x pH 7.4 (PBS), Fetal Bovine Serum (FBS) were purchased from Gibco® by Life Technologies™ (Invitrogen Corporation, Paisley, UK). L929 cells (ATCC® CCL-1™) were purchased from ATCC® (Manassas, VA, USA). MKN28 cell line was a kind gift from Professor Dr. Bruno Sarmento, Instituto de Investigação e Inovação em Saúde (i3S). All components were used without further purification.

All the weighting measurements were performed using a Kern ABT-120-SDM digital analytical balance (Kern & Sohn; Balingen, Germany). The pH measurements were obtained using a Crison pH meter GLP22 with a Crison 52-02 tip (Crison; Barcelona, Spain). Milli-Q water was purified by an Ultra-pure water system (Milli-Q, Sartorius, Arium® Cartige 1 and 2, Sartorius Stedin Biotech; Göttingen, Germany) by a reverse osmosis process.

## 2.2 AMOXICILLIN STABILITY STUDIES

The study of AMX stability under different conditions, namely by changing light, temperature and sonication time, allowed to assess the optimal conditions to prepare and store AMX-loaded LNPs.

Briefly, a solution of AMX with a final concentration of 1.67 mg/mL was placed in the ultrasounds bath (Ultrasonic Cleaner, Soltec Soluzioni Technologiche Srl; Basaldella di Campoformido, UD, Italy) until the AMX was completely dissolved in Milli-Q water. Then, 42 mL of AMX solution were divided into 7 tubes, under different conditions, represented in the **Table**

**2.1**. For the samples exposed to high temperatures (conditions 3 to 5), a hot-bath (Medingen E5 Bath-Termostat, The Medingen Group LLC; Rochester, NY, USA) at 70ºC was used. In the conditions 4 to 7 the samples were exposed to sonication (VCX-130 Vibra-Cell™ with a CV-18 probe, Sonics & Materials Inc; Newtown, CT, USA) at 70% amplitude during a variable period of time. All samples were left in 7 different conditions during 40 minutes.

The absorbance of the diluted samples (1:100) was measured by UV-Vis spectroscopy using a V-660 spectrophotometer (Jasco Corporation, Software: Spectra Manager V.2, Jasco Corporation; Easton, MD, USA) from 200 to 500 nm.

**Table 2.1:** Scheme of the 7 different conditions of light, temperature and sonication tested for AMX stability assessment. RT, room temperature.

| | Light/Dark | Temperature | Sonication time ( at 70% amplitude) |
|---|---|---|---|
| Condition 1 | Light | RT | ✗ |
| Condition 2 | Dark | RT | ✗ |
| Condition 3 | Dark | 70ºC | ✗ |
| Condition 4 | Dark | 70ºC | 2.50 minutes |
| Condition 5 | Dark | 70ºC | 5 minutes |
| Condition 6 | Dark | RT | 2.50 minutes |
| Condition 7 | Dark | RT | 5 minutes |

## 2.3 SCREENING OF LIPIDS

An initial screening, using different lipids or combinations of lipids, was performed to evaluate the affinity of AMX to each one. For this screening, 9 different solid lipids were selected: Gelucire 43/01, Cetyl palmitate, Compritol 888 ATO, Precirol ATO 5, Softisan 100, Gelucire 44/14, Dynasan 116, Imwitor 900 K and Imwitor 491. These lipids were used to synthetize LNPs by the modified free organic-solvent emulsification/sonication method (described in detail in section 2.4.1). The affinity of LNPs to AMX was evaluated by their EE and LC (described in detail in the section 2.6). Additionally, the particle size, PDI and zeta potential were also determined (described in detail in the section 2.6).

## 2.4 LNPS PREPARATION

### 2.4.1 MODIFIED FREE ORGANIC-SOLVENT EMULSIFICATION/SONICATION METHOD

In the modified free organic-solvent emulsification/sonication method (**Figure 2.1**), the lipid phase containing the desired lipids or lipids combination and the stabilizer Tween®80 were melted in a hot bath at a temperature above their melting point (from 60ºC to 80ºC), in order to fuse the lipids. For the synthesis of AMX-loaded LNPs, a solution of AMX with a final

concentration of 1.67 mg/mL was prepared. The solution was placed in an ultrasounds bath until being completely dissolved in Milli-Q water. Then, the fused lipids were dispersed in 6 mL of pre-heated AMX solution (aqueous phase) at the same temperature. The emulsion was promoted by sonication for 5 minutes at 70% amplitude. After sonication, the nanoemulsion was cooled in ice for 30 seconds. The process of cooling is a crucial step in the synthesis of LNPs, since it allows the crystallization of the lipid and, therefore the formation of NPs [81]. Further, the cold formulations were stored in glass flasks at RT. Placebos were prepared in a similar manner without the addition of drug to the aqueous phase. The LNPs were protected from light during the whole process of synthesis and storage.

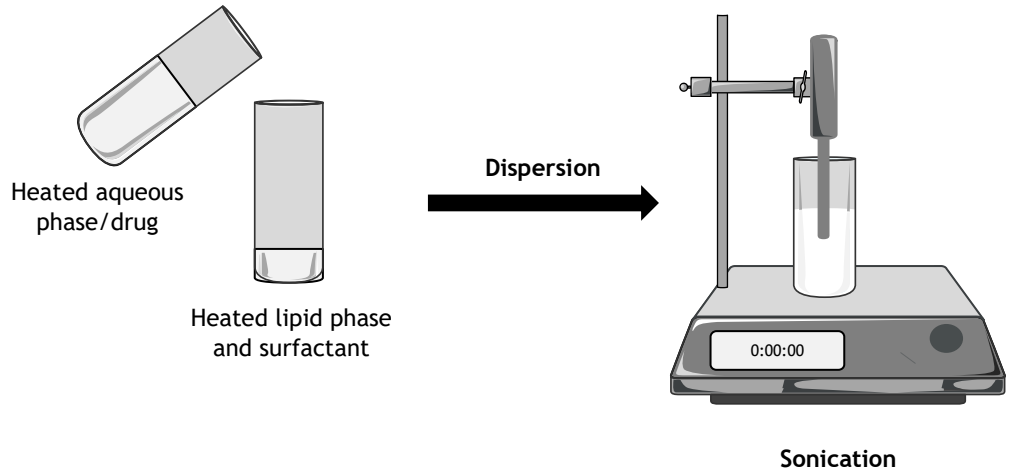


**Figure 2.1:** Scheme of the modified free organic-solvent emulsification/sonication method.

### 2.4.2 DOUBLE EMULSION METHOD

In the double emulsion method (**Figure 2.2**), the lipid phase containing the solid lipid was dissolved in 2 mL of chloroform. When the LNPs were also composed of linolenic acid, this fatty acid was dissolved in chloroform in combination with the solid lipid. Further, 0.5 mL of AMX solution was added to the lipid phase. The AMX solution was prepared by dissolving 19.90 mg of AMX in a small volume of NaOH 1M (around 3 drops) until is completely dissolved. Further, Milli-Q water was added to a final volume of 0.5 mL. In the case of placebos, the same volume of Milli-Q water was added to the lipid phase. The emulsion was promoted by sonication for 30 seconds at 70% amplitude. In the formulations containing DOPE as a surfactant, 20 mg of this lipid previously dissolved in chloroform were added. Then, 4 mL of Tween®80 solution were added to the emulsion. Once more, the emulsion was homogenized by sonication for 2 minutes at 70% amplitude. The nanoemulsion was transferred to a flask and 4 mL of Tween®80 solution (50mg/ 4 mL) were added. The flask was placed in a stirring plate at RT (IKA 2930701 RT 15 Power IKAMAG 15-Position Analog Magnetic Stirrer Hotplate 115V, IKA WORKS Inc; Staufen im Breisgau, Germany) with agitation during 2h30 to 3h to evaporate the chloroform. During the preparation and storage, the LNPs were protected from light.

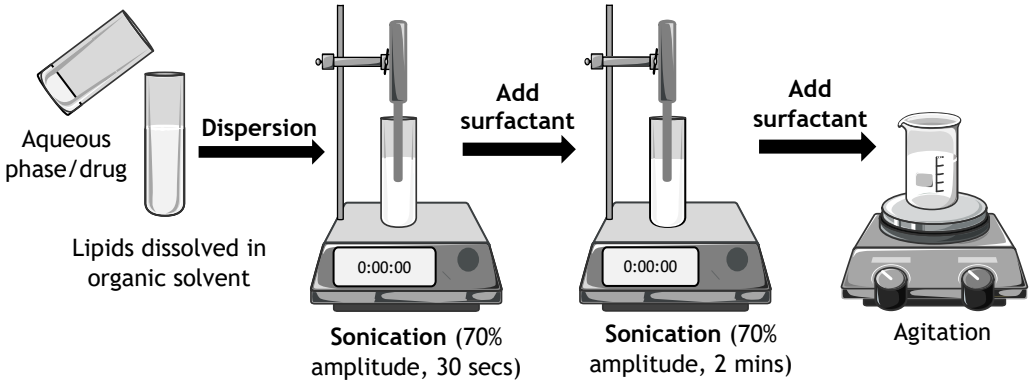


**Figure 2.2:** Scheme of the double emulsion method.

In preliminary experiments, several concentrations of Tween®80 solution and lipid and AMX quantities were tested in order to stablish the best conditions for LNPs preparation.

## 2.5 LYOPHILIZATION

Aqueous suspensions of NPs stored for long periods of time usually become instable due to the formation of aggregates, among other phenomena [82]. Therefore, in an attempt to improve the stability of these systems water is removed [82]. Freeze-drying, also known as lyophilization is a commonly used industrial process which consists on removing water from a frozen sample by sublimation and desorption under vacuum [82]. Before samples' freezing, usually a cryoprotectant is added to the formulations for protection of NPs against freezing and desiccation stresses [82].

LNPs were lyophilized using a programmable freeze-dryer (LyoQuest -85 laboratory freeze dryer, Telstar Group; Terrassa, Barcelona, Spain). Aerosil cryoprotectant was added to the SLNs suspensions before freezing at -80ºC in a GFL Upright Freezer 6481(GFL Gesellschaft für Labortechnik mbH; Burgwedel, Germany). The aerosil was screened at the following concentrations: 1% and 2% of total solid lipid mass for its cryoprotectant efficiency. The samples were lyophilized for 48h at -80ºC and pressure of 0.5 bar.

## 2.6 LNPS CHARACTERIZATION

### 2.6.1 PARTICLE SIZE MEASUREMENTS

Dynamic light scattering (DLS) is a common technique to determine particle size in colloidal suspensions [83]. The particles suspended in a liquid solvent undergo random movement (Brownian movement) due to interactions with the solvent molecules [83, 84]. During the particle size measurement by DLS technique, the NPs suspension is exposed to a light beam [85]. Due to the random motion of NPs, the direction and intensity of the incident light is changed in a process known as scattering [85]. Thus, from these variations the diffusion

coefficient of NPs can be measured [85]. Considering that NPs are spherical particles, the hydrodynamic diameter of the particles can be calculated from their diffusion coefficients [85].

The produced NPs were characterized by its mean hydrodynamic diameter and PDI in a Particle Size Analyser (Brookhaven Instruments Corporation; Software: Particle Sizing v.5 Brookhaven Instruments; Holtsville, NY, USA). The system was operating at a fixed light incidence angle of 90º, at 25ºC, with a dust cut-off set to 30 and the refractive index of the particles set to 1.59. Prior to measurements, NPs suspensions were diluted (1:100) in Milli-Q water. In the case of lyophilized NPs, the powder was ressuspended in Milli-Q water and filtered with a single use syringe filter (Ministart, pore size 0.8 µm, Satorius Stedin Biotech; Goettingen, Germany). For each sample, 6 runs, each one with ten cycles, were performed.

### 2.6.2 The Zeta Potential Measurements

When particles are in contact with an aqueous solution, a rearrangement of the local free ions in the solution occurs [86]. Thus, the electrical double layer is formed [86]. This double layer is composed by a compact layer and a diffuse layer [86]. In the compact layer, the ions of the solvent are immobile due to the strong electrostatic attraction to the particle surface [86]. On other hand, in the diffuse layer the ions are mobile, since they have a weaker attraction to the particle surface [86]. The zeta potential is defined as the electrostatic potential at the boundary between the dispersion medium and the stationary layer of fluid attached to the dispersed particle [87]. Electrophoretic light scattering (ELS) is a common technique to measure the zeta potential [88]. In this technique, two electrodes are inserted on the formulation [88]. An incident light causes an electrophoretic movement of the particles in the electric field created by the electrodes [88]. The velocity of the particles motion to the electrode of the opposite charge is measured by the deviation of the laser light scattering spectrum, which allows the calculation of the zeta potential [89].

Zeta potential is an important physical property of particles in suspension, being related with their stability and their surface morphology [88]. Therefore, the measurement of this potential can be useful to characterize the stability of NPs for an extended period.

The zeta potential of all samples was determined using a Zeta Potential Analyser (ZetaPALS, Brookhaven Instruments Corporation; Software: PALS Zeta Potential Analyser v.5 Brookhaven Instruments; Holtsville, NY, USA). The system was operating at 25ºC, with a fixed light incidence angle of 90º. The Smoluchowski mathematical model was used to perform the analysis. Prior to measurements, all samples were diluted (1:100) in Milli-Q water. In the case of lyophilized NPs, the powder was resssuspended in Milli-Q water and filtered with a single use syringe filter. For each sample, 6 runs, each one with 5 cycles, were performed.

### 2.6.3 Amoxicillin Encapsulation Efficiency

In the first step of the NPs optimization, namely in the screening of lipids and method of synthesis, the EE was determined by calculating the difference between the total amount of

AMX used to prepare the formulation and the amount of free AMX remaining in the aqueous phase [90]. Formulations were diluted (1:100) in Milli-Q water and transferred into Amicon® Ultra-4 Centrifugal Filter Devices, ultracel® - 50k (50000 NMWL) (MERK Milipore, Ltd; Cork, Ireland). Centrifugation was performed using an Allegra® X-15R centrifuge (Beckman Coulter; Pasadena, CA, USA) with a spin at 3900 rpm for 20 minutes or until complete separation between SLNs retained in the filter and the aqueous phase corresponding to the supernatant. The unentrapped AMX was present in the supernatant. The EE was calculated as follows:

$$EE\ (\%) = \frac{Total\ amoxicillin\ amount - Unentrapped\ amoxicillin}{Total\ amoxicillin\ amount} \times 100$$

For further studies, the EE of AMX was determined from the measurement of the amount of AMX encapsulated in the NPs. Formulations were diluted (1:50) in Milli-Q water and transferred into Amicon® Ultra-4 Centrifugal Filter Devices, ultracel® - 50k (50000 NMWL). Centrifugation was performed using the Allegra® X-15R centrifuge with a spin at 1500 rpm for 25 minutes or until complete separation between SLNs retained in the filter and the aqueous phase corresponding to the supernatant. The filter unit was centrifuged in an inverted position at 4500 rpm during 5 minutes to isolate the pellet were NPs with the encapsulated AMX were present. The pellet was then dissolved in 2 mL of acetonitrile and centrifuged at 4750 rpm until the lipids were deposited. The entrapped AMX was present in the solution of acetonitrile. The EE was calculated as follows:

$$EE\ (\%) = \frac{Entrapped\ amoxicillin\ amount}{Total\ amoxicillin\ amount} \times 100$$

Both the unentrapped and entrapped AMX were quantified by UV-Vis spectroscopy performing scans from 200 to 500 nm.

### 2.6.4 Amoxicillin Loading Capacity

LC is defined as the percentage of drug incorporated into the NPs relative to the total amount of lipid in the NPs [90]. The LC was calculated as follows:

$$LC\ (\%) = \frac{EE \times Total\ amoxicillin\ amount}{Total\ lipid\ amount} \times 100$$

### 2.6.5 Transmission Electron Microscopy

TEM was used to assess NPs size and morphology by acquisition of two-dimensional images of NPs. Using TEM technique, an electron beam is emitted from an electron gun and a condenser-lens system focus the beam onto the sample [91]. The electrons interact with the thin sample and part of it is transmitted [91]. Further, the transmitted electrons are focused by a lens system (objective, intermediate and projector lenses) into an image on a fluorescent screen [91].

For TEM analysis, lyophilized formulations were prepared using a 1:10 dilution while the NPs suspensions were prepared using a 1:4 dilution. Both dilutions were performed using Milli-Q water. Further, samples were prepared by placing 10 µl of solution on a copper-mesh grid and left to rest for 1 to 2 minutes at RT. After this period, the excess was removed with filter paper. For contrast, 10 µl of 0.75% uranyl acetate solution were placed on the grid and left to rest for 30 seconds at RT. After this period, the excess was removed with filter paper. The samples were observed in a JEM-1400 Transmission Electron Microscope (JEOL Ltd., Tokyo, Japan) with an acceleration voltage of 80 kV.

### 2.6.6 Differential Scanning Calorimetry Analysis

Structural alterations of materials are accompanied by heat exchanges, as capture of heat during melting or emission of heat during crystallization. Differential scanning calorimetry (DSC) is designed to measure these heat exchanges during temperature scans and allows to draw conclusions on the structural properties of a sample. DSC is commonly used to evaluate the lipid phases in the nanoparticle composition and the modifications that the addition of components may provoke on the lipid structure.

Prior to DSC analysis, the components of each formulation (F1, F2, F3, F4, P1, P2, P3, P4) were mixed in the same proportions of the correspondent LNPs (**Table 2.2**).

**Table 2.2:** Mixtures compositions studied by DSC technique.

| | Cetyl palmitate (mg) | Tween®80 (mg) | Linolenic acid (mg) | DOPE (mg) | AMX (mg) |
|---|---|---|---|---|---|
| **Bulk solid lipid (L)** | 20 | - | - | - | - |
| **Mixture F1** | 54.4 | 39.6 | - | - | 6.1 |
| **Mixture P1** | 57.9 | 42.1 | - | - | - |
| **Mixture F2** | 54.4 | 38.1 | 1.5 | - | 6.1 |
| **Mixture P2** | 57.9 | 40.5 | 1.6 | - | - |
| **Mixture F3** | 54.4 | 33.5 | - | 6.1 | 6.1 |
| **Mixture P3** | 57.9 | 35.7 | - | 6.5 | - |
| **Mixture F4** | 54.4 | 32.0 | 1.5 | 6.1 | 6.1 |
| **Mixture P4** | 57.9 | 34.0 | 1.6 | 6.5 | - |

The degree of lipid crystallinity and the lipid polymorphism of lyophilized SLNs were analysed by DSC. This technique was performed using a DSC 200 F3 Maia® (NETZSCH, Selb, Germany) equipped with an automatic sample changer. The samples were weighted directly in aluminium pans and an empty pan was used as reference. Further, the samples were scanned between 10ºC and 80ºC at a heating rate of 5ºC/min and a cooling rate of 40ºC/min, under a dynamic atmosphere of nitrogen. This characterization method was performed on the lyophilized SLNs as well as on the bulk materials used in the preparation of the SLNs. The results were obtained using *Proteus*® 5.2.1 software (NETZSCH, Selb, Germany). Lyophilized unloaded and AMX-loaded SLNs were analysed in triplicate, while bulk mixtures and solid lipid were analysed in duplicate. The degree of crystallinity or recrystallization index (RI) give an estimation of the amount of recrystallized solid and is calculated by the following equation [42]:

$$RI = \frac{\Delta \mathrm{H\ SLN}\ (\mathrm{J}/g)}{\Delta \mathrm{H\ bulk\ material}\ (\mathrm{J}/g)\ \times fraction\ of\ lipid\ phase} \times 100$$

where ΔH SLN is the melting enthalpy of the LNPs, ΔH bulk material is the melting enthalpy of the bulk material and the fraction of lipid phase relatively the whole sample.

## 2.7 EXPERIMENTAL DESIGN AND OPTIMIZATION OF FORMULATIONS

The BBD was used to optimize and evaluate the effect of different processing variables on the SLNs characteristics [50].

In this study a 15-run, 3-factor, 3-level BBD was applied, were lipid mass ($X_1$), concentration of Tween®80 in the first phase ($X_2$) and AMX mass ($X_3$) were considered as independent variables. These variables were studied at three different levels as low (-1), medium (0) and high (1) stablished from preliminary experimentation. The coded and actual values of the variables are given in **Table 2.3**.

**Table 2.3:** Independent variables and their levels in the BBD.

| | Studied levels | | |
|---|---|---|---|
| | Low (-1) | Medium (0) | High (1) |
| Independent variables | | | |
| $X_1$: Lipid mass (mg) | 150 | 200 | 250 |
| $X_2$: Tween®80 concentration in the first phase (mg/4 mL) | 15 | 35 | 55 |
| $X_3$: AMX mass (mg) | 10 | 20 | 30 |

The experimental runs were generated and further evaluated using STATISTICA Software (v12, StatSoft Inc; Tulsa, OK, USA). The generated design matrix by the software is represented in **Table 2.4**.

**Table 2.4:** Formulations studied by the BBD.

| | Lipid (mg) | Tween®80 in the 1st phase (mg/4 mL) | AMX (mg) |
|---|---|---|---|
| **1** | 150 | 15 | 20 |
| **2** | 250 | 15 | 20 |
| **3** | 150 | 55 | 20 |
| **4** | 250 | 55 | 20 |
| **5** | 150 | 35 | 10 |
| **6** | 250 | 35 | 10 |
| **7** | 150 | 35 | 30 |
| **8** | 250 | 35 | 30 |
| **9** | 200 | 15 | 10 |
| **10** | 200 | 55 | 10 |
| **11** | 200 | 15 | 30 |
| **12** | 200 | 55 | 30 |
| **13** | 200 | 35 | 20 |
| **14** | 200 | 35 | 20 |
| **15** | 200 | 35 | 20 |

The formulations represented in **Table 2.4** were characterized by their particle size, PDI and LC. Additionally, the zeta potential was also measured, however it was not considered in the BBD design. Therefore, particle size ($Y_1$), PDI ($Y_2$) and LC ($Y_3$) were defined as dependent variables. The values of particle size, PDI and LC obtained for each formulation were inserted into the software. Then, the best model among the linear, two-factor interaction and quadratic models was chosen, due to the best correlation between the expected and the observed values. Each model is associated to an equation and, as an example, the non-linear quadratic model equation is as follows [52]:

$$Y = A_0 + A_1 X_1 + A_2 X_2 + A_3 X_3 + A_4 X_1 X_2 + A_5 X_2 X_3 + A_6 X_1 X_3 + A_7 X_1^2 + A_8 X_2^2 + A_9 X_3^2$$

where, Y is the measured response of the dependent variables associated with each factor-level combination; $A_0$ is an intercept; $A_1$ to $A_3$ are the linear coefficients; $A_4$ to $A_6$ are the interaction coefficients; $A_7$ to $A_9$ are the squared coefficients; and $X_1$, $X_2$, $X_3$ are the coded levels of independent variables [49, 52]. The terms $X_1 X_2$, $X_2 X_3$ and $X_1 X_3$ represent the linear interaction terms, while $X_i^2$ represents the quadratic term. To evaluate the fitness of the model, the predicted $R^2$ was evaluated. Three-dimension surface plots were used to evaluate the relationship between the independent and dependent variables.

Further, the optimal values for each dependent variable were selected and submitted in the software (**Table 2.5**). The desirability function was used to obtain points regarding the constraints in which $Y_1$ and $Y_2$ were at their minimum levels, while $Y_3$ was at its maximum level [49]. According to what was desirable for the dependent variables, the software suggests an

optimal formulation and the expected values of particle size, PDI and LC. This formulation was used for further studies.

**Table 2.5:** Dependent variables and their desirability levels in the BBD.

| Dependent variables | Desirability | | |
|---|---|---|---|
| | High | Medium | Low |
| $Y_1$: Particle Size (nm) | 70 | 150 | 250 |
| $Y_2$: PDI | 0 | 0.1 | 0.2 |
| $Y_3$: LC (%) | 20 | 4 | 0 |

## 2.8 STABILITY STUDIES

To evaluate the physical stability of the prepared SLNs, measurements of particles size, PDI, zeta potential and LC were performed at 0, 1, 2, 4 and 8 weeks after the synthesis of the SLNs. The lyophilized SLNs were stored at RT, while the SLNs suspensions were kept at 4ºC. The ressuspended lyophilized SLNs were prepared by weighting 50 mg of powder and ressuspend it in 10 mL of Milli-Q water to a final concentration of 5 mg/mL. Then, the ressuspended SLNs were stored at 4ºC and RT. All formulations were protected from light during the synthesis and the storage.

## 2.9 *IN VITRO* AMOXICILLIN RELEASE STUDY

*In vitro* release studies were assessed by dialysis diffusion technique. A cellulose dialysis bag (Float-A-Lyzer®G2 Dialysis Device, 3.5 – 5 kD MWCO, SpectrumLabs; Rancho Dominguez, CA, USA) was filled with 1.0 mL of sample for the screening methods and 1.5 mL for further *in vitro* release studies with lyophilized SLNs and SLNs suspensions. In lyophilized SLNs, the samples were prepared by resuspension of 82.2 mg of formulation into 1.5 mL of Milli-Q water.

As previously mentioned, the stomach has an acidic pH (1 to 2), while the region between the mucus layer and the epithelial cells has a pH near to neutral (4 to 6) [22, 70]. Thus, the interest of this study was focused in simulate the pH gradient verified in the gastrointestinal tract in order to mimic AMX release after oral administration. To this end, the samples were incubated for 3h in 75 mL of simulated gastric fluid (HCl/NaCl solution, pH 1.2 prepared according to the European Pharmacopoeia 8.0) for the methods screening study. For further studies, the medium complexity was increased by using the fasted state simulated gastric fluid (FaSSGF: NaCl/HCl solution, pH 1.6 with SIF®Powder), which contains bile salts and lecithins. After, the samples were placed for 1h in 75 mL of acetate buffer solution (a buffer solution containing sodium acetate and acetic acid glacial, pH 5, as described in [92]). The acetate

buffer was used to simulate the gastric mucosa environment. After this period, samples were placed in 75 mL of HEPES buffer solution (a buffer solution containing HEPES hemisodium salt and NaCl, pH 7.4, as described in [92]) until the end of the study in order to mimic the physiological conditions. At regular intervals, aliquots were collected for a UV-Vis microplate (Corning® 96-well UV Microplates, Corning Inc.; Corning, NY, USA) and replaced with the same volume of fresh medium. Throughout the *in vitro* release study, all samples were incubated at 37ºC under gentile stirring and protected from light. The AMX release was quantified by UV-Vis spectroscopy using a microplate reader (BioTek Instruments Inc., Synergy HT, Software: Gen5 v1.08.4, BioTek Instruments Inc.; Winooski, VT, USA) at 277 nm. The cumulative percentage of released AMX was determined calculating the average of the triplicate samples, indicating the standard deviation (SD).

## 2.10 *IN VITRO* CELL VIABILITY STUDIES

The effect of the prepared SLNs on cell viability was evaluated using the MTT assay. The assay was performed for both L929 and MKN28 cells in duplicate. These cell lines were previously cultured at 37ºC in a 5% $CO_2$ athmosphere (Unitherm CO2 Incubator 3503 Uniequip; Planegg, Germany). L929 was cultured in DMEM supplied with 10% FBS and 1% Pen Strep. On the other hand, MKN28 cells were cultured in RPMI culture medium supplied with 10% FBS and 1% Pen Strep. Firstly, L929 cells at 80 to 90% of confluence were detached from the culture flask by physical detachment using a cell scraper (Nunc™ Cell Scrapers, Thermofisher Scientific; Waltham, MA USA). In the case of MKN28 cell line, at 80 to 90% of confluence the cells were detached by chemical detachment using 0.25% trypsin-EDTA. Further, both cell lines were centrifuged using the Heraeus Multifuge X1R centrifuge (Thermo Fisher Scientific; Waltham, MA, USA) at 300 g and re-suspended in fresh medium. Viable cells were counted using a Neubauer chamber (Improved Neubaur Bright-line, Boeco; Hamburg, Germany).

The collected cells were seeded in 96-well tissue culture test microplates (Tissue Culture OrPlates, surface treated flat bottom, Orange Scientific; Braine-l' Alleud, Belgium) at a density of $10^5$ cells/well. The L929 cells were supplemented with 100 µl of DMEM medium while the MKN28 cells were supplemented with the same volume of RPMI medium. All cells were incubated at 37ºC in a 5% $CO_2$ atmosphere until the cells presented 80 to 90% of confluence when observed using the Motic® AE2000 Binocular Inverted Microscope (Motic Electric Group Co., Ltd; Xiamen, Fujian, China). Then, the culture medium was discarded and 100 µl of SLNs formulations with different concentrations (0.5 mg/mL, 1.0 mg/mL and 2.0 mg/mL) were added to the cells. A positive control (culture medium) was included to normalize and compare the results. The cells were incubated for 24h (L929 cells) or 4h (MKN28 cells) at 37ºC in a 5% $CO_2$ atmosphere. After incubation time, the medium was discarded and 100 µl of MTT solution (5 mg/mL MTT in PBS stock solution diluted to a final concentration of 0.5 mg/mL in culture medium) was added to each cell seeded well and incubated for 2h (L929 cells) or 3h (MKN28 cells) at 37ºC in a 5% $CO_2$ atmosphere, to allow the formation of formazan crystals. Then, the

medium was rejected and 100 µl of DMSO were added to the wells, in order to dissolve the formazan crystals. The absorbance was measured at 590 and 630 nm using a microplate reader. The latter was used for background subtraction. Cell viability was determined according as follows:

$$Cell\ viability\ (\%) = \frac{Experimental\ absorbance}{Mean\ of\ absorbance\ of\ the\ positive\ control} \times 100$$

## 2.11 STATISTICAL ANALYSIS

Statistical analysis was performed using GraphPad Prism Software (v5.03 for Windows; GraphPad Software Inc, San Diego, CA, USA). The measurements were repeated at least 3 times and data expressed as mean ± SD. Data was analysed using two-way analysis of variance (ANOVA). A *P* value of <0.05 was considered statistically significant.

# Chapter 3 - Results and discussion

## 3.1 AMOXICILLIN STABILITY STUDIES

An initial study was performed to evaluate which are the main parameters that influence AMX stability during the LNPs preparation and their storage. With that purpose, an AMX solution (1.67 mg/mL) was exposed to different light, temperature and sonication conditions. Changes in the AMX UV-Vis absorbance spectrum were evaluated, since previous studies performed by Gozlan et al. (2013) observed that AMX degradation products increased or decreased the absorbance when compared with the non-degraded AMX spectrum [93].

Firstly, the influence of light was evaluated by placing AMX at RT protected and unprotected from light. In the sample exposed to light, a decrease in absorbance was observed (**Figure 3.1**), which is a consequence of AMX degradation. Due to the influence of light in AMX stability, the remaining conditions were performed protecting AMX from light. Further, the effect of temperature was also evaluated by placing AMX into a hot bath at 70ºC. A slight increase in the AMX absorbance (70ºC Dark) was detected when compared to the sample at RT (RT Dark). Hence, the temperature apparently influences the AMX stability to a lesser extent than light condition. Sonication is a required process to obtain nanoemulsions during the preparation of LNPs. The effect of the sonication time on AMX stability was also investigated. For that purpose, AMX at RT and 70ºC were exposed to 2.50 and 5 minutes of sonication at 70% of amplitude. **Figure 3.1** shows that the sample exposed to 70ºC and sonication during 5 minutes had the highest absorbance. On the other hand, sonication time apparently does not have an evident influence on the samples at RT.

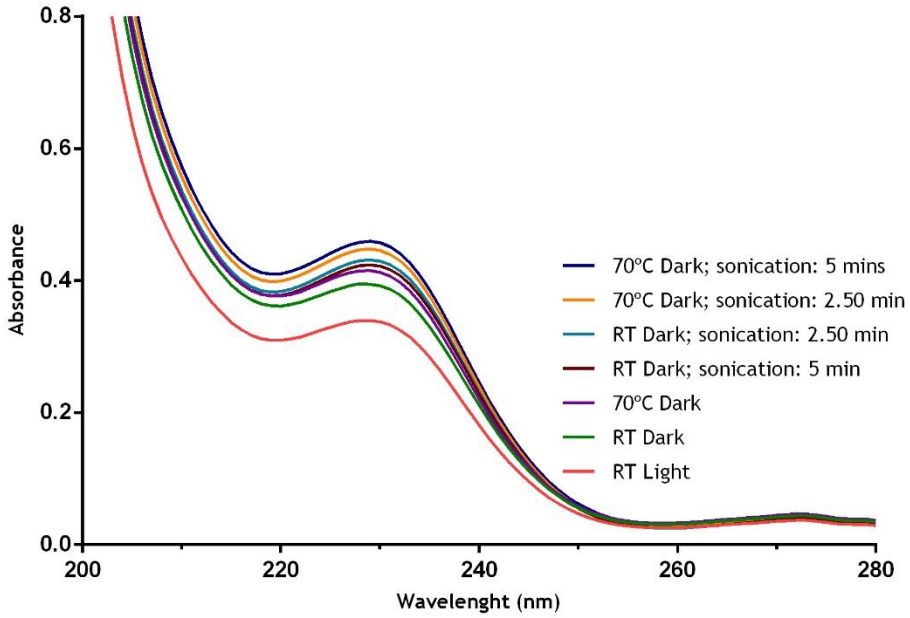


**Figure 3.1:** UV-Vis analysis of different conditions, viz. light (light/dark), temperature (RT/70°C) and sonication (2.50/5 minutes), to perform AMX stability studies. RT, Room temperature.

In the current work two methods were used to prepare LNPs: the modified free organic-solvent emulsification/sonication method and the double emulsion technique. In the first method, high temperatures are used to fuse the lipids above their melting point. On the other hand, the double emulsion technique does not require high temperatures, being usually performed at RT. The absence of high temperatures is an advantage of double emulsion, since using AMX is less susceptible to degradation at RT than at 70°C. The sonication time does not seem to influence the AMX stability. Nevertheless, sonication at high temperatures affects the AMX stability in a higher extent than sonication at RT.

## 3.2 LIPID SCREENING

Drug delivery systems such as NPs should have a high drug LC, thereby reducing the quantity of matrix materials for administration [94]. In LNPs, EE and LC are widely dependent on the drug solubility in the lipid matrix [94]. Besides, the drug release profile of the LNPs is also associated to drug solubility in the lipids [94]. Therefore, the design of LNPs should consider the affinity of the drug to the lipid phase of the NPs.

In this study, an initial lipid screening was performed using 9 different solid lipids (Gelucire 43/01, Cetyl palmitate, Compritol 888 ATO, Precirol ATO 5, Softisan 100, Gelucire 44/14, Dynasan 116, Imwitor 900 k, Imwitor 491) to prepare LNPs using the modified free organic-solvent emulsification/sonication method. Further, to evaluate the affinity of AMX to each one of the selected lipids, the LNPs were characterized by their EE and LC. Additionally, the particle size, PDI and zeta potential were also determined. The results obtained with the three most promising lipids are presented in **Table 3.1**.

**Table 3.1:** Composition and characterization of the NPs composed of the three most promising lipids (Gelucire 43/01, Cetyl palmitate, Compritol 888 ATO).

| Composition | Mass (mg) | Melting Point (°C) | Size (nm) | PDI | Zeta Potential (mV) | EE (%) | LC (%) |
|---|---|---|---|---|---|---|---|
| Gelucire 43/01 | 250 | 43 | 247 | 0.195 | -34 | 50 | 2.1 |
| Tween®80 | 50 | | | | | | |
| AMX | 10 | | | | | | |
| Cetyl palmitate | 250 | 54 | 210 | 0.148 | -38 | 51 | 2.1 |
| Tween®80 | 50 | | | | | | |
| AMX | 10 | | | | | | |
| Compritol 888 ATO | 150 | 70 | 444 | 0.169 | -24 | 34 | 1.4 |
| Tween®80 | 50 | | | | | | |
| AMX | 10 | | | | | | |

The three formulations prepared using Gelucire 43/01, Cetyl palmitate and Compritol 888 ATO appeared white and milky, with low viscosity. SLNs composed of Gelucire 43/01 presented high EE, however this waxy solid has a low melting point of 43ºC (**Table 3.1**). Since the human body temperature is around 37ºC, these SLNs could become more fluid when administered to humans and release their content before their arrival to the target organ or tissue. Particle size is also a crucial characteristic of NPs that must be considered in the design of these delivery systems, since it determines the *in vivo* distribution, biological fate, toxicity and targeting ability of NPs [94]. Moreover, particle size can influence LC, drug release and the stability of NPs during storage time [94]. **Table 3.1** shows that SLNs composed of Compritol 888 ATO had a size of 444 ± 2 nm. According to Lopes and her co-workers (2014), some authors defend that NPs with more than 200 nm have a decreased diffusion into the gastric mucosa [70]. Furthermore, Hasani *et al*. (2009) observed that NPs with smaller sizes (50 and 200 nm) showed higher mucoadhesion than particles of 750 nm in the inflamed tissue of gastric ulcers [95]. Hence, Compritol 888 ATO NPs were excluded due to their size. Cetyl palmitate was selected the most promising solid lipid, taking into account the suitable melting point for oral administration, the high EE and the lower zeta potential, which represents a higher stability.

The low LC verified for the three formulations suggests a low affinity of AMX to the solid lipids. This result was expected, since AMX is considered a low permeability drug according to Biopharmaceutics Classification System, with low affinity to lipid phases [77, 78]. In order to select the most suitable preparation technique to improve LC in the NPs composed of cetyl palmitate, a methods screening was performed.

## 3.3 METHODS SCREENING

SLNs were prepared by two different methods: modified free organic-solvent emulsification/sonication and double emulsion. The AMX-loaded SLNs and their corresponding placebos obtained by both methods were characterized by their particle size, PDI, EE and LC. Zeta potential was not evaluated since the particles prepared by both methods showed to be stable.

The size and PDI of the formulations obtained from the modified/emulsification and double emulsion methods were studied for one week (**Figures 3.2** and **3.3**). The formulations prepared by both methods were stable during one week, with no significant differences ($P$>0.05) over time in both particle size and PDI. Besides, the placebos were compared with the AMX-loaded SLNs synthesized using the same method. For the modified emulsification/sonication method no significant differences ($P$>0.05) were observed when comparing the placebo with AMX-loaded SLNs both at 0 and 1 week. On other hand, significant differences ($P$<0.05) were observed between placebo and AMX-loaded SLNs synthetized by the double emulsion technique in both weeks. This phenomenon suggests that AMX stabilized the NPs, since both the size and PDI were decreased comparing to the placebo formulations.

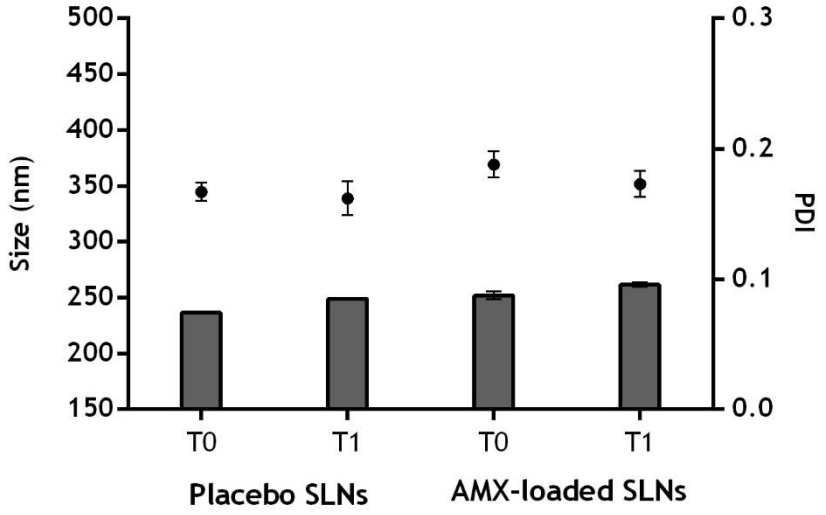


**Figure 3.2:** Physical stability of the formulations obtained by modified emulsification/sonication method over time (0 (T0) and 1 (T1) weeks). Bars represent the size (left Y axis) and the dots the PDI (right Y axis). Values represent mean ± SD. No significant differences in size and PDI were observed over time and between placebo and AMX-loaded SLNs formulations ($P$>0.05).

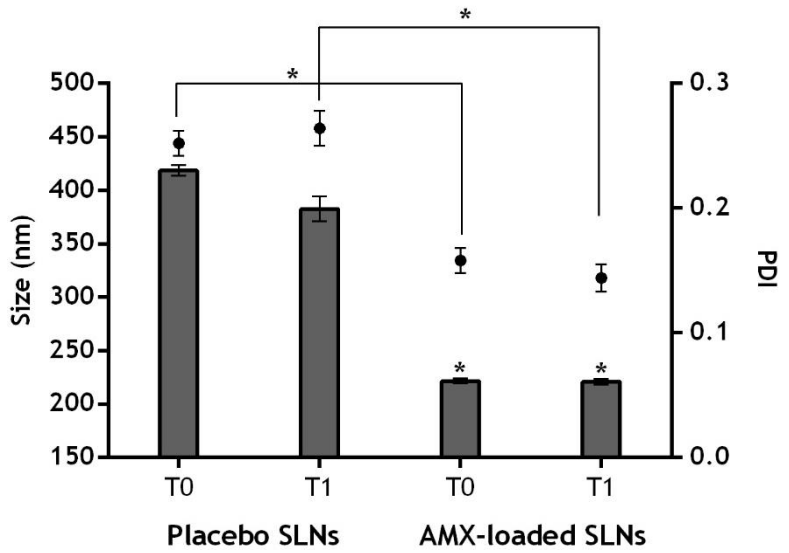


**Figure 3.3:** Physical stability of the formulations obtained by double emulsion method over time (0 (T0) and 1 (T1) weeks). Bars represent the size (left Y axis) and the dots the PDI (right Y axis). Values represent mean ± SD. *P<0.05 relatively to the Placebo SLNs. No significant differences in size and PDI were observed over the time for any of the formulations (P>0.05).

The EE and the LC determined for the AMX-loaded SLNs prepared using both methods are represented in the **Figure 3.4** It is possible to observe that both formulations showed similar EE. Regarding to the LC, the formulation synthetized by the double emulsion method showed the highest value due to the use of a lower lipid quantity and the formation of aqueous compartments where AMX is encapsulated. Nonetheless, the differences in EE and LC between the two formulations are not statistically significant (*P*>0.05).

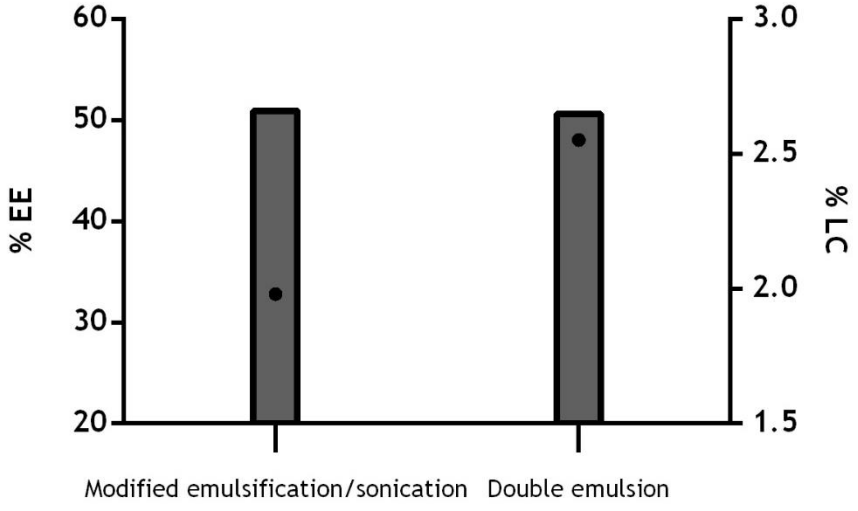


**Figure 3.4:** EE and LC of the formulations obtained by the modified emulsification/sonication and the double emulsion methods. Bars represent the EE (left Y axis) and the dots the LC (right Y axis). No significant differences were observed between the two formulations (*P*>0.05).

The profile of drug release is influenced by the method of drug encapsulation [94]. Thus, an *in vitro* AMX release study simulating the oral administration of AMX-loaded SLNs at body

temperature (37ºC) was performed in an attempt to predict the *in vivo* kinetics [81]. In **Figure 3.5**, an initial burst release is verified, mainly due to adsorbed or weakly bounded AMX onto the NPs surface [94]. Following, a sustained release profile is observed in both methods. However, the formulation prepared using the double emulsion technique showed a higher release percentage at the mucus layer pH, near to where the bacterium *H. pylori* is located [22, 70]. Hence, NPs prepared by the double emulsion technique have a high potential as vehicles for AMX controlled release to the target bacteria.

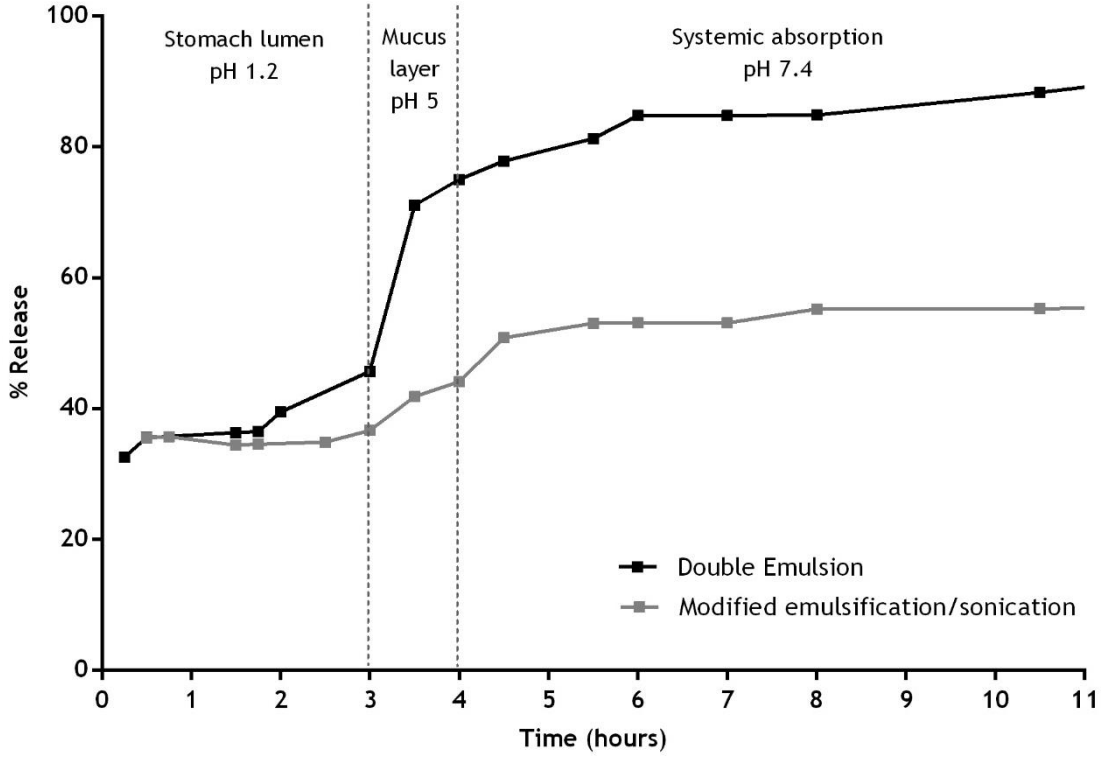


**Figure 3.5:** *In vitro* AMX release in three simulated conditions to mimic oral administration at 37°C: stomach lumen (pH 1.2), mucus layer (pH 5) and physiological medium (pH 7.4). Vertical lines represent media changes.

Due to highest LC and the suitable release profile of AMX-loaded SLNs obtained by the double emulsion technique, this method was selected for further studies.

## 3.4 Experimental Design and Optimization of Formulations

After the initial lipid and method screening, an experimental design was applied to optimize the composition of the SLNs prepared by the double emulsion method. The aim of the optimization process consists in the determination of the most suitable concentration of Tween®80 solution and quantities of cetyl palmitate and AMX for the preparation of SLNs. In the previous experiments, the SLNs were composed of the solid lipid and Tween®80. For the

experimental design, all formulations were prepared using the components of the ideal formulation (cetyl palmitate, Tween®80, DOPE, linolenic acid and AMX).

Preliminary experiments were performed by changing Tween®80 concentration in the first phase. From these experiments, it was verified that the increase of the Tween®80 percentage relatively to the solid lipid mass lead to non-homogeneous formulations, with higher particle sizes and PDI (**Table 3.2**). Therefore, for the BBD the concentration of Tween®80 was limited to a range of 15-55 mg/4 mL in the first phase of the double emulsion technique, being fixed at 50 mg/4 mL in the second phase.

**Table 3.2:** Composition and characterization of the formulations analysed in preliminary experiments. The NPs were characterized by their particle size, PDI and zeta potential. FP1, formulation 1; FP2, formulation 2; FP3, formulation 3; FP4, formulation 4; FP5, formulation 5.

| | **FP1** | **FP2** | **FP3** | **FP4** | **FP5** |
|---|---|---|---|---|---|
| Cetyl palmitate (mg) | 150 | 200 | 250 | 250 | 250 |
| Tween®80 (mg) | 175 | 125 | 100 | 75 | 65 |
| Linolenic acid (mg) | 5 | 5 | 5 | 5 | 5 |
| DOPE (mg) | 20 | 20 | 20 | 20 | 20 |
| AMX (mg) | 20 | 0 | 20 | 20 | 20 |
| **Size (nm)** | 572 | 482 | 213 | 199 | 195 |
| **PDI** | 0.364 | 0.328 | 0.149 | 0.1 | 0.118 |
| **Zeta Potential (mV)** | -64 | -26 | -60 | -49 | -47 |

From the preliminary experiments, the solid lipid mass (150-250 mg), Tween®80 concentration (15–55 mg/4 mL) in the first phase of the double emulsion technique and AMX mass (10–30 mg) were selected as critical parameters for LNPs preparation. Thus, these parameters were defined as independent formulation variables for the 3-factor, 3-level BBD. Moreover, the levels low, medium and high were defined according to results obtained in the preliminary experiments. The BBD consisted in 15 experimental runs, from which 15 formulations were prepared and characterized (**Table 3.3**). The formulation variables were studied as a function of particle size, PDI and LC. As previously mentioned, particle size is an important parameter for gastric diffusion [70]. Regarding to PDI, this parameter was selected as a dependent variable due to the importance of having a monodisperse population, which leads to a higher particles stability. EE was not considered for the experimental optimization design. Instead, LC was selected since this parameter represents the exact percentage of AMX entrapped in the NPs. Besides, LC calculation already considers the EE of the formulations. Zeta potential was also discarded as a possible dependent variable in the BBD analysis, since all the formulations were stable, with zeta potential values ranging between -40 mV and -55 mV (data not shown).

**Table 3.3:** Formulations studied by the BBD and the corresponding particle size ($Y_1$), PDI ($Y_2$) and LC ($Y_3$).

| | Lipid (mg) | Tween®80 in the 1st phase (mg/4 mL) | AMX (mg) | Particle Size ± SD (nm) | PDI ± SD | LC (%) |
|---|---|---|---|---|---|---|
| **1** | 150 | 15 | 20 | 195 ± 2 | 0.09 ± 0.03 | 3.48 |
| **2** | 250 | 15 | 20 | 203 ± 3 | 0.15 ± 0.03 | 4.48 |
| **3** | 150 | 55 | 20 | 213.5 ± 0.9 | 0.096 ± 0.005 | 9.31 |
| **4** | 250 | 55 | 20 | 273 ± 4 | 0.14 ± 0.02 | 5.89 |
| **5** | 150 | 35 | 10 | 178 ± 2 | 0.11 ± 0.02 | 1.82 |
| **6** | 250 | 35 | 10 | 183 ± 2 | 0.11 ± 0.02 | 3.54 |
| **7** | 150 | 35 | 30 | 239 ± 2 | 0.15 ± 0.01 | 5.30 |
| **8** | 250 | 35 | 30 | 198 ± 2 | 0.14 ± 0.02 | 5.18 |
| **9** | 200 | 15 | 10 | 199 ± 2 | 0.146 ± 0.009 | 3.08 |
| **10** | 200 | 55 | 10 | 193 ± 2 | 0.12 ± 0.02 | 5.31 |
| **11** | 200 | 15 | 30 | 266 ± 3 | 0.136 ± 0.008 | 6.74 |
| **12** | 200 | 55 | 30 | 173 ± 3 | 0.1 ± 0.02 | 6.08 |
| **13** | 200 | 35 | 20 | 188.3 ± 0.7 | 0.11 ± 0.02 | 5.15 |
| **14** | 200 | 35 | 20 | 192 ± 3 | 0.134 ± 0.009 | 5.18 |
| **15** | 200 | 35 | 20 | 197 ± 2 | 0.11 ± 0.03 | 4.40 |

A quadratic model was used to fit the values of all dependent variables obtained from the characterization of the 15 formulations prepared in this experimental design. The plots of the observed vs. predicted values for the particle size, PDI and LC and the corresponding $R^2$ are represented in **Figures 3.6**, **3.7** and **3.8**, respectively. These figures show that the quadratic model is the most suitable model to analyse the dependent variables in study, which is confirmed by the high $R^2$.

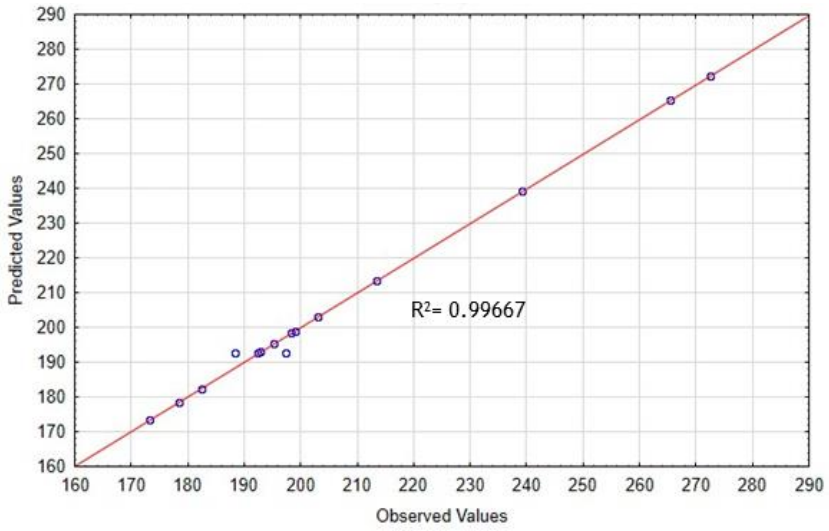


**Figure 3.6:** Observed vs. predicted values plot obtained for particle size using the quadratic model ($R^2$=0.99667). Predicted values and observed values are represented in nm.

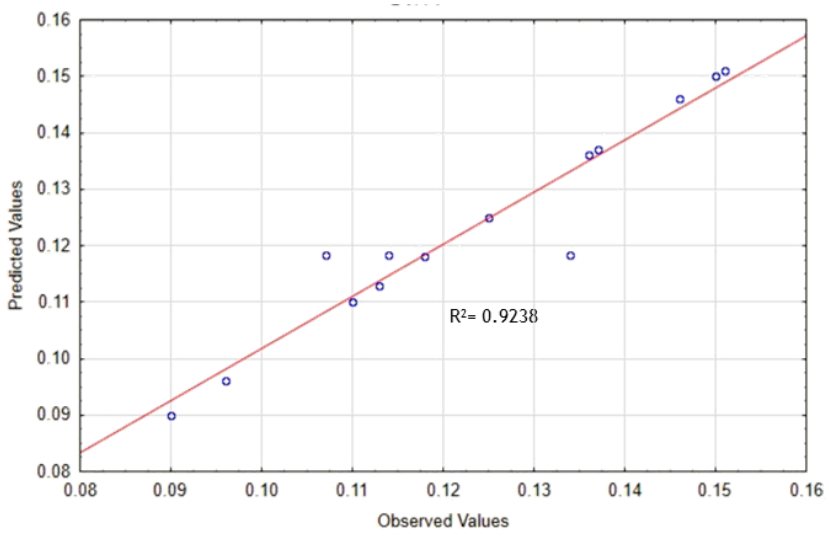


**Figure 3.7:** Observed vs. predicted values plot obtained for PDI using the quadratic model ($R^2$=0.9238).

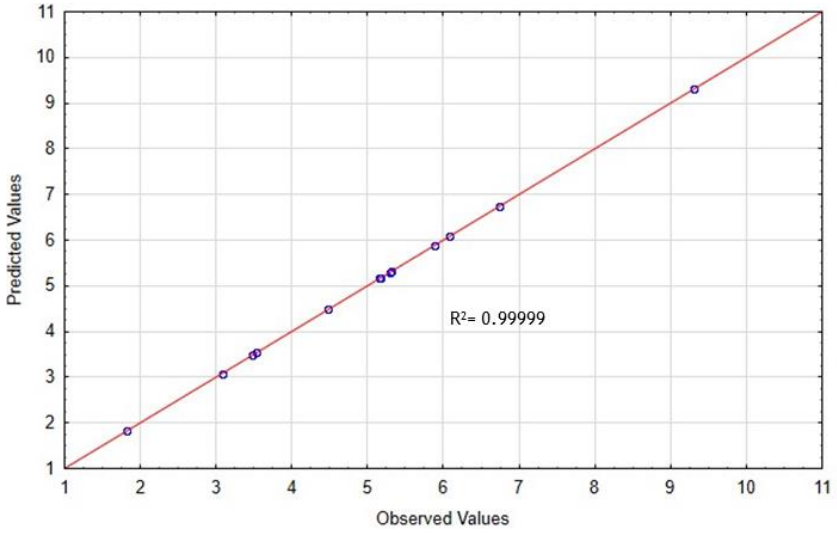


**Figure 3.8:** Observed vs. predicted values plot obtained for LC using the quadratic model ($R^2$=0.99999). Predicted values and observed values are represented in percentage.

From the BBD analysis, it was possible to obtain the interaction coefficients and corresponding *P*-values for the particle size, PDI and LC (**Table 3.4**). The synergistic and antagonistic effects are represented by positive and negative signs, respectively [96].

**Table 3.4:** Regression analysis for particle size ($Y_1$), PDI ($Y_2$) and LC ($Y_3$). CE, interaction coefficients; Int, Intercept; L, linear; Q, Quadratic. Highlighted values represent statistically significant *P*-values associated to the corresponding interaction coefficients (*P*<0.05).

| | Particle Size | | PDI | | LC | |
|---|---|---|---|---|---|---|
| | **CE** | ***P*-value** | **CE** | ***P*-value** | **CE** | ***P*-value** |
| **Int** | 209.4667 | 0.000040 | 0.125750 | 0.001033 | 5.01750 | 0.000001 |
| **1 - lipid mass (L)** | 8.0667 | 0.041649 | 0.015917 | 0.092883 | -0.27000 | 0.000444 |
| **Lipid mass (Q)** | -5.1083 | 0.049967 | 0.000896 | 0.828826 | 0.17979 | 0.000488 |
| **2 - T80 1st phase concentration (L)** | 6.4167 | 0.063558 | -0.004417 | 0.486725 | 1.33750 | 0.000018 |
| **T80 1st phase concentration (Q)** | -9.1083 | 0.016558 | -0.000854 | 0.836570 | -0.49146 | 0.000065 |
| **3 - AMX mass (L)** | 16.7167 | 0.010182 | 0.010583 | 0.179917 | 1.22250 | 0.000022 |
| **3 - AMX mass (Q)** | 1.6167 | 0.306269 | -0.005604 | 0.264096 | 0.42354 | 0.000088 |
| **1(L) by 2 (L)** | 12.8000 | 0.030308 | -0.004750 | 0.567698 | -1.10500 | 0.000048 |
| **1(L) by 2 (Q)** | -12.9500 | 0.015155 | -0.014000 | 0.105725 | 0.50250 | 0.000115 |
| **1(Q) by 2 (L)** | -23.2250 | 0.004786 | -0.004000 | 0.504179 | -0.70875 | 0.000058 |
| **1(L) by 3 (L)** | -11.2500 | 0.038722 | -0.004250 | 0.605787 | -0.46000 | 0.000276 |
| **1(Q) by 3 (L)** | -3.7250 | 0.147141 | -0.008500 | 0.228335 | -0.08625 | 0.003898 |
| **2(L) by 3 (L)** | -21.5500 | 0.011014 | 0.004250 | 0.605787 | -0.72250 | 0.000112 |

### 3.4.1 Effect of Formulation Variables on Particle Size

According to **Table 3.3**, the particle size of the 15 formulations prepared for the optimization design was found to be in a range of 173-273 nm. The equation representing the linear and quadratic interactions for the dependent variable $Y_1$ is the following:

$$Y1 = 209.4667 + 8.0667\,X_1 - 5.1083X_1^2 + 6.4167X_2 - 9.1083\,X_2^2 + 16.7167X_3 + 1.6167X_3^2 + 12.8X_1X_2 - 12.95X_1X_2^2 - 23.225X_1^2X_2 - 11.25X_1X_3 - 3.725X_1^2X_3 - 21.55X_2X_3$$

where $X_1$, $X_2$ and $X_3$ represents the variation of one variable at a time and consists in linear interactions; $X_1X_2$, $X_1X_2^2$, $X_1^2X_2$, $X_1X_3$, $X_1^2X_3$, $X_2X_3$, $X_1^2$, $X_2^2$ and $X_3^2$ show how the dependent variables in study are affected when two variables are change simultaneously [96].

According to this equation, the lipid mass and the AMX mass individually revealed a significant influence in particle size (*P*<0.05). These independent variables demonstrate a positive interaction with the particle size, when analysed individually. Thus, increasing the lipid mass or the AMX mass leads to an increase in the particle size. On the other hand, the concentration of surfactant per se does not significantly influence the particle size (*P*>0.05).

The mathematically interactions between the independent variables and their effect on particles size (previous equation) can be elucidated by response surface plots (**Figure 3.9**). In

these plots, one independent variable is fixed at a level, while the remaining two are variable among the axis of the plot. Simultaneous increase in lipid and AMX mass demonstrated a significant negative effect on the particle size as shown in **Figure 3.9 (A)**. On the other hand, **Figure 3.9 (B)** represents the influence of AMX mass and the surfactant concentration when the lipid mass was fixed at a constant level. A simultaneous increase of both AMX mass and surfactant concentration demonstrated a negative effect. This relationship is also verified by the negative sign of the corresponding interaction coefficient ($A_5$ =-21.55). The simultaneous increase in lipid mass and surfactant concentration positively affects the particle size, as verified by **Figure 3.9 (C)** and by the interaction coefficient ($A_4$ = 12.8000).

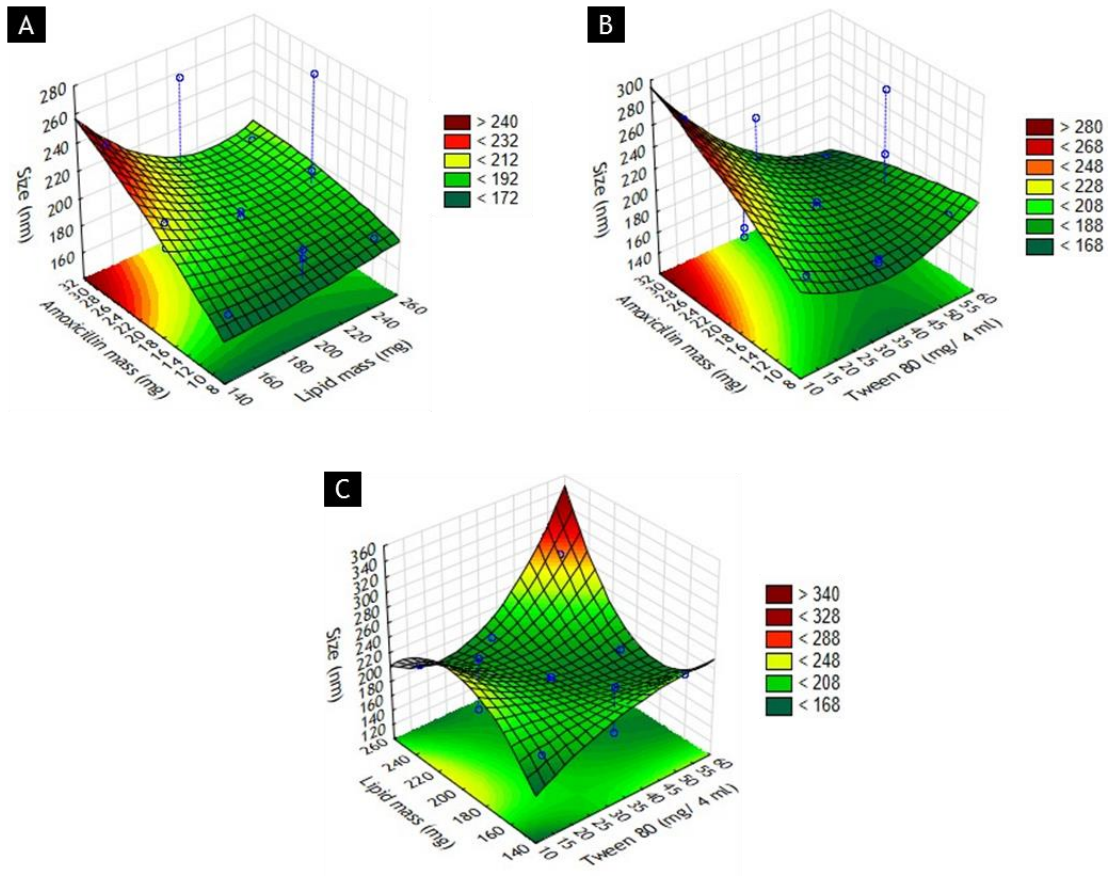


**Figure 3.9:** Response surface plots of variances in particles size by changing (A) AMX mass and lipid mass, (B) AMX mass and Tween®80 concentration and (C) lipid mass and Tween®80 concentration.

### 3.4.2 Effect of Formulation Variables on PDI

Regarding to PDI, the regression equation obtained from BBD analysis is the following:

$$Y2 = 0.125750 + 0.015917X_1 + 0.000896X_1^2 - 0.004417X_2 - 0.000854X_2^2 + 0.010583X_3 - 0.005604X_3^2 - 0.004750X_1X_2 - 0.014000X_1X_2^2 - 0.004000X_1^2X_2 - 0.004250X_1X_3 - 0.008500X_1^2X_3 + 0.004250X_2X_3$$

where $X_1$, $X_2$ and $X_3$ represents the variation of one variable at a time and consists in linear interactions; $X_1X_2$, $X_1X_2^2$, $X_1^2X_2$, $X_1X_3$, $X_1^2X_3$, $X_2X_3$, $X_1^2$, $X_2^2$ and $X_3^2$ show how the dependent variables in study are affected when two variables are change simultaneously [96].

In **Figure 3.10** the three response surface plots relatively to PDI are represented. The simultaneous increase in lipid and AMX mass demonstrates a negative effect on PDI, which is shown in **Figure 3.10 (A)**. On the contrary, a positive effect on the PDI is demonstrated with the simultaneous increase of AMX mass and surfactant concentration (Figure **3.10 (B)**). Additionally, the simultaneous increase of lipid mass and surfactant concentration shows a negative effect, which can be verified in **Figure 3.10 (C)**. Besides these conclusions, **Table 3.4** shows that the selected independent variables had no statistically significant ($P$>0.05) effect on PDI, regardless of the type of interactions studied (linear or quadratic). This phenomenon is probably due to the low PDI values obtained for the 15 formulations, which indicates that all of the studied suspensions were monodispersed and stable.

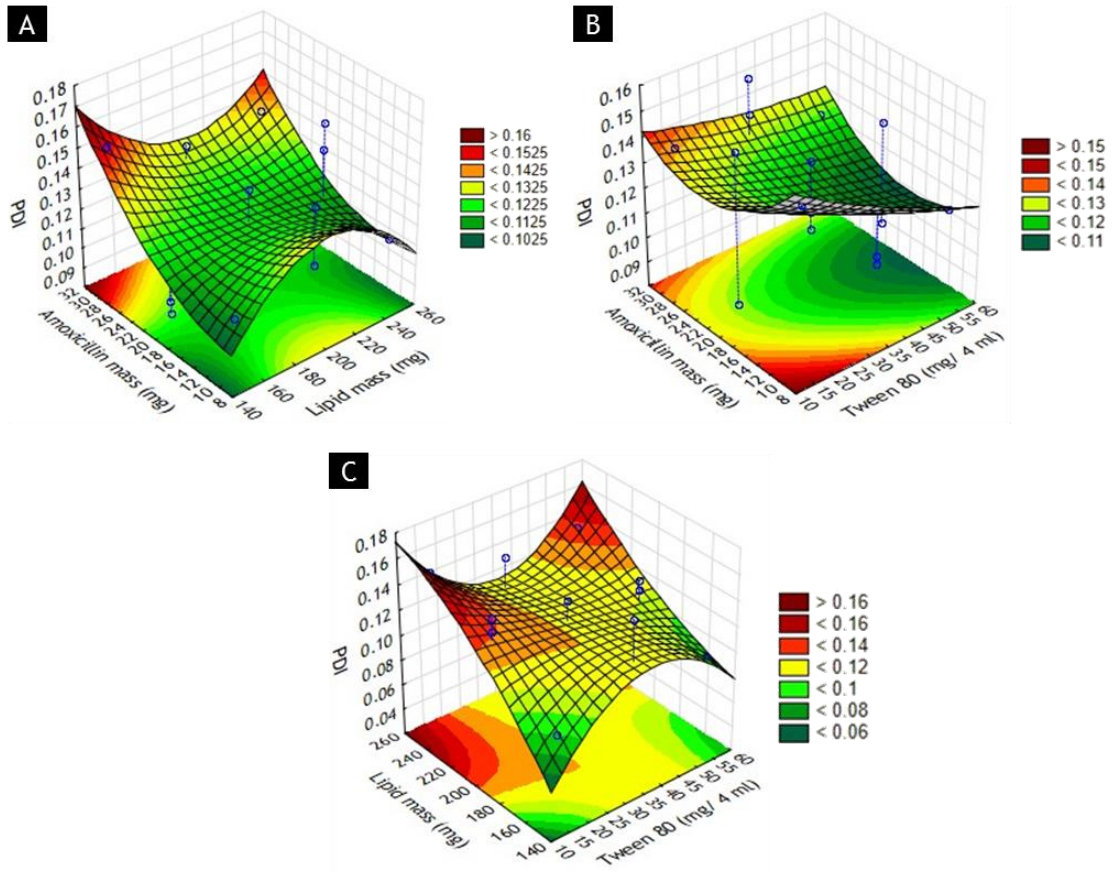


**Figure 3.10:** Response surface plots of variances in PDI by changing (A) AMX mass and lipid mass, (B) AMX mass and Tween®80 concentration and (C) lipid mass and Tween®80 concentration.

### 3.4.3 Effect of Formulation Variables on LC

The regression equation obtained from BBD analysis is the following:

$$Y3 = 5.01750 - 0.27000X_1 + 0.17979X_1^2 + 1.33750X_2 - 0.49146X_2^2 + 1.22250X_3 + 0.42354X_3^2 - 1.10500X_1X_2 + 0.50250X_1X_2^2 - 0.70875X_1^2X_2 - 0.46000X_1X_3 - 0.08625X_1^2X_3 - 0.72250X_2X_3$$

where $X_1$, $X_2$ and $X_3$ represents the variation of one variable at a time and consists in linear interactions; $X_1X_2$, $X_1X_2^2$, $X_1^2X_2$, $X_1X_3$, $X_1^2X_3$, $X_2X_3$, $X_1^2$, $X_2^2$ and $X_3^2$ show how the dependent variables in study are affected when two variables are change simultaneously [96].

The LC value calculated for the 15 formulations in study was found to be in a range of 1.5-9.5%. In **Figure 3.11** the three response surface plots relatively to LC are represented. The simultaneous increase in lipid and AMX mass demonstrates a significant negative effect ($P$<0.05) on LC, which is shown in **Figure 3.11 (A)**. Similar, the simultaneous increase in AMX mass and surfactant concentration and the simultaneously increase of the lipid mass and surfactant concentration have a negative effect (P<0.05) on LC, which can be verified in **Figure 3.11 (B)** and **(C)**, respectively.

Additionally, the *p*-values shown in **Table 3.4** regarding to LC analysis are all lower than 0.05, revealing that all the linear and quadratic interactions between the independent variables have a statistically significant effect on the LC.

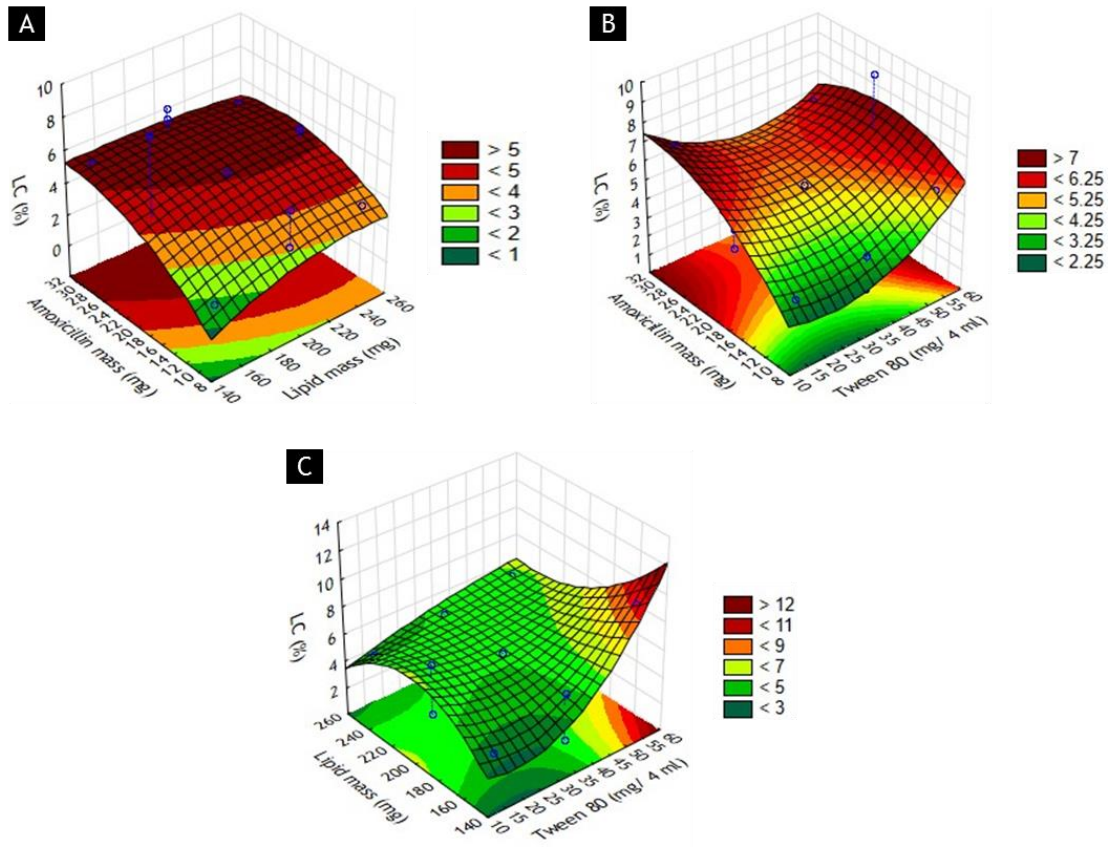


**Figure 3.11:** Response surface plots of variances in LC by changing (A) AMX mass and lipid mass, (B) AMX mass and Tween®80 concentration and (C) lipid mass and Tween®80 concentration.

### 3.4.4 ESTABLISHMENT OF THE IDEAL FORMULATION

The optimal lipid mass, surfactant concentration and AMX mass values were determined using the STATISTICA v12 software (**Table 3.5**). Furthermore, the particle size, PDI and LC of the optimal formulation were predicted by the software (**Table 3.5**). The optimization process performed using BBD was successful, since the experimental values obtained for the dependent variables in study were in the range of the 95% confidence limits.

**Table 3.5:** Composition and characterization of the optimal formulation obtained by BBD, with the predicted and experimental values for particle size, PDI and LC. The low and high 95% confidence limits for each dependent variable is also represented. Predict, Predicted; Exp, Experimental.

| | **Composition of the optimal formulation** | | | | |
|---|---|---|---|---|---|
| | Lipid Mass (mg) | Tween®80 concentration in the 1st phase (mg/4 mL) | | AMX mass (mg) | |
| | 178.5 | 55 | | 19.90 | |
| | **Characterization of the optimal formulation** | | | | |
| | Predict | Exp | -95% Confidence | +95% Confidence | **Goal** |
| **Particle size (nm)** | 184.15 | 197.43 | 170.36 | 199.9 | Minimize |
| **PDI** | 0.103 | 0.137 | 0.06 | 0.144 | Minimize |
| **LC (%)** | 7.47 | 7.47 | 7.42 | 7.51 | Maximize |

## 3.5 LNPS CHARACTERIZATION

The optimal formulation (F4) obtained by the BBD was compared with three other formulations (F1, F2, F3). The only difference between the four formulations was the NPs composition (**Figure 3.12**). The respective placebos (P1, P2, P3 and P4) for each formulation were also studied. The main goal of studying these formulations is to be able to evaluate in future studies which are the most important parameters in the interactions NPs-bacteria. For that purpose, the four formulations and the corresponding placebos were characterized. Besides, *in vitro* drug release and cell viability studies were performed. All studies were performed in triplicate.

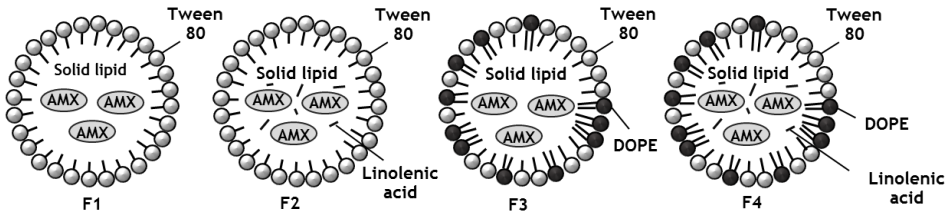


| | | | | |
|---|---|---|---|---|
| **Cetyl palmitate (mg)** | 178.5 | 178.5 | 178.5 | 178.5 |
| **T80 (mg/ 8 mL)** | 130 | 125 | 110 | 105 |
| **Linolenic acid (mg)** | - | 5 | - | 5 |
| **DOPE (mg)** | - | - | 20 | 20 |
| **AMX (mg)** | 19.90 | 19.90 | 19.90 | 19.90 |

**Figure 3.12:** Schematic representation and composition of the four formulations (F1, F2, F3 and F4) studied in this work. The corresponding placebos (P1, P2, P3 and P4) were also studied (not represented).

The four formulations and the corresponding placebos prepared by the double emulsion technique were visually white and milky. Besides, these liquid suspensions had a low viscosity and AMX deposits were not visible in any formulation. In **Figure 3.13**, P4 suspension after synthesis is visualized. The remaining formulations had a similar appearance, independently of being placebo or AMX-loaded SLNs. Therefore, all the formulations appeared stable by visual observation.

**Figure 3.13:** P4 formulation synthetized by double emulsion technique.

After synthesis, formulations from different batches were maintained in different conditions to evaluate the most suitable approach for long-term storage (**Figure 3.14**). Therefore, a batch was lyophilized at -80ºC during 48h to obtain a powder from the suspensions. Another batch

was lyophilized in the same conditions for further resuspension of the powder. The resuspensions were stored at RT and 4ºC, to compare the effect of the temperature in the formulations stability. Besides, the formulations were also stored as suspensions at 4ºC, without being exposed to a lyophilization process.

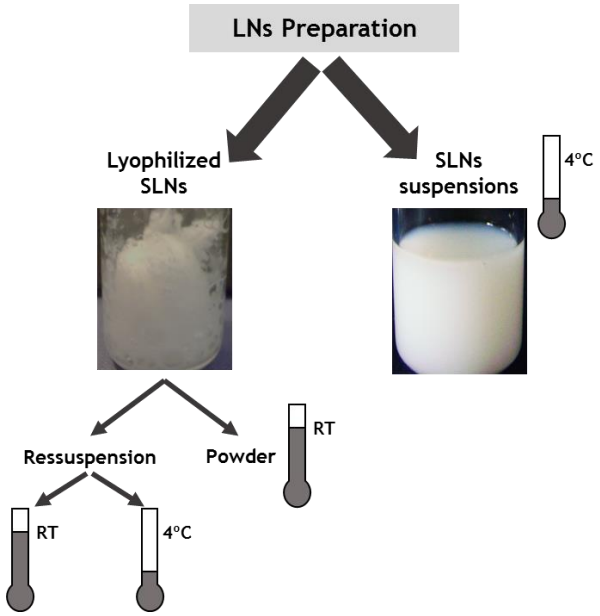


**Figure 3.14:** Schematic representation of all formulations studied in this work and their different conditions of storage. RT, Room Temperature.

### 3.5.1 LYOPHILIZED SLNS

For the lyophilization process, a preliminary experiment was performed to select the most suitable aerosil concentration. The addition of cryoprotectant to the formulations is a crucial step in the lyophilization of SLNs, since cryopreservation is responsible to decrease the SLNs aggregation that usually occurs due to stress during the process of freeze-drying [97]. In this study, two different aerosil concentrations were added to the formulations previously obtained: 1% and 2% of the solid lipid mass. After lyophilization, no evident differences were observed in particle size for the formulations with different concentrations of cryoprotectant (data not shown). Therefore, the lower concentration of cryoprotectant was chosen for further studies.

The formulations prepared in this work were lyophilized at -80ºC for 48h and a white powder was obtained from the process. Then, the lyophilized SLNs were stored at RT, protected from light for 1 month.

#### 3.5.1.1 TRANSMISSION ELECTRON MICROSCOPY

TEM was used to assess SLNs size distribution and to obtain information about the surface morphology. The morphology of the formulations can be observed in **Figure 3.15**. The images reveal that the AMX-loaded SLNs were almost spherical with smooth surfaces. The same morphology was verified for placebo formulations. Besides, aqueous compartments in the SLNs structure are visible after the lyophilization process. In **Figure 3.15 (C)** the presence of

vacuoles in not shown, however other TEM images of the F3 formulation revealed the presence of multiple vacuoles (data not shown). The existence of inner compartments in the SLNs matrix is a consequence of the LNPs preparation method, since NPs obtained by the double emulsion technique can contain few to many small compartments, depending on their size [98]. Regarding the particle size, most of the NPs visualized by TEM had a size in the range of 300-500 nm.

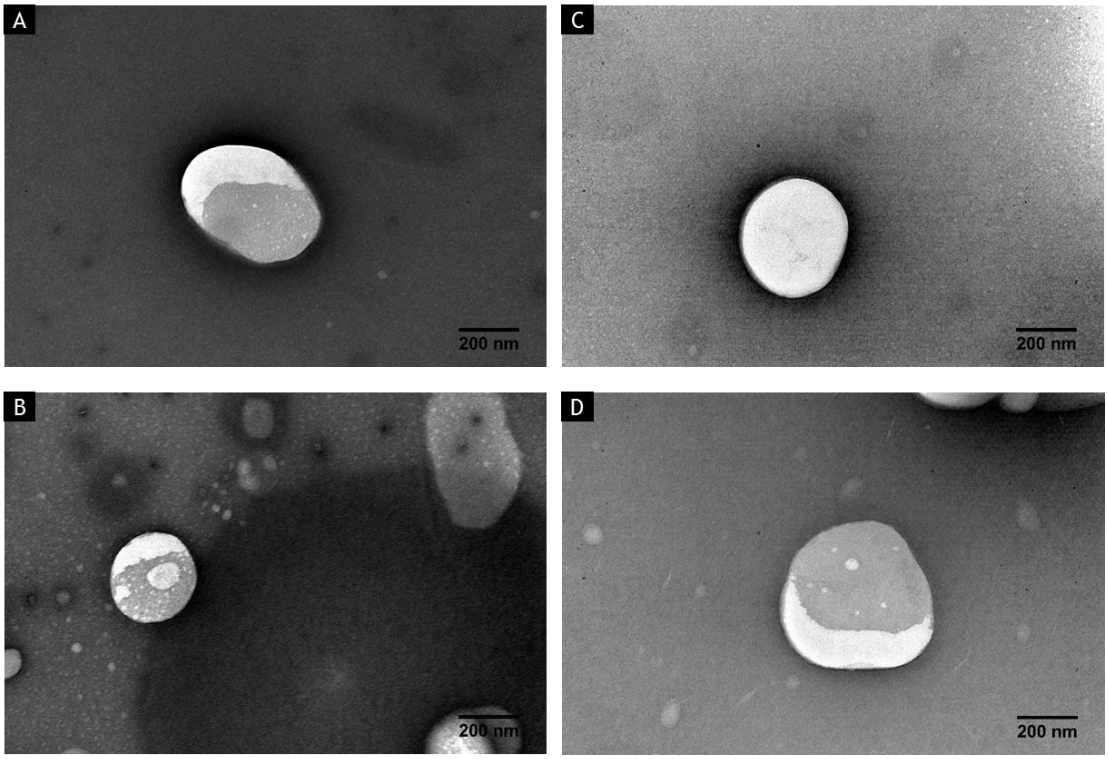


**Figure 3.15:** TEM images of the lyophilized SLNs. (A) F1 formulation, magnification 100000X. (B) F2 formulation, magnification 100000X. (C) F3 formulation, magnification 100000X. (D) F4 formulation, magnification 100000X.

### 3.5.1.2 Differential Scanning Calorimetry Analysis

DSC is a highly sensitive technique that allows measuring how physical properties of a sample change, along with temperature against time [42]. In this thermoanalytical technique it is possible to indirectly detect polymorphic forms by the analysis of transition temperatures and melting enthalpies [42].

The bulk solid lipid (cetyl palmitate) used to prepared the formulations was analysed by DSC technique (**Table 3.6**). Cetyl palmitate was heated to 80ºC, which lead to thermal transitions [99]. The heating curve of the bulk lipid showed two distinct polymorphic modifications [81]. The first peak (45ºC) corresponded to the α-polymorphic form of the crystal lipid, while the second peak with a sharp form reveals the melting point of the ß- polymorphic form (58.25ºC) (**Appendix 2**). The melting point of the bulk lipid proves the solid state of the lipid matrix at RT [100].

Further, the lyophilized SLNs were compared with the corresponding bulk mixtures. According to **Table 3.6**, the melting points of the SLNs were approximately 3–4°C below the melting temperature of the corresponding bulk mixtures. This occurrence, described as the Gibbs-Thompson effect is due to the larger surface area-to-volume ratio of nanoparticles, and has already been reported for lipid nanoparticles [101]. The high surface energy associated with the nanoparticles results in an energetically suboptimal state which is responsible for lowering the melting point of the lipid material [102]. Besides, a broader peak in the DSC thermograms of the SLNs when compared to the bulk lipid suggests that there is a range of thermal transitions, which is a consequence of the SLNs structure [99].

Regarding to enthalpy, all samples revealed a negative value. Therefore, an exothermic phase transition process occurred. The bulk solid lipid shows the lowest value (-188.3 J/g) (**Table 3.6**), which indicates a higher crystallinity state when compared with the bulk mixtures and the SLNs developed.

According to the **Table 3.6**, F1 SLNs and P1 SLNs present the lower RI values, which suggests that these SLNs have a lower level of organization in the crystal lattice when compared with the remaining SLNs analysed. In fact, the remaining SLNs present a RI value near to 100%. Therefore, these formulations show a crystallinity state similar to the mixtures.

**Table 3.6:** DSC parameters of bulk cetyl palmitate, placebos and AMX-loaded SLNs and the corresponding bulk mixtures: melting temperatures, enthalpy and RI. Values are represented as mean ± SD. SLNs samples were analysed in triplicate whereas bulk mixtures and bulk solid lipid samples were analysed in duplicate. RI percentages were calculated relatively to the respective placebo bulk mixture, except for the cetyl palmitate (bulk solid lipid). RI, recrystallization index.

| | Melting point (ºC) | Enthalpy (J/g) | RI (%) |
|---|---|---|---|
| Cetyl palmitate | 58.2 ± 0.2 | - 188 ± 2 | 100 |
| F1 SLNs | 53.6 ± 0.2 | - 91 ± 3 | 80 |
| P1 SLNs | 53.8 ± 0.6 | - 85 ± 3 | 70 |
| Mixture F1 | 56.55 ± 0.05 | - 109.8 ± 0.4 | 97 |
| Mixture P1 | 56.8 ± 0.1 | - 121 ± 6 | 100 |
| F2 SLNs | 54.1 ± 0.3 | - 93 ± 3 | 102 |
| P2 SLNs | 53.8 ± 0.3 | - 99 ± 6 | 102 |
| Mixture F2 | 57.4 ± 0.3 | - 90 ± 3 | 98 |
| Mixture P2 | 58.00 ± 0.00 | - 98 ± 2 | 100 |
| F3 SLNs | 53.80 ± 0.08 | - 93 ± 3 | 101 |
| P3 SLNs | 54.0 ± 0.6 | - 93 ± 2 | 94 |
| Mixture F3 | 57.3 ± 0.4 | - 89 ± 4 | 97 |
| Mixture P3 | 58.0 ± 0.2 | - 98 ± 5 | 100 |
| F4 SLNs | 53.9 ± 0.5 | - 95 ± 2 | 103 |
| P4 SLNs | 53.8 ± 0.3 | - 82 ± 2 | 83 |
| Mixture F4 | 57.6 ± 0.5 | - 89 ± 1 | 96 |
| Mixture P4 | 57.9 ± 0.2 | - 99 ± 2 | 100 |

DSC thermograms for the formulations F1, F2 and F3 are represented in the **Appendix 3**, **Appendix 4** and **Appendix 5**, respectively. The thermograms for the corresponding placebos and bulk materials mixtures are also represented (**Appendix 3** to **5**). The previously mentioned thermograms will not be described in detail in this work.

For the formulation optimized by BBD (F4 formulation), DSC thermogram can be observed in **Figure 3.16**. The DSC thermograms of the corresponding placebo SLNs and bulk mixtures (F4 and P4 mixtures) are also shown in **Figure 3.16**. The respective melting parameters are shown in **Table 3.6**. For the mixtures F4 and P4 the maximum peak occurred at 57.6ºC and 57.9ºC (**Table 3.6** and **Figure 3.16**). These temperatures are very similar to the bulk cetyl palmitate ß- polymorphic form melting point (58.25ºC). Regarding to F4 and P4 SLNs, the maximum peak took place at 53.9ºC and 53.8ºC, respectively. Thus, the SLNs revealed a lower melting transition temperature than the respective bulk mixtures. Regarding to enthalpy, SLNs and the corresponding bulk mixtures showed similar melting enthalpy values in the range of -80 to -100 J/g.

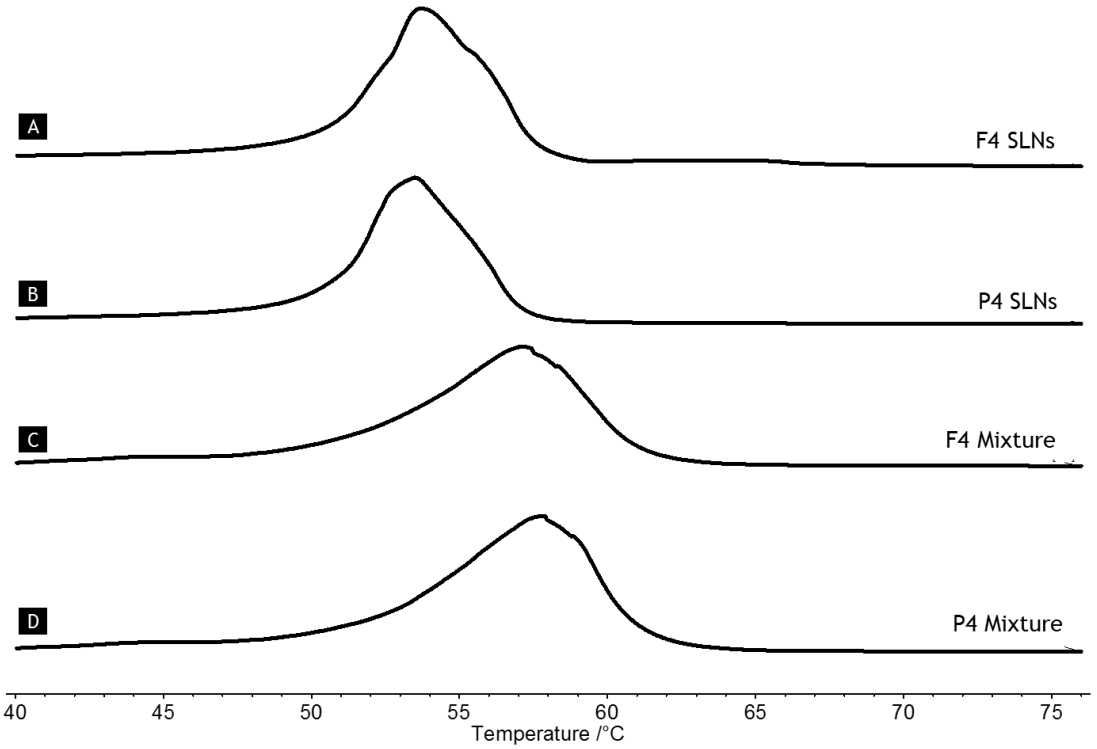


**Figure 3.16:** Differential scanning calorimetry thermograms of: (A) F4 SLNs, (B) P4 SLNs, (C) F4 mixture and (D) P4 mixture.

The DSC technique can also be used to assess the interaction of drugs with the lipid material and to stablish the effect of AMX encapsulation on the melting behavior of the prepared SLNs. According to **Table 3.6**, an incorporation of AMX does not affect the melting point, since the AMX-loaded SLNs and their corresponding placebos have similar values of this parameter. Regarding to the RI, an increase is verified for the AMX-loaded SLNs when compared with their respective placebos SLNs, except for the F2 formulation (**Table 3.6**). The increase in RI verified with the encapsulation of AMX into SLNs suggest a slightly higher level of organization in the crystal lattice of the AMX-loaded SLNs [81].

### 3.5.1.3 STABILITY STUDIES

Stability studies were performed during 1 month. In these studies, particles size, PDI, zeta potential and LC were evaluated at the weeks 0, 1, 2 and 4 after the NPs synthesis. The measurements performed at week 0 correspond to the characterization of SLNs suspensions previous to the lyophilization process. The data from EE is not shown, however it was used to calculate the LC.

The particle size of the AMX-loaded SLNs and the corresponding placebos was measured over time and it is represented in **Figure 3.17**. For all the formulations, a significant increase in the particles size was verified from week 0 to week 1. Before the lyophilization, all formulations

had a size lower than 300 nm. In week 1, after the lyophilization process, all the measurements revealed sizes between 300-450 nm. In weeks 2 and 4 the measurements showed a similar particle size with no significant differences when compared to week 1, except for the formulation P4. In this formulation a significant decrease was observed at week 4, when compared to weeks 1 and 2.

The particle sizes obtained by the DLS technique are similar to the results obtained by TEM. Nevertheless, these techniques have a completely different basis concept and sample's preparation [81]. In the DLS technique the samples are highly hydrated and the diameter of NPs is based on the hydrodynamic radius [81]. On the other hand, TEM analysis gives a direct measurement of the size of the particles in a planar grid [81].

From these results, it is suggested that the lyophilization process is responsible for the reorganization of the SLNs structure in a way that leads to an increase in particle size. Therefore, due to the high particle size, the diffusion of NPs into the gastric mucosa can be compromised [70].

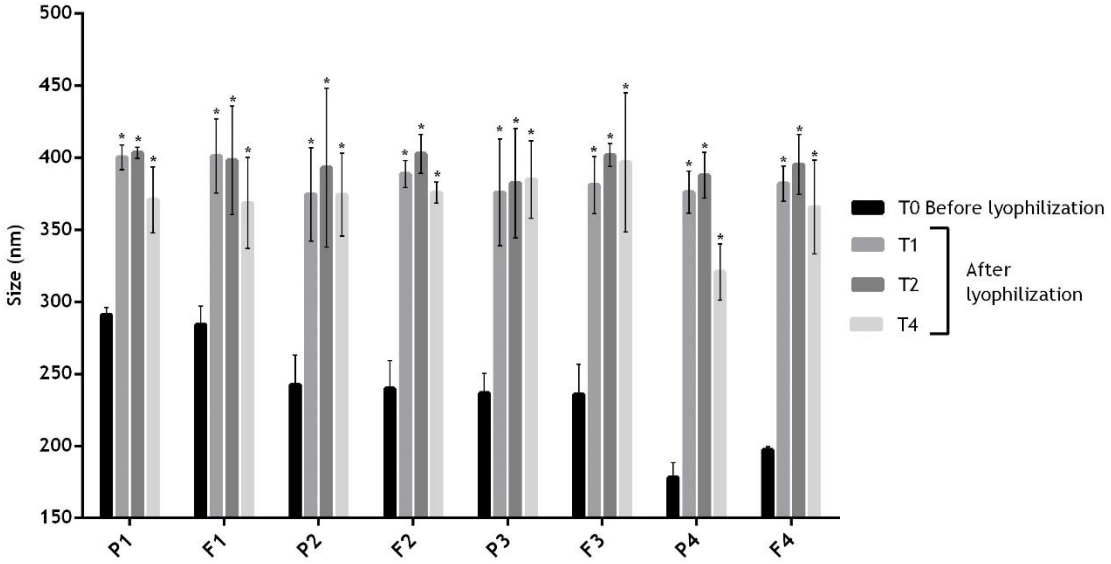


**Figure 3.17:** Evaluation of the particle size of the lyophilized formulations over time (0 (T0), 1 (T1), 2 (T2) and 4 (T4) weeks). Bars represent the size (left Y axis). Values represent the mean ± SD of the readings. *$P$<0.05 relatively to the correspondent week 0. No significant changes in particle size were verified from week 1 to week 4, except for the formulation P4.

On other hand, the lyophilization process did not affected the PDI of the SLNs, since no significant changes were observed between week 0 and week 1 in all formulations studied (**Figure 3.18**). In fact, the PDI measurements revealed very similar values over time for both the formulations and the corresponding placebos. An exception can be observed for the formulation P4, since a significant increase was observed at week 2, when compared to week 0. However, the PDI of the formulation appears to maintain stable at week 4, with no significant differences when compared to week 0.

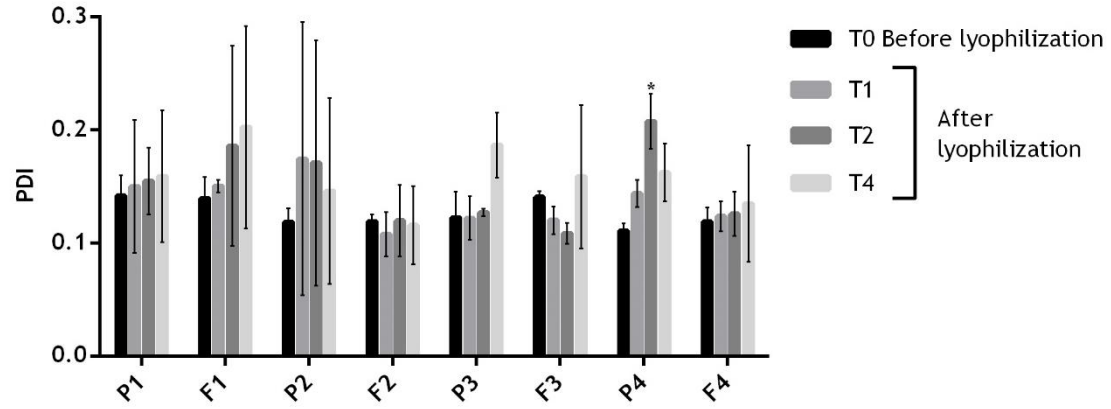


**Figure 3.18:** Evaluation of the PDI of the lyophilized formulations over time (0 (T0), 1 (T1), 2 (T2) and 4 (T4) weeks). Bars represent the PDI (left Y axis). Values represent the mean ± SD of the readings. *$P$<0.05 relatively to the correspondent week 0. No significant changes in PDI were verified from week 1 to week 4.

Another important parameter to evaluate NPs' stability over time is the zeta potential. It characterizes the surface charge of NPs, which is influenced by both the NPs composition and the medium where they are dispersed [94]. In general, when the absolute value of zeta potential is above 30 mv, the dispersion is stable due to the electrostatic repulsion between the particles [103]. Zeta potentials between 5 and 15 mV result in limited flocculation and between 0 and 5 mV a maximum flocculation occurs [103]. Despite that some significant changes in particle size were verified over time (**Figure 3.19**), it is possible to observe that all the formulations presented a highly negative zeta potential average, greater than |30| mV. Therefore, regarding the lipid composition variations among the SLNs, the results suggest that all formulations were stable and did not tend to form aggregates due to electric repulsion between the particles.

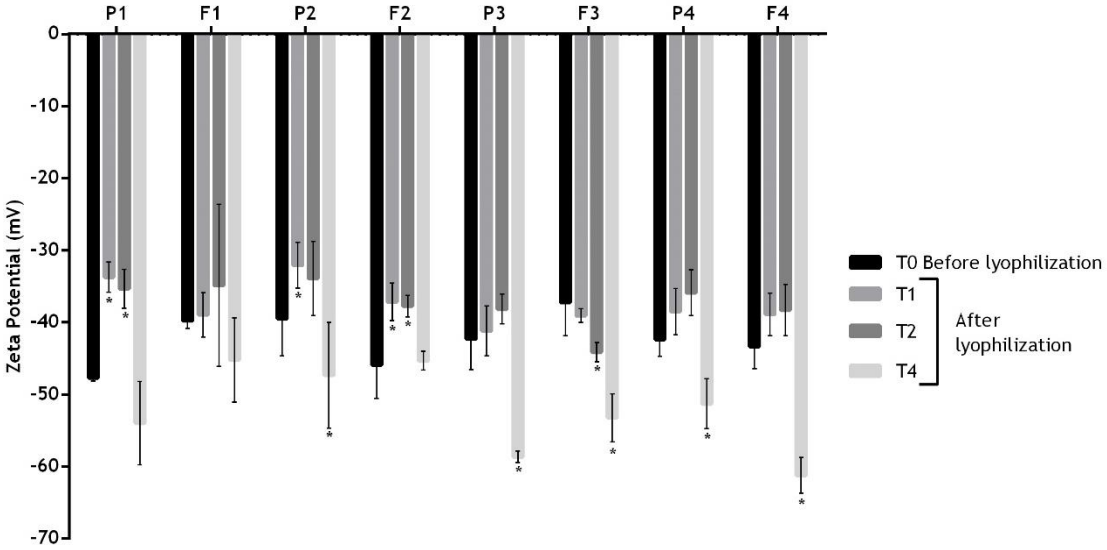


**Figure 3.19:** Evaluation of the zeta potential of the lyophilized formulations over time (0 (T0), 1 (T1), 2 (T2) and 4 (T4) weeks). Bars represent the zeta potential (left Y axis). Values represent the mean ± SD of the readings. *$P$<0.05 relatively to the correspondent week 0.

The LC of the AMX-loaded SLNs is shown in **Figure 3.20**. For the 4 formulations, the values of LC are satisfactorily high, with averages between 5.7 and 7.5 in week 0, before lyophilization. The formulation F1 did not have significant variations in the LC, during the study period. On the other hand, the remaining formulations significantly decreased their LC after the lyophilization process. This indicates a reorganization that leads to AMX expulsion during the lyophilization. However, from week 1 to week 4 the LC of all formulations maintained stable, which leads to the conclusion that during that period of storage no significant AMX release was observed.

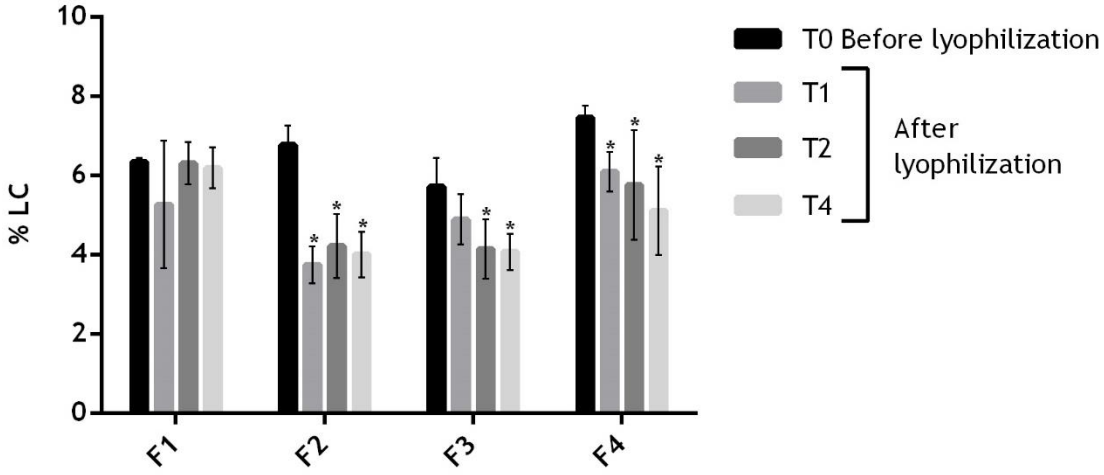


**Figure 3.20:** Evaluation of the LC of the lyophilized formulations over time (0 (T0), 1 (T1), 2 (T2) and 4 (T4) weeks). Bars represent the LC (left Y axis). Values represent the mean ± SD of the readings. *$P$<0.05 relatively to the correspondent week 0. No significant changes in LC were verified from week 1 to week 4.

Although the results from particle size, PDI, zeta potential and LC suggested that the formulations were stable during 4 weeks, visual observation of the AMX-loaded SLNs revealed a color change from white to yellow, which indicates that AMX was degraded. This color change can be observed in **Figure 3.21.** Due to this phenomenon and to the changes in the particle size resulted from the lyophilization, this process was considered inadequate for the SLNs in study. An optimization of the liophilization conditions is needed, however once it can be a time-consuming process, this possibility was for the time, left behind. Therefore, a new approach involved the evaluation of SLNs suspensions stability over storage time.

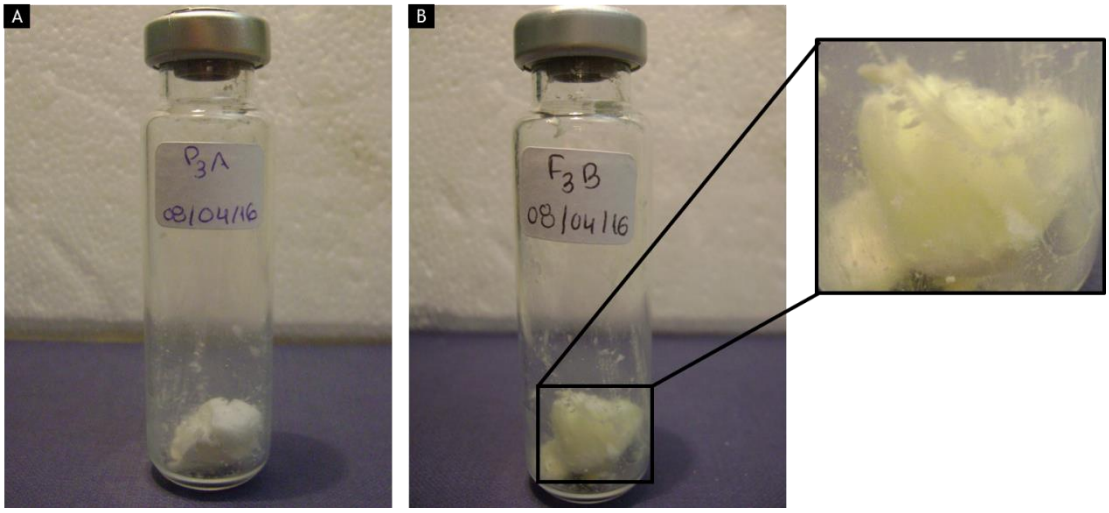


**Figure 3.21:** Lyophilized SLNs synthetized by double emulsion technique, after 1 month of storage at RT: A) P3 formulation (placebo), B) F3 formulation.

The ressuspended SLNs were stored at both RT and 4ºC, protected from light for 2 weeks. Particle size, PDI, zeta potential and LC stability studies were performed during 2 weeks (**Appendix 6** to **13**). The measurements performed at week 0 corresponded to the characterization of SLNs suspensions previous to lyophilization process. As a consequence of liophilization, ressuspended SLNs revealed a significant increase in the particles size from week 0 to week 1. The stability study of the ressuspended SLNs was discontinued due to the AMX degradation verified on liophilized SLNs after 1 month of storage.

### 3.5.2 SLNs SUSPENSIONS

The SLNs suspensions synthetized by the double emulsion technique were stored at 4ºC, protected from light during at least 2 months.

#### 3.5.2.1 TRANSMISSION ELECTRON MICROSCOPY

TEM images (**Figure 3.22**) were analysed for all formulations in study in order to assess SLNs size distribution and to obtain information about the surface morphology. The TEM images revealed that both placebos and AMX-loaded SLNs had a spherical shape, which leads to the conclusion that SLNs morphology is not affected by the encapsulation of AMX. In **Figure 3.22 (A)**, the presence of vacuoles is observed, which was also identified in the remaining formulations analysed by TEM. The presence of vacuoles in AMX-loaded SLNs suggests that AMX is entrapped in these cellular comportments. The presence of vacuoles in the structure of the SLNs prepared was expected since in the double emulsion technique the NPs obtained can contain from few to many small compartments, depending on their size [98]. Furthermore, the TEM images revealed no visible aggregation of SLNs.

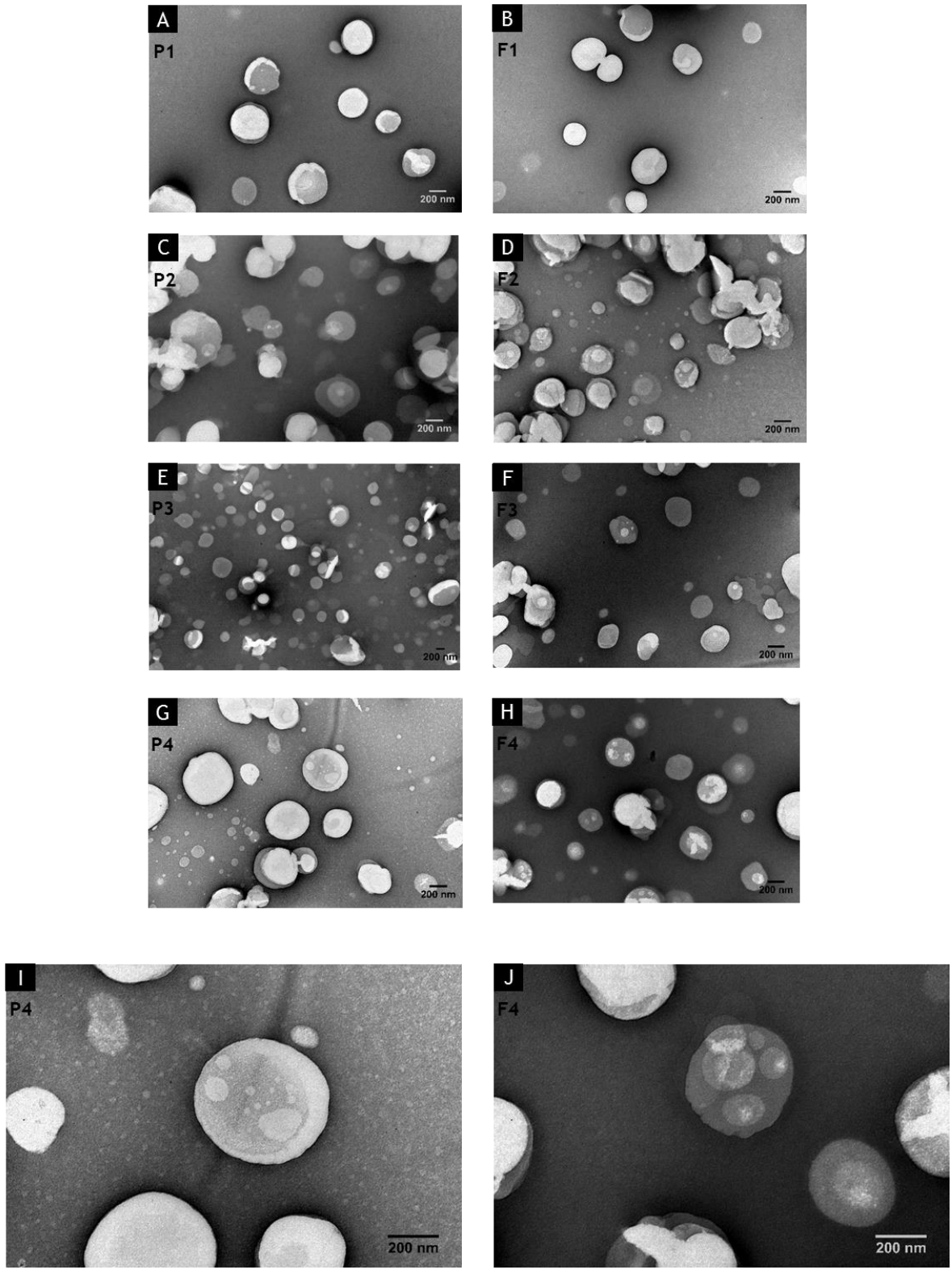


**Figure 3.22:** TEM images of the SLNs suspensions. (A) P1 formulation, magnification 50000X. (B) F1 formulation, magnification 50000X. (C) P2 formulation, magnification 50000X. (D) F2 formulation, magnification 50000X. (E) P3 formulation, magnification 25000X. (F) F3 formulation, magnification 50000X. (G) P4 formulation, magnification 50000X. (H) F4 formulation, magnification 50000X. (I) P4 formulation, magnification 100000X. (J) F4 formulation, magnification 100000X.

### 3.5.2.2 STABILITY STUDIES

Stability studies were performed during 2 months. In these studies, particle size, PDI, zeta potential and LC were evaluated at weeks 0, 1, 2, 4 and 8 after the synthesis. The data from EE is not shown, however it was used to calculate the LC.

The particle size of the AMX-loaded SLNs and the corresponding placebos measured by DLS are represented in **Figure 3.23**. Both placebo and AMX-loaded SLNs showed stability over the 8 weeks of study, with no statistically significant variations observed. However, the formulation P4 showed a significant increase in size at weeks 2 and 4 when compared with week 0. All the formulations studied showed a homogenous size distribution with a mean diameter lower than 300 nm. P4 and F4 formulations had the smallest particle sizes at week 0, with a mean diameter of 178.3 and 197.4 nm, respectively. The results obtained in **Figure 3.23** suggest that AMX encapsulation into the NPs does not influence the particle size.

The particle sizes obtained by the DLS technique are slightly lower than the sizes obtained by TEM. The differences in diameter observed by both techniques can be justified by the fact that DLS analysis is a technique based on light dispersion, while TEM provides a direct measurement of the particle size in a planar grid [81].

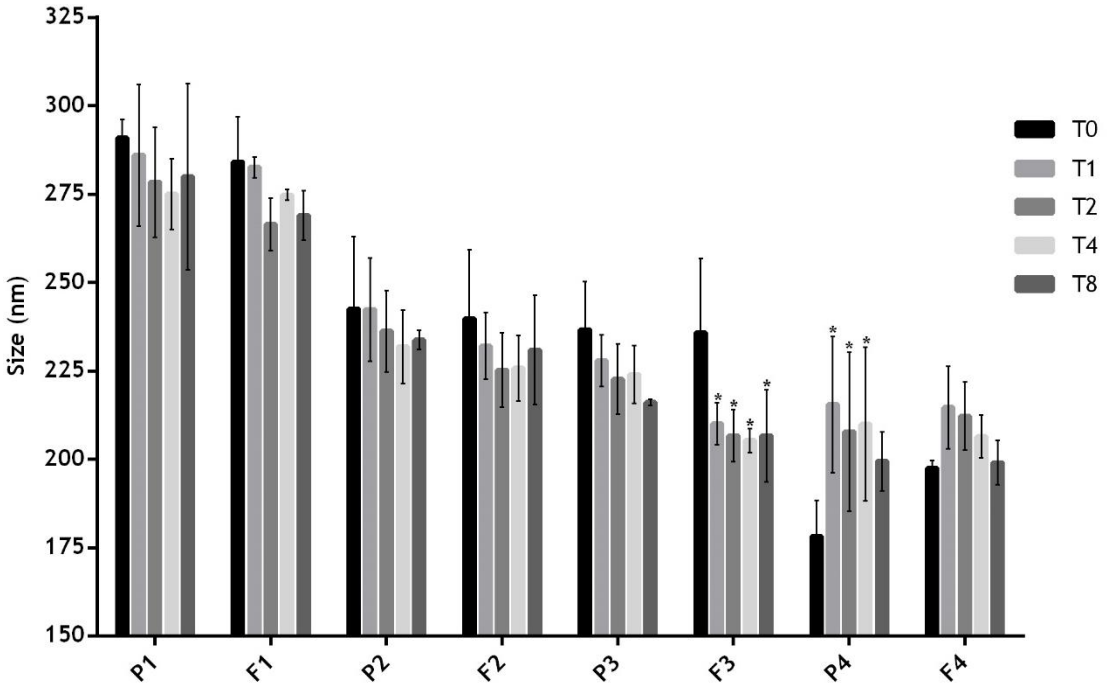


**Figure 3.23:** Evaluation of the particle size of the SLNs suspensions over time (0 (T0), 1 (T1), 2 (T2), 4 (T4) and 8 (T8) weeks). Bars represent the size (left Y axis). Values represent the mean ± SD of the readings. *$P$<0.05 relatively to the correspondent week 0.

Meanwhile, the PDI values obtained for all formulations were lower than 0.2 during the 8 weeks of study (**Figure 3.24**), which suggests that the particles were stable and had an acceptable monodispersed distribution, with low variability and no aggregation [81].

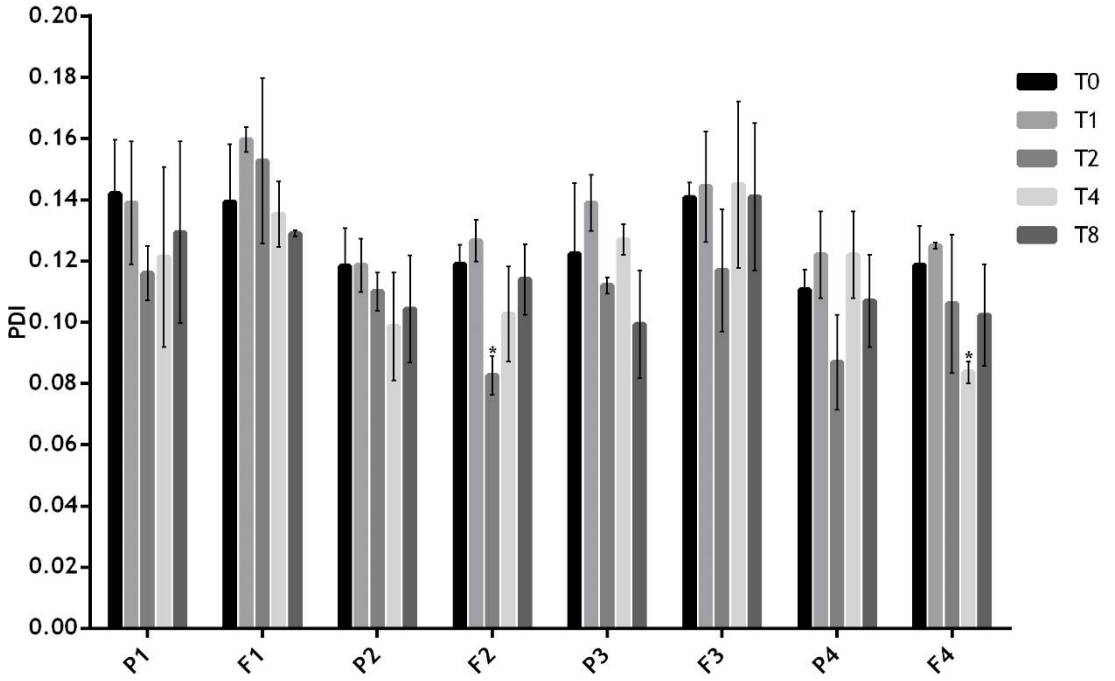


**Figure 3.24:** Evaluation of the PDI of the SLNs suspensions over time (0 (T0), 1 (T1), 2 (T2), 4 (T4) and 8 (T8) weeks). Bars represent the PDI (left Y axis). Values represent the mean ± SD of the readings. *$P$<0.05 relatively to the correspondent week 0.

As is shown in **Figure 3.25**, all formulations presented a high negative zeta potential average, between -35 to -60 mV over the 8 weeks of study. These values predict a long-term stability of the NPs. Besides, they apparently suggest that the incorporation of AMX did not affected the physical stability of the suspensions. Therefore, the SLNs suspensions prepared in this work are stable for at least 8 weeks due to the electrostatic repulsion, which leads to no tendency to form aggregates.

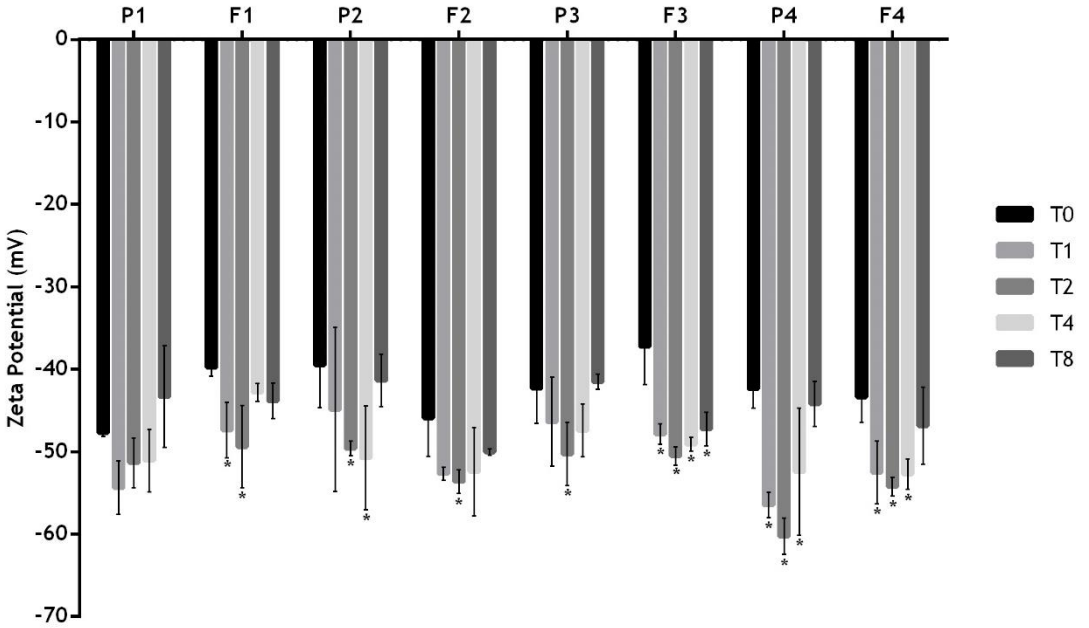


**Figure 3.25:** Evaluation of the zeta potential of the SLNs suspensions over time (0 (T0), 1 (T1), 2 (T2), 4 (T4) and 8 (T8) weeks). Bars represent the zeta potential (left Y axis). Values represent the mean ± SD of the readings. *$P$<0.05 relatively to the correspondent week 0.

The LC of the AMX-loaded SLNs over the 8 weeks is represented in **Figure 3.26**. The percentage of LC in all the formulations is considered satisfactorily high. After NPs synthesis, the formulations F1, F2, F3 showed an average LC of 6.34, 6.78 and 5.73, respectively. As expected from BBD, the optimal formulation F4 presented a LC of 7.47 at week 0, having the highest value of LC from the four formulations. After 8 weeks a significant decrease of the LC percentage was verified in the formulations F2 and F4, when compared to week 0. Nevertheless, F2 and F4 formulations still had LC percentages higher than 6.0 and 6.7, respectively.

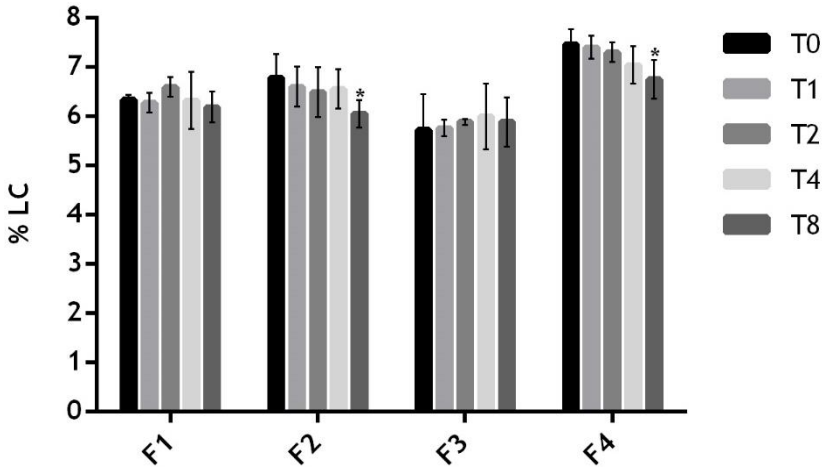


**Figure 3.26:** Evaluation of the LC of the SLNs suspensions over time (0 (T0), 1 (T1), 2 (T2), 4 (T4) and 8 (T8) weeks). Bars represent the LC (left Y axis). Values represent the mean ± SD of the readings. *$P$<0.05 relatively to the correspondent week 0.

According to the stability results over the 8 weeks of study, it is possible to conclude that the SLNs suspensions prepared by the double emulsion technique were stable for at least 2 months when stored at 4ºC and protected from light. Therefore, these LNPs can be considered suitable systems for AMX encapsulation. In contrast to the color change from white to yellow observed in the lyophilized SLNs, in the SLNs suspensions a white color was observed after 1 month, which indicates that AMX did not degraded (**Figure 3.27**).

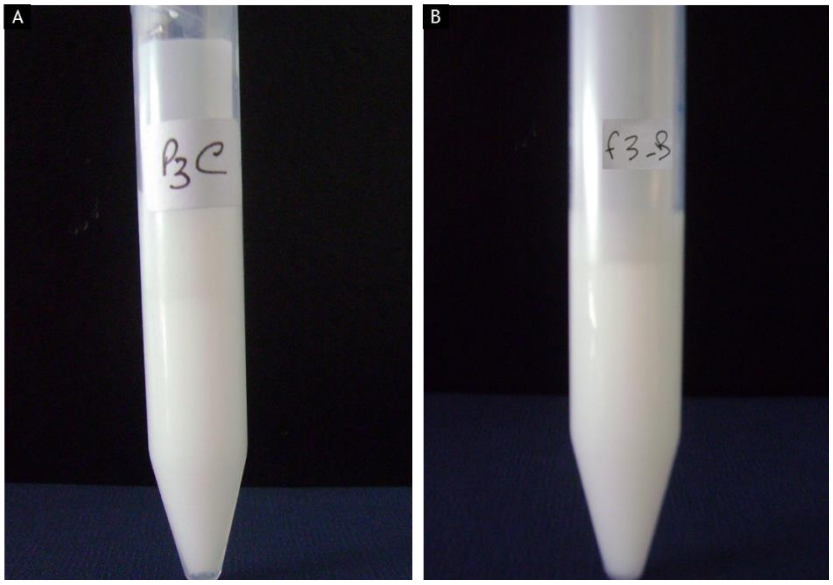


**Figure 3.27:** SLNs suspensions synthetized by double emulsion technique, after 1 month of storage at 4ºC: A) P3 formulation (placebo), B) F3 formulation.

## 3.6 *IN VITRO* AMOXICILLIN RELEASE STUDY

An *in vitro* AMX release study was performed at body temperature (37ºC) for both the lyophilized SLNs and the SLNs suspensions (**Figures 3.28** and **3.29**). In this study, the gastrointestinal conditions to which the SLNs are exposed after oral administration were simulated to predict the *in vivo* kinetics of the NPs [81]. The SLNs were exposed to gastric medium (pH 1.6) for 3 hours and then to a pH 5 buffer simulating the mucus layer medium during 1 hour. Afterwards, the SLNs were exposed to a pH 7.4 buffer to simulate the systemic circulation environment.

**Figures 3.28** and **3.29** showed an initial burst release for both lyophilized and suspensions NPs. It is hypothesised that this initial percentage of release corresponds to the non-encapsulated AMX. Hence, since all formulations have an initial release around or inferior to 25%, it is believed that the prepared SLNs have a higher EE and, consequently, a higher LC than the values measured during LNPs characterization and stability studies. After the initial burst release, all formulations remained stable at the gastric medium (pH 1.6) with low release of AMX in the first 3 hours of study (**Figures 3.28** and **3.29**). In fact, in the SLNs suspensions (**Figure 3.29**) during the 3 initial hours less than 30% of AMX was released. Thus, the acidic pH of the gastric medium, bile salts, lecithins and the high temperature do not seem to

compromise the SLNs as AMX delivery systems to target the mucus layer. During the study, the formulations (F1, F2, F3 and F4) revealed identical release profiles (**Figures 3.28** and **3.29**). However, the SLNs suspension corresponding to the ideal formulation (F4) obtained by the BBD (**Figure 3.29**) presented an increased release of AMX at pH 5 compared to the remaining formulations. The higher AMX release at pH 5 verified in the formulation F4 suggests that this formulation is the most suitable for *H. pylori* targeting, due to the location of these bacteria at the interface between the mucus layer and epithelial cells.

Comparing the release profiles of the formulations and the free AMX, it can be observed in the **Figures 3.28** and **3.29** that AMX is released much faster in the native form than when entrapped into the SLNs. In fact, even comparing with the formulation with highest release (F4), the release profile is significant ($P<0.05$) lower than the profile of the free AMX from 1.50 hours until the total release of the drug (**Figure 3.29**). A similar difference was verified for the lyophilized F4 formulation (**Figure 3.28**).

According to the results obtained from the *in vitro* release study, the encapsulation of AMX into the SLNs promotes a more sustainable and controlled release. Therefore, SLNs are a suitable oral delivery system of AMX for the treatment of *H. pylori* infections.

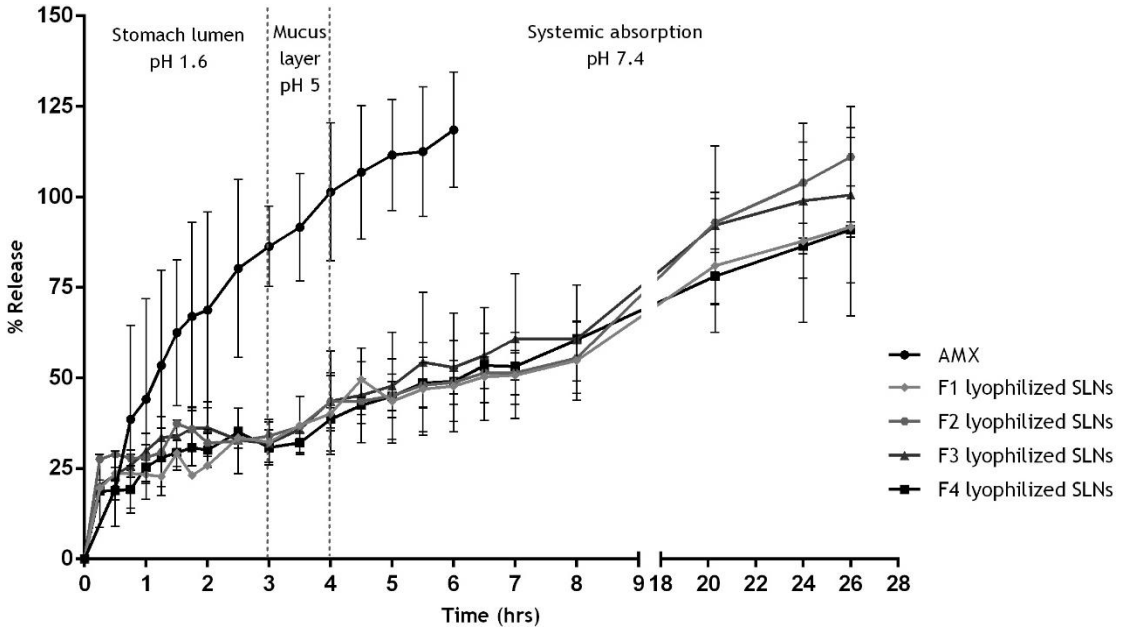


**Figure 3.28:** *In vitro* AMX release profiles from lyophilized SLNs (F1, F2, F3 and F4) and free AMX, simulating the gastrointestinal transit conditions, at body temperature (37ºC). Vertical lines represent media changes. AMX, free amoxicillin.

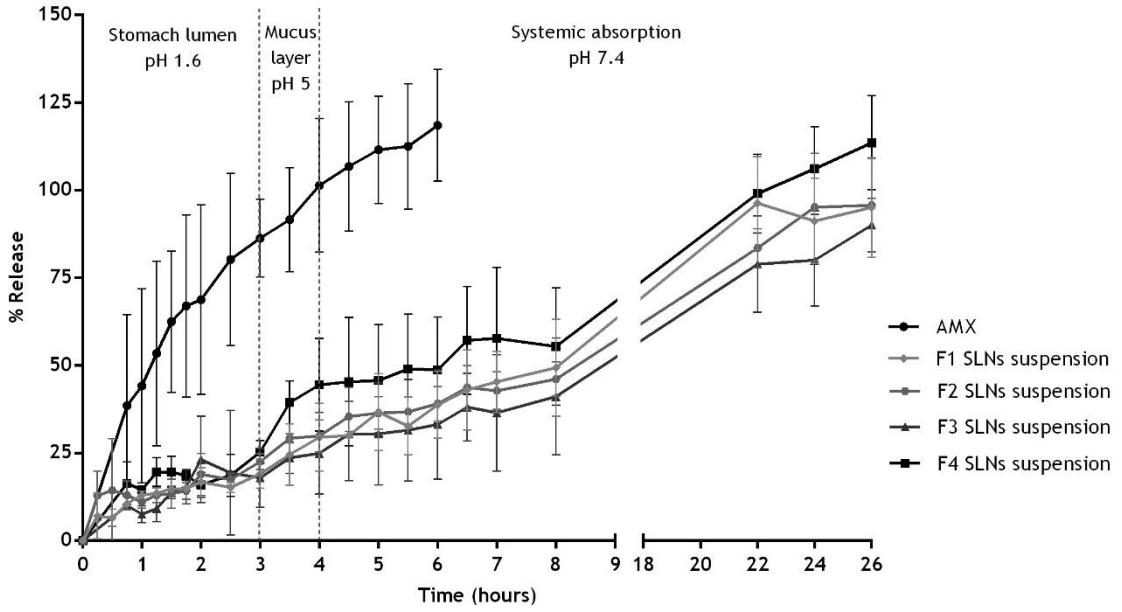


**Figure 3.29:** *In vitro* AMX release profiles from SLNs suspensions (F1, F2, F3 and F4) and free AMX, simulating the gastrointestinal transit conditions, at body temperature (37ºC). Vertical lines represent media changes. AMX, free amoxicillin.

## 3.7 *IN VITRO* CELL VIABILITY STUDIES

In order to assess the effects of the developed SLNs on cellular viability of fibroblasts and gastric cells, an MTT assay was performed in L929 cells (**Figure 3.30**) and MKN28 cells (**Figure 3.31**), respectively. L929 cells were selected for the cell viability study, since this cell line is recommended by ISO international standard 10993-5 for the MTT cytotoxicity test [104]. MKN28 gastric cells were selected to evaluate gastric cytotoxicity of the developed SLNs. In this assay, viability of the cells incubated with the NPs and the free AMX at different concentrations was compared with the mean of positive control (incubated with culture medium).

The MTT assay performed with L929 cells (**Figure 3.30**) showed that cell viability percentage was higher than 80%. In **Figure 3.30**, the samples with a higher concentration (2 mg/mL) slightly decreased cell viability when compared to concentrations 0.5 and 1 mg/mL. This effect is not verified for the formulations F3 and F4. Nevertheless, no significant ($P$>0.05) cytotoxic effects were verified in cells incubated with SLNs, regardless of being AMX-loaded SLNs or placebos. Therefore, this result suggests that the entrapment of AMX into SLNs does not increase the SLNs cytotoxicity when tested with the L929 cell line. Moreover, free AMX also revealed no significant effects on cell viability at the tested concentrations.

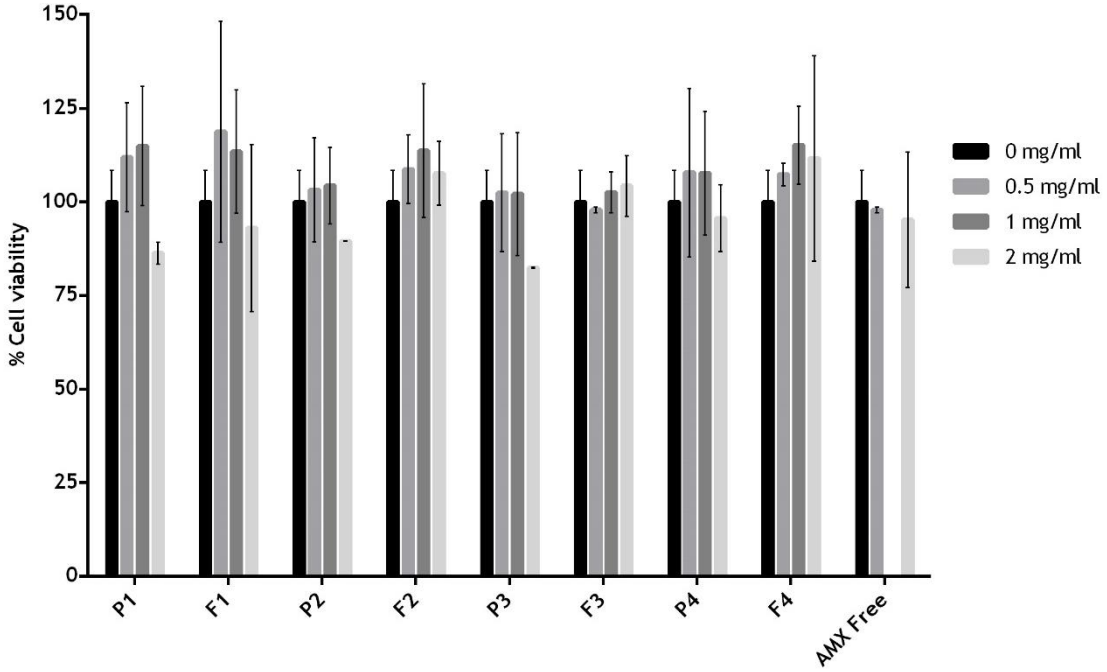


**Figure 3.30:** L929 cell viability assessed by MTT assay as a function of the different formulations and concentrations of SLNs tested (0, 0.5, 1 and 2 mg/mL). For free AMX only the concentrations 0, 0.5 and 2 mg/mL were tested. Values represent mean ± SD. No statistically significant differences were observed for both formulations and free AMX relatively to the mean positive control, regardless the concentration ($P$>0.05).

The MTT assay performed with MKN28 cells (**Figure 3.31**) revealed that no significant ($P$>0.05) cytotoxic effects were observed in the cells incubated with the developed formulations and the free AMX, when compared to the mean positive control (culture medium). Thus, cells incubated with both AMX-loaded and placebo SLNs presented a cell viability around 100% (**Figure 3.31**), which indicates that the encapsulation of AMX into SLNs does not lead to cytotoxicity effects in MKN28 cells. Moreover, free AMX also revealed no significant effects on cell viability at the tested concentrations.

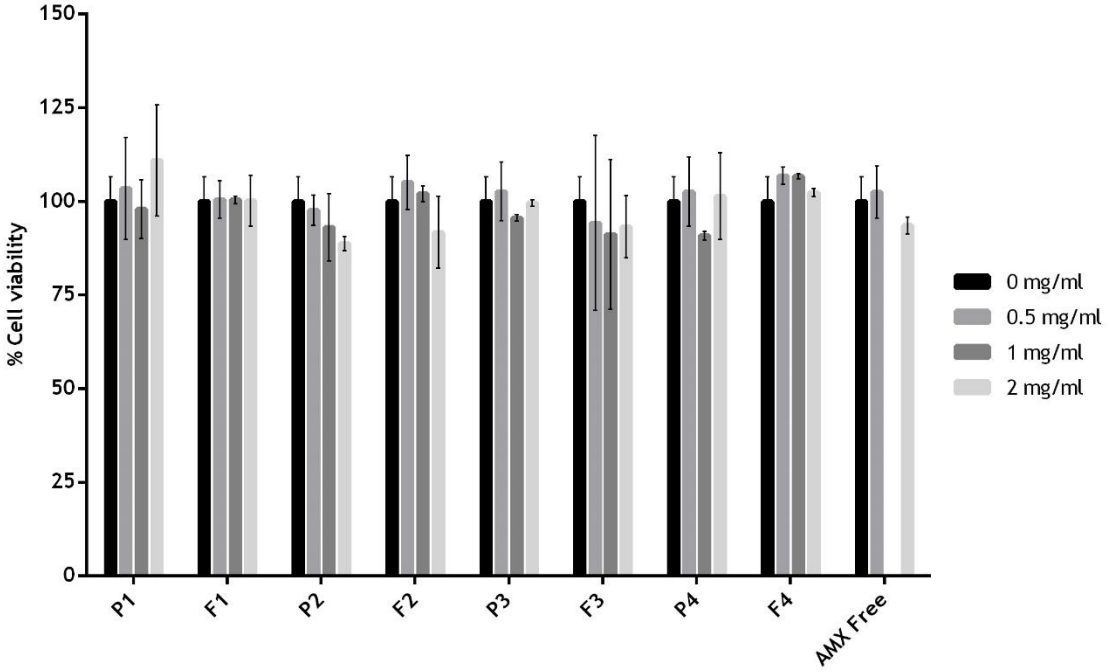


**Figure 3.31:** MKN28 cell viability assessed by MTT assay as a function of the different formulations and concentrations of SLNs tested (0, 0.5, 1 and 2 mg/mL). For free AMX only the concentrations 0, 0.5 and 2 mg/mL were tested. Values represent mean ± SD. No statistically significant differences were observed for both formulations and free AMX relatively to the mean positive control, regardless the concentration ($P$>0.05).

The MTT assays results for both L929 and MKN28 cell lines suggest that the developed AMX-loaded SLNs and the corresponding placebos does not interfere with cell viability. Therefore, these SLNs have potential to be a safe AMX delivery system for oral administration. It is noteworthy, that both 1 mg/mL and 2 mg/mL of the nanoparticles, contain a drug concentration of 0.112 mg/mL and 0.223 mg/mL, respectively. These drug concentrations are higher than the amoxicillin plasmatic concentration (0.0146 mg/mL) and the amoxicillin concentration in the gastric juice (0.00013 mg/mL) reported in the literature [105].

*-This page was intentionally left blank-*

# Chapter 4 - Conclusions

The increasing antibiotic resistance with loss of antibiotic efficacy and the lack of new antibiotics in the market have become a worldwide challenge to provide adequate treatment for infectious diseases [7, 14].

*H. pylori* infections affects around 50% of the global population, being the main cause of peptic ulcer and gastric cancer [22, 70]. Due to the last clinical outcome, *H. pylori* is classified as a human carcinogenic bacterium [22]. The current triple therapy applied to *H. pylori* infections lacks of efficacy due to the degradation of both AMX and clarithromycin in the acidic pH and due to the gastric transit that is responsible for an insufficient time of the antibiotics in the stomach [22, 70]. This requires multiple doses, leading to adverse side effects and lack of patient compliance [22, 70]. Ultimately, the early discontinuation of the therapy may lead to the development of antimicrobial resistance [70, 74]. Thus, novel effective therapies are necessary to overcome the limitations of the currently available treatments.

In the present work, AMX-loaded SLNs were developed as a potential effective therapy against *H. pylori* infections. The optimized SLNs composed of cetyl palmitate, linolenic acid, DOPE, Tween®80 and AMX were synthetized by the double emulsion technique. The optimal SLNs formulation obtained by the BBD revealed a particle size around 200 nm and a low PDI of approximately 0.137. The particle size of the SLNs developed is suitable for their diffusion into the gastric mucosa, which allows to overcome the limitations associated with the low permeability of AMX [70, 77, 78]. Besides, LC was superior to 7%. These values of particle size, PDI and LC were in accordance with the predicted by the experimental design applied, which indicates the success of the optimization process. The ideal formulation was compared with other three formulations that varied in the presence/absence of the therapy adjuvant and the targeting. Morphology studies revealed that both lyophilized SLNs and SLNs suspensions were almost spherical NPs and had smooth surfaces. In addition, stability studies showed that lyophilized SLNs at RT were stable for only 1 month, while SLNs suspensions stored at 4ºC were stable for at least 2 months. It seems that amoxicillin's encapsulation in NPs in suspension protect the drug from degradation, which is one of the limitations of the current treatment. Further studies are necessary to corroborate this hypothesis. In *in vitro* release studies, both lyophilized SLNs and SLNs suspensions revealed an initial burst release, which may be attributed to the release of non-encapsulated AMX (less than 30%), followed by a sustained and more controlled phase. In the F4 suspension, it was observed a slight higher release at the pH 5 medium, which simulates the mucus layer medium. This preferential release at pH 5 can be suitable for the *H. pylori* targeting. Further, all formulations revealed a high stability to a simulated stomach medium, with almost null release during 3 hours of exposure. This is in agreement to what was projected to overcome the limitations of the free drug administration.

The cytotoxicity of the SLNs developed was assessed through MTT assays on fibroblasts and gastric cells (L929 and MKN28 cell lines, respectively). All SLNs suspensions revealed no cytotoxicity at the tested concentrations when compared with the positive control.

In summary, it is expected that AMX degradation and its low diffusion across the mucus layer can be overcome by the SLNs developed, which can improve the therapeutic efficacy of this antibiotic in the treatment of *H. pylori* infections. Besides, it is believed that the addition of linolenic acid and DOPE will enhance the therapy as an adjuvant and a targeting, respectively. Nevertheless, further studies are required to assess their effect on *H. pylori* bacteria.

# Chapter 5 - Future Work

For future work, stability studies of the SLNs suspensions stored at 4ºC are expected to continue in order to define the SLNs shelf-time. Further, the stability of the developed SLNs will be assessed in a simulated gastric fluid medium containing enzymes to a more comprehensive translation into the *in vivo* gastric environment.

Cell permeability studies will be performed using the transwell assay on MKN28 cells. Further, to increase the complexity of the cell permeability model, mucins will be added.

Interactions NPs-bacteria will be performed to evaluate the efficiency of DOPE to target the bacteria. Additionally, the efficacy of the SLNs developed against *H. pylori* will be assessed through the determination of the minimal inhibitory concentration.

Ultimately, studies in healthy and disease animal models should be performed to evaluate the *in vivo* efficacy of the SLNs developed.

*-This page was intentionally left blank-*

# References


1. Cohen, M.L., *Changing patterns of infectious disease*. Nature, 2000. **406**(6797): p. 762-767.
2. Huh, A.J. and Y.J. Kwon, *"Nanoantibiotics": a new paradigm for treating infectious diseases using nanomaterials in the antibiotics resistant era.* J Control Release, 2011. **156**(2): p. 128-45.
3. World Health Organization Press, W.P., *Antimicrobial resistance: global report on surveillance*. 2014: France. p. 1-256.
4. Pelgrift, R.Y. and A.J. Friedman, *Nanotechnology as a therapeutic tool to combat microbial resistance*. Advanced Drug Delivery Reviews, 2013. **65**(13–14): p. 1803-1815.
5. World Health Organization, W. *Antibiotic resistance: Fact sheet*. 2015 October 2015 [cited 2016 January 01]; Available from: http://www.who.int/mediacentre/factsheets/antibiotic-resistance/en/.
6. Walsh, C., *Molecular mechanisms that confer antibacterial drug resistance.* Nature, 2000. **406**(6797): p. 775-81.
7. Mathers, C., D.M. Fat, and J.T. Boerma, *The global burden of disease: 2004 update*. 2008: World Health Organization.
8. Xie, S., et al., *Biodegradable nanoparticles for intracellular delivery of antimicrobial agents.* Journal of Controlled Release, 2014. **187**: p. 101-117.
9. Harde, H., M. Das, and S. Jain, *Solid lipid nanoparticles: an oral bioavailability enhancer vehicle*. Expert Opin Drug Deliv, 2011. **8**(11): p. 1407-24.
10. MacGregor, R.R. and A.L. Graziani, *Oral administration of antibiotics: a rational alternative to the parenteral route.* Clin Infect Dis, 1997. **24**(3): p. 457-67.
11. Ojer, P., et al., *Toxicity evaluation of nanocarriers for the oral delivery of macromolecular drugs.* Eur J Pharm Biopharm, 2015. **97**(Pt A): p. 206-17.
12. Pond, S.M. and T.N. Tozer, *First-pass elimination. Basic concepts and clinical consequences.* Clin Pharmacokinet, 1984. **9**(1): p. 1-25.
13. Beaulac, C., et al., *Eradication of mucoid Pseudomonas aeruginosa with fluid liposome-encapsulated tobramycin in an animal model of chronic pulmonary infection.* Antimicrobial Agents and Chemotherapy, 1996. **40**(3): p. 665-669.
14. Abed, N. and P. Couvreur, *Nanocarriers for antibiotics: a promising solution to treat intracellular bacterial infections.* Int J Antimicrob Agents, 2014. **43**(6): p. 485-96.
15. Laroui, H., et al., *Nanotechnology in diagnostics and therapeutics for gastrointestinal disorders.* Dig Liver Dis, 2013. **45**(12): p. 995-1002.
16. Alemán, J., et al., *Definitions of terms relating to the structure and processing of sols, gels, networks, and inorganic-organic hybrid materials (IUPAC Recommendations 2007).* Pure and Applied Chemistry, 2007. **79**(10): p. 1801-1829.
17. Bowman, D., J. D'Silva, and G. Van Calster, *Defining nanomaterials for the purpose of regulation within the European Union.* The European Journal of Risk Regulation, 2010: p. 115.
18. Wilczewska, A.Z., et al., *Nanoparticles as drug delivery systems.* Pharmacol Rep, 2012. **64**(5): p. 1020-37.
19. Hajipour, M.J., et al., *Antibacterial properties of nanoparticles.* Trends in Biotechnology, 2012. **30**(10): p. 499-511.
20. Moritz, M. and M. Geszke-Moritz, *The newest achievements in synthesis, immobilization and practical applications of antibacterial nanoparticles.* Chemical Engineering Journal, 2013. **228**: p. 596-613.
21. Shahverdi, A.R., et al., *Synthesis and effect of silver nanoparticles on the antibacterial activity of different antibiotics against Staphylococcus aureus and Escherichia coli.* Nanomedicine, 2007. **3**(2): p. 168-71.
22. Lopes, D., et al., *Targeting strategies for the treatment of Helicobacter pylori infections*, in *Nano Based Drug Delivery*, J. Naik, Editor. 2015, IAPC Publishing: Croatia. p. 604.

23. Abeylath, S.C. and E. Turos, *Drug delivery approaches to overcome bacterial resistance to beta-lactam antibiotics*. Expert Opin Drug Deliv, 2008. **5**(9): p. 931-49.
24. Zhang, L., et al., *Development of nanoparticles for antimicrobial drug delivery*. Curr Med Chem, 2010. **17**(6): p. 585-94.
25. Gao, W., J.M. Chan, and O.C. Farokhzad, *pH-Responsive nanoparticles for drug delivery*. Mol Pharm, 2010. **7**(6): p. 1913-20.
26. Lin, Y.H., et al., *Development of pH-responsive chitosan/heparin nanoparticles for stomach-specific anti-Helicobacter pylori therapy*. Biomaterials, 2009. **30**(19): p. 3332-42.
27. Weissig, V., T.K. Pettinger, and N. Murdock, *Nanopharmaceuticals (part 1): products on the market*. Int J Nanomedicine, 2014. **9**: p. 4357-73.
28. Evers, P., *Nanotechnology in medical applications: the global market*. BCC Research, 2015.
29. Das, S. and A. Chaudhury, *Recent advances in lipid nanoparticle formulations with solid matrix for oral drug delivery*. AAPS PharmSciTech, 2011. **12**(1): p. 62-76.
30. Battaglia, L. and M. Gallarate, *Lipid nanoparticles: state of the art, new preparation methods and challenges in drug delivery*. Expert Opin Drug Deliv, 2012. **9**(5): p. 497-508.
31. Pardeike, J., A. Hommoss, and R.H. Müller, *Lipid nanoparticles (SLN, NLC) in cosmetic and pharmaceutical dermal products*. International Journal of Pharmaceutics, 2009. **366**(1–2): p. 170-184.
32. Severino, P., et al., *Current state-of-art and new trends on lipid nanoparticles (SLN and NLC) for oral drug delivery*. J Drug Deliv, 2012. **2012**: p. 750891.
33. Fricker, G., et al., *Phospholipids and lipid-based formulations in oral drug delivery*. Pharm Res, 2010. **27**(8): p. 1469-86.
34. Ali Khan, A., et al., *Advanced drug delivery to the lymphatic system: lipid-based nanoformulations*. Int J Nanomedicine, 2013. **8**: p. 2733-44.
35. Müller, R.H., K. Mäder, and S. Gohla, *Solid lipid nanoparticles (SLN) for controlled drug delivery – a review of the state of the art*. European Journal of Pharmaceutics and Biopharmaceutics, 2000. **50**(1): p. 161-177.
36. Xie, S., et al., *Preparation and evaluation of ofloxacin-loaded palmitic acid solid lipid nanoparticles*. International Journal of Nanomedicine, 2011. **6**: p. 547-555.
37. DeMerlis, C.C. and D.R. Schoneker, *Review of the oral toxicity of polyvinyl alcohol (PVA)*. Food and Chemical Toxicology, 2003. **41**(3): p. 319-326.
38. Wissing, S.A., O. Kayser, and R.H. Muller, *Solid lipid nanoparticles for parenteral drug delivery*. Advanced Drug Delivery Reviews, 2004. **56**(9): p. 1257-72.
39. Mehnert, W. and K. Mäder, *Solid lipid nanoparticles: production, characterization and applications*. Advanced Drug Delivery Reviews, 2001. **47**(2–3): p. 165-196.
40. Üner, M. and G. Yener, *Importance of solid lipid nanoparticles (SLN) in various administration routes and future perspectives*. International Journal of Nanomedicine, 2007. **2**(3): p. 289-300.
41. Selvamuthukumar, S. and R. Velmurugan, *Nanostructured lipid carriers: a potential drug carrier for cancer chemotherapy*. Lipids Health Dis, 2012. **11**: p. 159.
42. Shah, R., et al., *Lipid nanoparticles: Production, characterization and stability*. 2015: Springer.
43. Cortesi, R., et al., *Production of lipospheres as carriers for bioactive compounds*. Biomaterials, 2002. **23**(11): p. 2283-94.
44. Singh, B., et al., *Developing oral drug delivery systems using formulation by design: vital precepts, retrospect and prospects*. Expert Opin Drug Deliv, 2011. **8**(10): p. 1341-60.
45. Lundstedt, T., et al., *Experimental design and optimization*. Chemometrics and Intelligent Laboratory Systems, 1998. **42**(1–2): p. 3-40.
46. Bezerra, M.A., et al., *Response surface methodology (RSM) as a tool for optimization in analytical chemistry*. Talanta, 2008. **76**(5): p. 965-977.
47. Singh, B., et al., *Developing micro-/nanoparticulate drug delivery systems using "design of experiments"*. Int J Pharm Investig, 2011. **1**(2): p. 75-87.
48. Ferreira, S.L.C., et al., *Box-Behnken design: An alternative for the optimization of analytical methods*. Analytica Chimica Acta, 2007. **597**(2): p. 179-186.

49. Varshosaz, J., M. Tabbakhian, and M.Y. Mohammadi, *Formulation and optimization of solid lipid nanoparticles of buspirone HCl for enhancement of its oral bioavailability.* J Liposome Res, 2010. **20**(4): p. 286-96.
50. Kaur, P., et al., *Development, optimization and evaluation of surfactant-based pulmonary nanolipid carrier system of paclitaxel for the management of drug resistance lung cancer using Box-Behnken design.* Drug Deliv, 2016. **23**(6): p. 1912-25.
51. Yasir, M. and U.V.S. Sara, *Preparation and optimization of haloperidol loaded solid lipid nanoparticles by Box–Behnken design.* Journal of Pharmacy Research, 2013. **7**(6): p. 551-558.
52. Hao, J., et al., *Development and optimization of solid lipid nanoparticle formulation for ophthalmic delivery of chloramphenicol using a Box-Behnken design.* Int J Nanomedicine, 2011. **6**: p. 683-92.
53. Negi, L.M., M. Jaggi, and S. Talegaonkar, *A logical approach to optimize the nanostructured lipid carrier system of irinotecan: efficient hybrid design methodology.* Nanotechnology, 2013. **24**(1): p. 015104.
54. Triplett, M., II and J. Rathman, *Optimization of β-carotene loaded solid lipid nanoparticles preparation using a high shear homogenization technique.* Journal of Nanoparticle Research, 2009. **11**(3): p. 601-614.
55. Marasini, N., et al., *Development and optimization of self-nanoemulsifying drug delivery system with enhanced bioavailability by Box-Behnken design and desirability function.* J Pharm Sci, 2012. **101**(12): p. 4584-96.
56. Zhang, Z., et al., *Solid lipid nanoparticles loading candesartan cilexetil enhance oral bioavailability: in vitro characteristics and absorption mechanism in rats.* Nanomedicine, 2012. **8**(5): p. 740-7.
57. Neves, A.R., et al., *Cellular uptake and transcytosis of lipid-based nanoparticles across the intestinal barrier: Relevance for oral drug delivery.* J Colloid Interface Sci, 2016. **463**: p. 258-65.
58. Fan, T., et al., *Design and evaluation of solid lipid nanoparticles modified with peptide ligand for oral delivery of protein drugs.* Eur J Pharm Biopharm, 2014. **88**(2): p. 518-28.
59. Ramalingam, P. and Y.T. Ko, *Improved oral delivery of resveratrol from N-trimethyl chitosan-g-palmitic acid surface-modified solid lipid nanoparticles.* Colloids and Surfaces B: Biointerfaces, 2016. **139**: p. 52-61.
60. Pandita, D., et al., *Solid lipid nanoparticles enhance oral bioavailability of resveratrol, a natural polyphenol.* Food Research International, 2014. **62**: p. 1165-1174.
61. Zhou, X., et al., *Nanostructured lipid carriers used for oral delivery of oridonin: an effect of ligand modification on absorption.* International Journal of Pharmaceutics, 2015. **479**(2): p. 391-8.
62. Neupane, Y.R., et al., *Lipid based nanocarrier system for the potential oral delivery of decitabine: formulation design, characterization, ex vivo, and in vivo assessment.* International Journal of Pharmaceutics, 2014. **477**(1-2): p. 601-12.
63. Luan, J., et al., *Nanostructured lipid carriers for oral delivery of baicalin: In vitro and in vivo evaluation.* Colloids and Surfaces A: Physicochemical and Engineering Aspects, 2015. **466**: p. 154-159.
64. Zhuang, C.-Y., et al., *Preparation and characterization of vinpocetine loaded nanostructured lipid carriers (NLC) for improved oral bioavailability.* International Journal of Pharmaceutics, 2010. **394**(1–2): p. 179-185.
65. How, C.W., et al., *Tamoxifen-loaded nanostructured lipid carrier as a drug delivery system: characterization, stability assessment and cytotoxicity.* Colloids Surf B Biointerfaces, 2013. **112**: p. 393-9.
66. Chen, C.C., et al., *Effects of lipophilic emulsifiers on the oral administration of lovastatin from nanostructured lipid carriers: physicochemical characterization and pharmacokinetics.* Eur J Pharm Biopharm, 2010. **74**(3): p. 474-82.
67. Tiwari, R. and K. Pathak, *Nanostructured lipid carrier versus solid lipid nanoparticles of simvastatin: comparative analysis of characteristics, pharmacokinetics and tissue uptake.* International Journal of Pharmaceutics, 2011. **415**(1-2): p. 232-43.
68. Dong, Z., et al., *Preparation and in vitro, in vivo evaluations of norfloxacin-loaded solid lipid nanopartices for oral delivery.* Drug Deliv, 2011. **18**(6): p. 441-50.

69. Severino, P., et al., *Sodium alginate-cross-linked polymyxin B sulphate-loaded solid lipid nanoparticles: Antibiotic resistance tests and HaCat and NIH/3T3 cell viability studies.* Colloids Surf B Biointerfaces, 2015. **129**: p. 191-7.
70. Lopes, D., et al., *Eradication of Helicobacter pylori: past, present and future.* Journal of Controlled Release, 2014. **189**: p. 169-186.
71. Suerbaum, S. and P. Michetti, *Helicobacter pylori infection.* N Engl J Med, 2002. **347**(15): p. 1175-86.
72. Malfertheiner, P., et al., *Management of Helicobacter pylori infection—the Maastricht IV/Florence consensus report.* Gut, 2012. **61**(5): p. 646-664.
73. Zullo, A., et al., *Standard triple and sequential therapies for Helicobacter pylori eradication: an update.* Eur J Intern Med, 2013. **24**(1): p. 16-9.
74. Egan, B.J., et al., *Treatment of Helicobacter pylori infection.* Helicobacter, 2008. **13 Suppl 1**: p. 35-40.
75. Thamphiwatana, S., et al., *In vivo treatment of Helicobacter pylori infection with liposomal linolenic acid reduces colonization and ameliorates inflammation.* Proc Natl Acad Sci U S A, 2014. **111**(49): p. 17600-5.
76. Lozniewski, A., et al., *Gastric penetration of amoxicillin in a human Helicobacter pylori-infected xenograft model.* Antimicrob Agents Chemother, 1999. **43**(8): p. 1909-13.
77. Amidon, G.L., et al., *A theoretical basis for a biopharmaceutic drug classification: the correlation of in vitro drug product dissolution and in vivo bioavailability.* Pharm Res, 1995. **12**(3): p. 413-20.
78. Lennernas, H., et al., *The effect of amiloride on the in vivo effective permeability of amoxicillin in human jejunum: experience from a regional perfusion technique.* Eur J Pharm Sci, 2002. **15**(3): p. 271-7.
79. Lingwood, C.A., M. Huesca, and A. Kuksis, *The glycerolipid receptor for Helicobacter pylori (and exoenzyme S) is phosphatidylethanolamine.* Infection and Immunity, 1992. **60**(6): p. 2470-2474.
80. Umamaheshwari, R.B. and N.K. Jain, *Receptor-mediated targeting of lipobeads bearing acetohydroxamic acid for eradication of Helicobacter pylori.* J Control Release, 2004. **99**(1): p. 27-40.
81. Neves, A.R., et al., *Novel resveratrol nanodelivery systems based on lipid nanoparticles to enhance its oral bioavailability.* Int J Nanomedicine, 2013. **8**: p. 177-87.
82. Abdelwahed, W., et al., *Freeze-drying of nanoparticles: formulation, process and storage considerations.* Adv Drug Deliv Rev, 2006. **58**(15): p. 1688-713.
83. Hoo, C.M., et al., *A comparison of atomic force microscopy (AFM) and dynamic light scattering (DLS) methods to characterize nanoparticle size distributions.* Journal of Nanoparticle Research, 2008. **10**(1): p. 89-96.
84. Brar, S.K. and M. Verma, *Measurement of nanoparticles by light-scattering techniques.* TrAC Trends in Analytical Chemistry, 2011. **30**(1): p. 4-17.
85. Lim, J., et al., *Characterization of magnetic nanoparticle by dynamic light scattering.* Nanoscale Research Letters, 2013. **8**(1): p. 381-381.
86. Sze, A., et al., *Zeta-potential measurement using the Smoluchowski equation and the slope of the current–time relationship in electroosmotic flow.* Journal of colloid and interface science, 2003. **261**(2): p. 402-410.
87. Honary, S. and F. Zahir, *Effect of zeta potential on the properties of nano-drug delivery systems-a review (Part 1).* Tropical Journal of Pharmaceutical Research, 2013. **12**(2): p. 255-264.
88. Xu, R., *Progress in nanoparticles characterization: sizing and zeta potential measurement.* Particuology, 2008. **6**(2): p. 112-115.
89. Ware, B., *Electrophoretic light scattering.* Advances in Colloid and Interface Science, 1974. **4**(1): p. 1-44.
90. Muchow, M., P. Maincent, and R.H. Muller, *Lipid nanoparticles with a solid matrix (SLN, NLC, LDC) for oral drug delivery.* Drug Dev Ind Pharm, 2008. **34**(12): p. 1394-405.
91. Reimer, L., *Transmission electron microscopy: physics of image formation and microanalysis.* Vol. 36. 2013: Springer.
92. Perrin, D., *Buffers for pH and metal ion control.* 2012: Springer Science & Business Media.

93. Gozlan, I., A. Rotstein, and D. Avisar, *Amoxicillin-degradation products formed under controlled environmental conditions: identification and determination in the aquatic environment*. Chemosphere, 2013. **91**(7): p. 985-92.
94. Singh, R. and J.W. Lillard, Jr., *Nanoparticle-based targeted drug delivery*. Exp Mol Pathol, 2009. **86**(3): p. 215-23.
95. Hassani, S., Y. Pellequer, and A. Lamprecht, *Selective adhesion of nanoparticles to inflamed tissue in gastric ulcers*. Pharm Res, 2009. **26**(5): p. 1149-54.
96. Mandpe, L. and V. Pokharkar, *Quality by design approach to understand the process of optimization of iloperidone nanostructured lipid carriers for oral bioavailability enhancement*. Pharm Dev Technol, 2015. **20**(3): p. 320-9.
97. Subedi, R.K., K.W. Kang, and H.K. Choi, *Preparation and characterization of solid lipid nanoparticles loaded with doxorubicin*. Eur J Pharm Sci, 2009. **37**(3-4): p. 508-13.
98. Iqbal, M., et al., *Double emulsion solvent evaporation techniques used for drug encapsulation*. International Journal of Pharmaceutics, 2015. **496**(2): p. 173-190.
99. Üner, M., E.F. Karaman, and Z. Aydoğmuş, *Solid lipid nanoparticles and nanostructured lipid carriers of loratadine for topical application: physicochemical stability and drug penetration through rat skin*. Tropical Journal of Pharmaceutical Research, 2014. **13**(5): p. 653-660.
100. Golmohammadzadeh, S., M. Mokhtari, and M.R. Jaafari, *Preparation, characterization and evaluation of moisturizing and UV protecting effects of topical solid lipid nanoparticles*. Brazilian Journal of Pharmaceutical Sciences, 2012. **48**(4): p. 683-690.
101. Kovacevic, A., et al., *Polyhydroxy surfactants for the formulation of lipid nanoparticles (SLN and NLC): effects on size, physical stability and particle matrix structure*. Int J Pharm, 2011. **406**(1-2): p. 163-72.
102. Shah, R.M., et al., *Physicochemical characterization of solid lipid nanoparticles (SLNs) prepared by a novel microemulsion technique*. J Colloid Interface Sci, 2014. **428**: p. 286-94.
103. Schwarz, C., et al., *Solid lipid nanoparticles (SLN) for controlled drug delivery. I. Production, characterization and sterilization*. Journal of Controlled Release, 1994. **30**(1): p. 83-96.
104. Standard, I., *10993-5. Biological evaluation of medical devices-Part 5: tests for in vitro cytotoxicity*. Geneva, Switzerland: International Organization for Standardization, 2009.
105. Goddard, A.F., et al., *Effect of omeprazole on the distribution of metronidazole, amoxicillin, and clarithromycin in human gastric juice*. Gastroenterology, 1996. **111**(2): p. 358-67.

*-This page was intentionally left blank-*

# Appendices

**Appendix 1:** Various SLNs and NLCs formulations studied for oral delivery of drugs/compounds.

| Formulation | Compound | Objective | LNPs composition | Method used | Particle Size (nm) | EE (%) | LC (%) | Ref. |
|---|---|---|---|---|---|---|---|---|
| NLCs and SLNs | Fluorescein isothiocyanate | Study cellular uptake through Caco-2 cell monolayers | **SLNs:** Cetyl palmitate, tween 60<br>**NLCs:** Cetyl palmitate, tween 60, miglyol 812 | High shear homogenization | 180 | - | 90.0 | [57] |
| SLNs | Salmon calcitonin | Improve oral bioavailability | Poloxamer 188, polyoxythylene, stearate, soybean phosphatidylcholin, stearic acid, tripalmitin<br>**Ligands:** CSK or IRQ | Double emulsion | **sCT IRQ-SLNs:** 409.9 ± 4.5<br>**sCT CSK-SLNs:** 244.4 ± 8.5 | **sCT-SLN:** 55.0 | **sCT-SLN:** 2.0 | [58] |
| SLNs | Candesartan cilexetil | Improve oral bioavailability | Soybean lecithin, glycerol monostearate, tween 80 | Film-homogenization | 24.3 ± 8.5 | 91.33 | - | [56] |
| SLNs | Resveratrol | Improve oral bioavailability and low water solubility | Palmitic acid, precirol ATO 5, gelucire 50/13, tween 80<br>**Functionalization:** palmitic acid-grafted *N*-trimethyl chitosan | Emulsification and ultrasonication | 258.28 ± 18.74 | 95.45 ± 2.18 | 3.56 | [59] |
| SLNs | Resveratrol | Enhance bioavailability | Stearic acid, poloxamer 188, phospholipon® 90 G | Solvent diffusion-solvent evaporation | 134.0 ± 7.6 | 88.9 ± 3.1 | 6.88 ± 0.11 | [60] |
| NLCs | Oridonin | Enhance oral bioavailability | Glycerin monostearate, octadecylamine, soybean lecithin S100, poloxamer 188<br>**Functionalization:** biotin | Melt dispersion-high pressure homogenization | 136.5 | 49.54 | 4.81 | [61] |
| SLNs | Buspirone HCl | Enhance bioavailability and pharmacokinetics | Cetyl alcohol, tween 20 | Emulsification-evaporation and sonification | 345.7 | 32.8 | - | [49] |

**Appendix 1:** Various SLNs and NLCs formulations studied for oral delivery of drugs/compounds.

| Formulation | Compound | Objective | LNPs composition | Method used | Particle Size (nm) | EE (%) | LC (%) | Ref. |
|---|---|---|---|---|---|---|---|---|
| NLCs | Decitabine | Enhance bioavailability and protection from acidic condition | Precirol ATO 5, transcutol HP, tween 80, polaxomer 188, solutol HS 15 | Cold high pressure homogenization | 116.64 ± 6.67 | 84.42 ± 5.38 | 8.54 ± 2.65 | [62] |
| NLCs | Baicalin | Improve dissolution and bioavalability | Glycerol monostearate, medium chain triglyceride, soybean lecithin, poloxamer 188 | Emulsion-evaporation and low temperature-solidification | 244.70 | 59.51 ± 0.57 | 3.54 ± 0.11 | [63] |
| NLCs | Vinpocetine | Improve oral absorption and bioavailability | Compritol 888 ATO, miglyol 812N, lecithin, solutol HS-15 | High pressure homogenization | 136.0 ± 4.2 | 95.3 ± 1.4 | - | [64] |
| NLCs | Simvastatin | Increase bioavailability and drug entrapment comparing with simvastatin loaded-SLN | Glycerin monostearate, oleic acid, poloxamer 407 | Solvent injection | 180.90 | 86.49 ± 2.83 | - | [67] |
| NLCs | Tamoxifen | Increase bioavailability | Softisan 154, olive oil, lecithin, polysorbate 80 | High-pressure homogenization | 46.55 ± 0.16 | 99.74 | 3.99 | [65] |
| NLCs | Lovastatin | Increase oral bioavailability | Precirol, squalene, pluronic F68, myverol 18-04 K, soybean phosphatidylcholine | Hot homogenization and ultrasonication | 180 - 290 | >70% | - | [66] |
| SLNs | Ofloxacin | Enhance pharmacological activity | Palmitic acid, PVA | Hot homogenization and ultrasonication | 156.33 ± 7.51 | 41.36 ± 1.50 | 4.40 ± 0.16 | [36] |
| SLNs | Norfloxacin | Enhance bioavailability and pharmacological activities | Stearic acid, PVA | Hot homogenization and ultrasonic | 301.00 ± 16.64 | 92.35 ± 2.24 | 8.58 ± 0.21 | [68] |
| SLNs (hybrid) | Polymyxin B sulphate | Improve residence time of the drug in mucosa and reduce the toxicity. | Cetyl alcohol, polysorbate 20 and trioleate sorbitan | High pressure homogenization | 439.5 ± 20.42 | 82.7 ± 5.5 | - | [69] |

**Appendix 2:** DSC thermogram of the bulk cetyl palmitate.

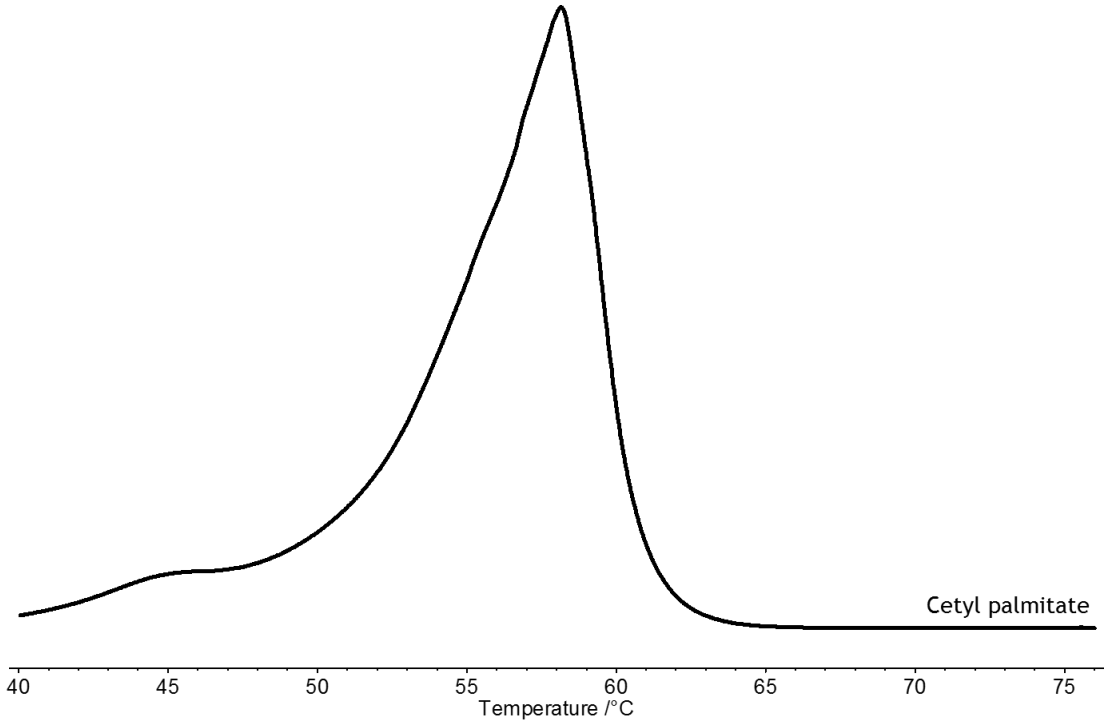


**Appendix 3:** DSC thermograms of: (A) F1 SLNs, (B) P1 SLNs, (C) F1 mixture and (D) P1 mixture.

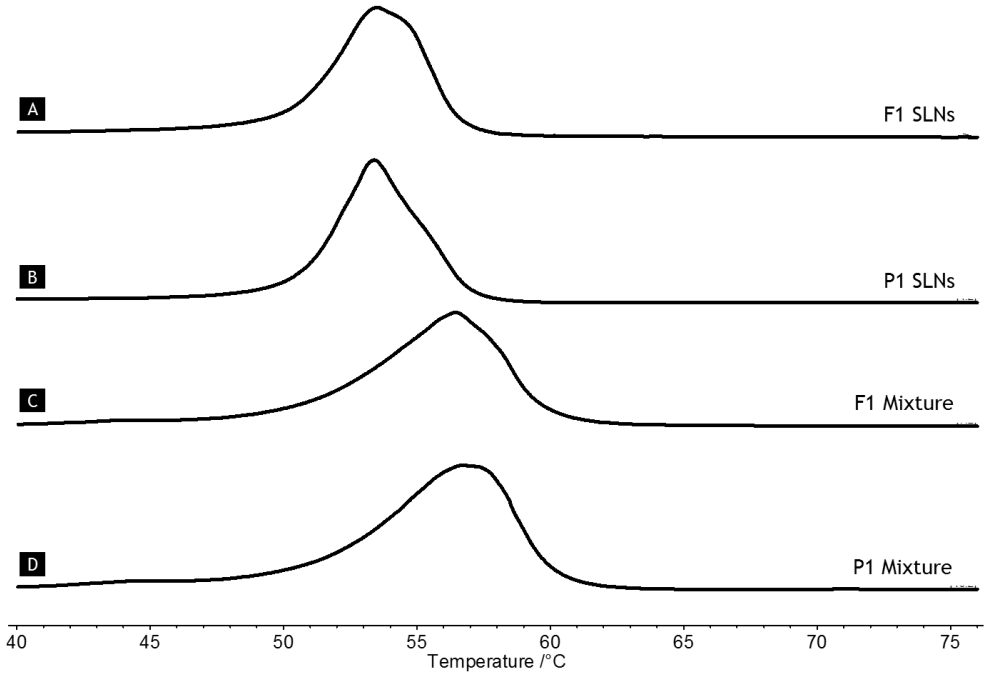

**Appendix 4:** DSC thermograms of: (A) F2 SLNs, (B) P2 SLNs, (C) F2 mixture and (D) P2 mixture.

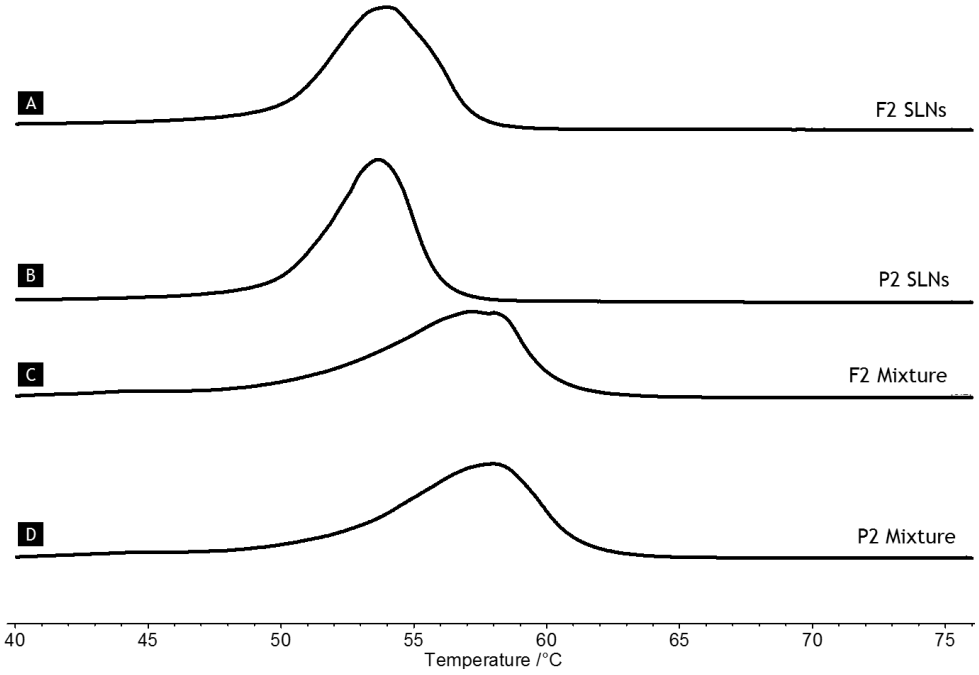


**Appendix 5:** DSC thermograms of: (A) F3 SLNs, (B) P3 SLNs, (C) F3 mixture and (D) P3 mixture.

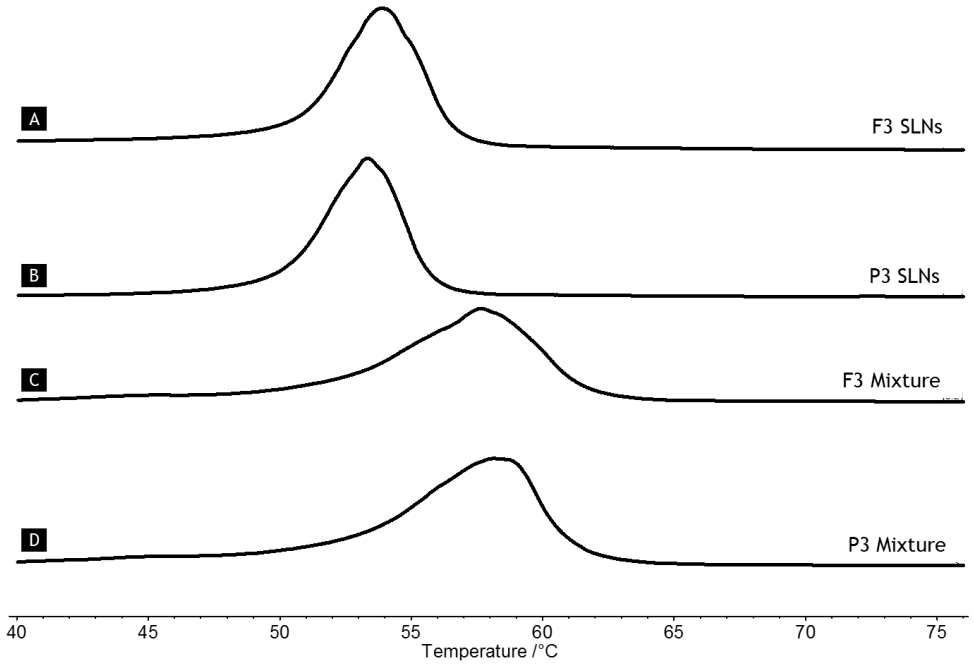

**Appendix 6:** Evaluation of the particle size of the ressuspended formulations stored at RT over time (0 (T0), 1 (T1) and 2 (T2) weeks). Bars represent the size (left Y axis). Values represent the mean ± SD of the readings. *P<0.05 relatively to the correspondent week 0.

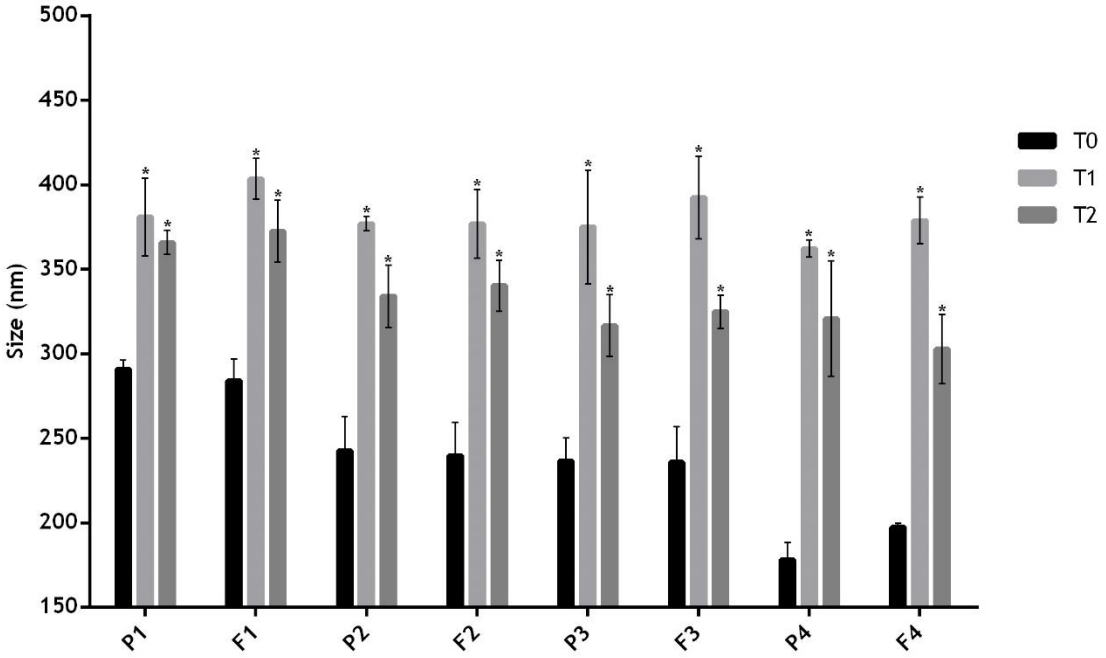


**Appendix 7:** Evaluation of the PDI of the ressuspended formulations stored at RT over time (0 (T0), 1 (T1) and 2 (T2) weeks). Bars represent the PDI (left Y axis). Values represent the mean ± SD of the readings. *P<0.05 relatively to the correspondent week 0.

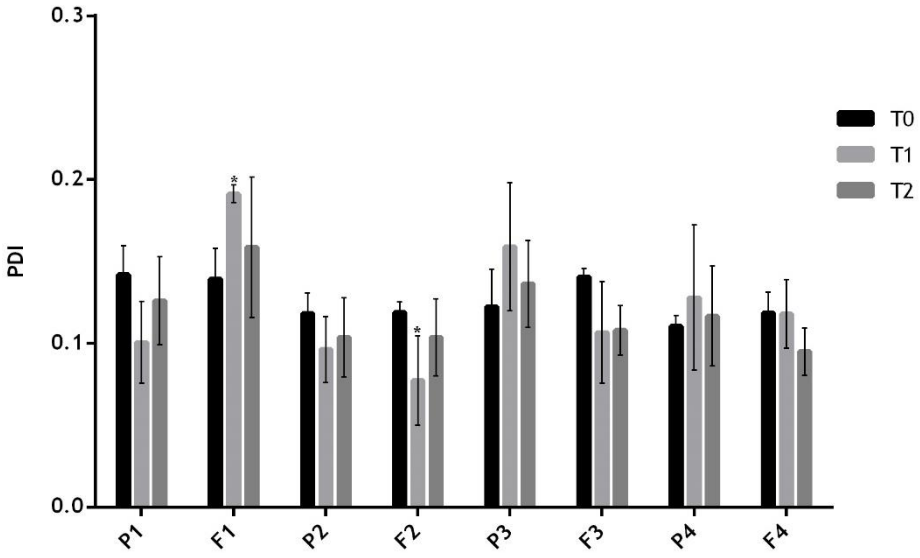

**Appendix 8:** Evaluation of the zeta potential of the ressuspended formulations stored at RT over time (0 (T0), 1 (T1) and 2 (T2) weeks). Bars represent the zeta potential (left Y axis). Values represent the mean ± SD of the readings. *P<0.05 relatively to the correspondent week 0.

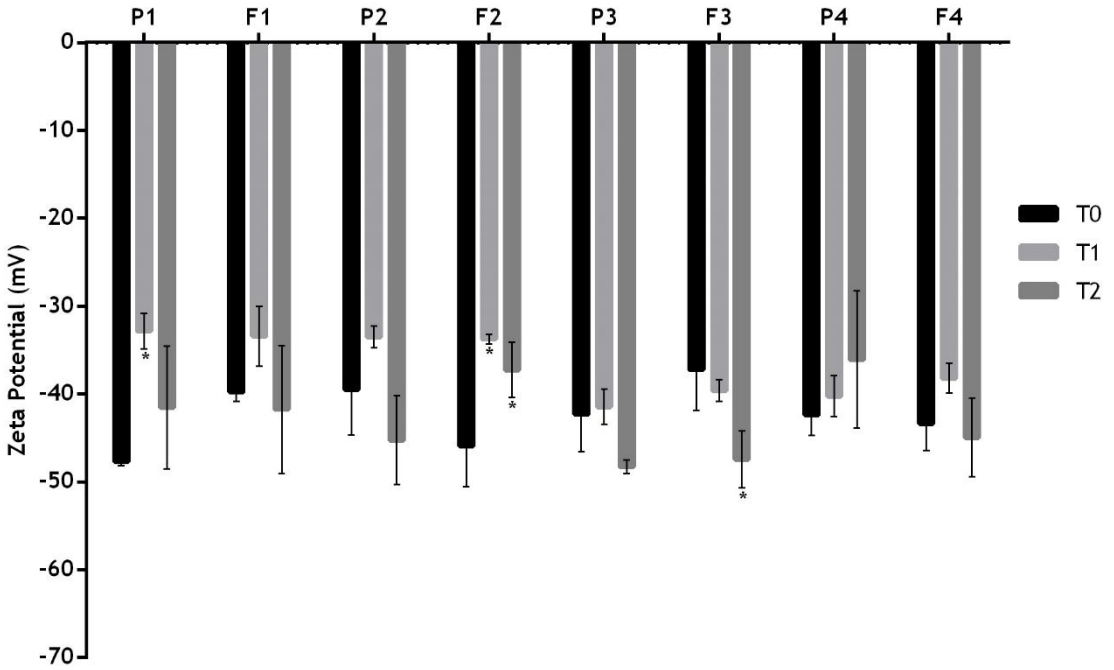


**Appendix 9:** Evaluation of the LC of the ressuspended formulations stored at RT over time (0 (T0), 1 (T1) and 2 (T2) weeks). Bars represent the LC (left Y axis). Values represent the mean ± SD of the readings. *P<0.05 relatively to the correspondent week 0.

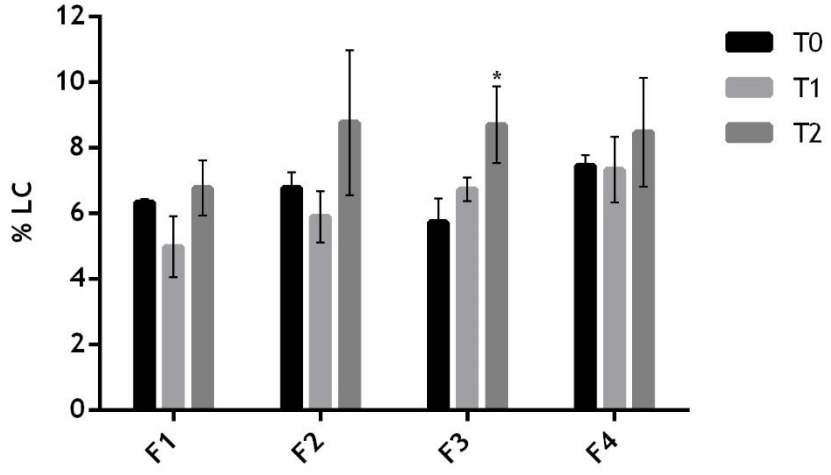

**Appendix 10:** Evaluation of the particle size of the ressuspended formulations stored at 4ºC over time (0 (T0), 1 (T1) and 2 (T2) weeks). Bars represent the size (left Y axis). Values represent the mean ± SD of the readings. *P<0.05 relatively to the correspondent week 0.

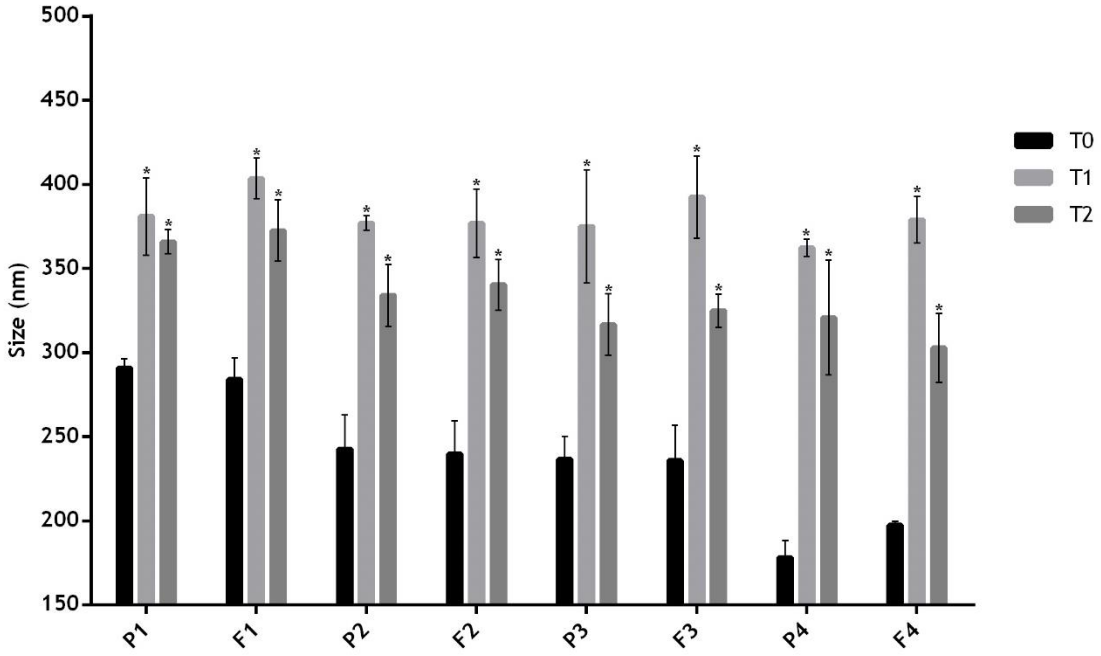


**Appendix 11:** Evaluation of the PDI of the ressuspended formulations stored at 4ºC over time (0 (T0), 1 (T1) and 2 (T2) weeks). Bars represent the PDI (left Y axis). Values represent the mean ± SD of the readings. *P<0.05 relatively to the correspondent week 0.

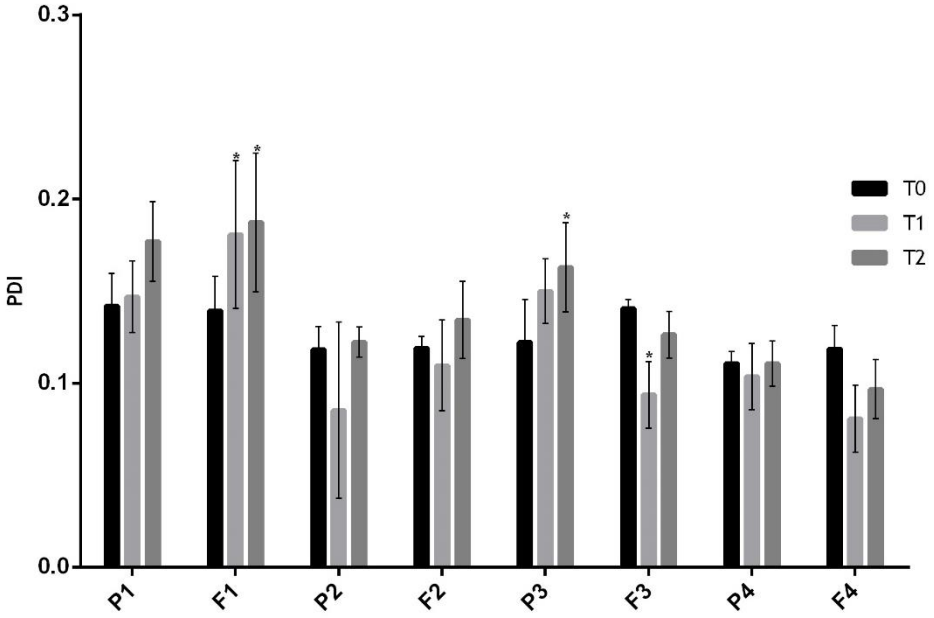

**Appendix 12:** Evaluation of the zeta potential of the ressuspended formulations stored at 4ºC over time (0 (T0), 1 (T1) and 2 (T2) weeks). Bars represent the zeta potential (left Y axis). Values represent the mean ± SD of the readings. *P<0.05 relatively to the correspondent week 0.

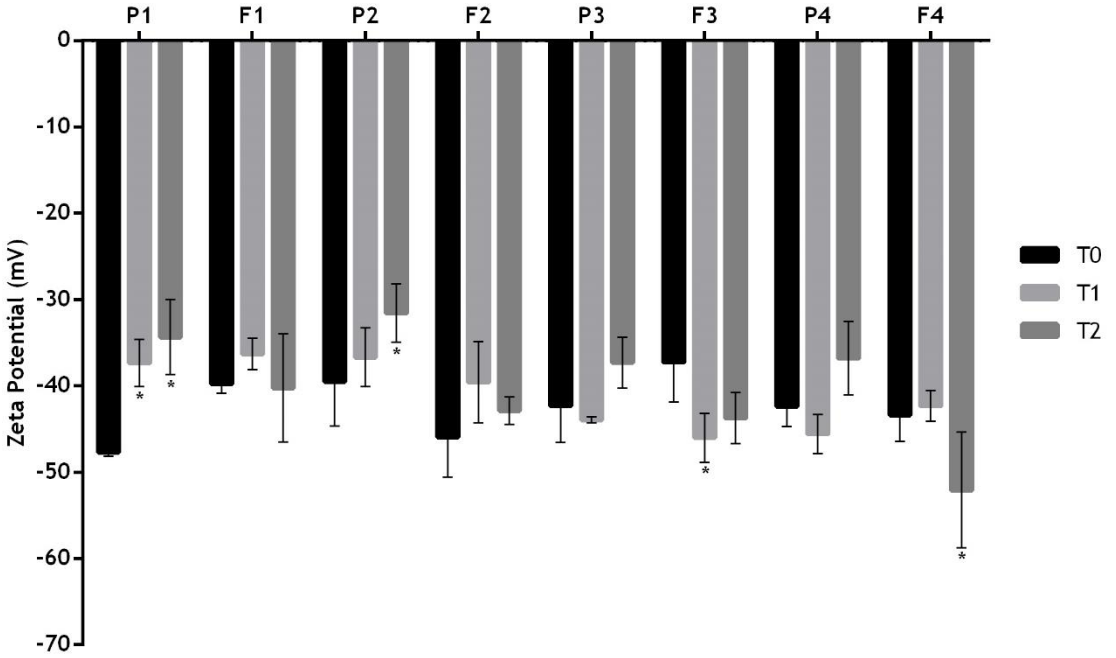


**Appendix 13:** Evaluation of the LC of the ressuspended formulations stored at 4ºC over time (0 (T0), 1 (T1) and 2 (T2) weeks). Bars represent the LC (left Y axis). Values represent the mean ± SD of the readings. *P<0.05 relatively to the correspondent week 0.